
Doctoral Dissertations

Student Theses and Dissertations

2011

Development of a versatile man-portable obscurant aerosol generator: characterization of aerosols in laboratory and field environments

Robert William Schaub

Follow this and additional works at: https://scholarsmine.mst.edu/doctoral_dissertations

 Part of the [Chemistry Commons](#)

Department: Chemistry

Recommended Citation

Schaub, Robert William, "Development of a versatile man-portable obscurant aerosol generator: characterization of aerosols in laboratory and field environments" (2011). *Doctoral Dissertations*. 2070. https://scholarsmine.mst.edu/doctoral_dissertations/2070

This thesis is brought to you by Scholars' Mine, a service of the Missouri S&T Library and Learning Resources. This work is protected by U. S. Copyright Law. Unauthorized use including reproduction for redistribution requires the permission of the copyright holder. For more information, please contact scholarsmine@mst.edu.

**DEVELOPMENT OF A VERSATILE MAN-PORTABLE OBSCURANT
AEROSOL GENERATOR: CHARACTERIZATION OF AEROSOLS IN
LABORATORY AND FIELD ENVIRONMENTS**

by

ROBERT WILLIAM SCHAUB

A DISSERTATION

Presented to the Faculty of the Graduate School of the
MISSOURI UNIVERSITY OF SCIENCE AND TECHNOLOGY

In Partial Fulfillment of the Requirements for the Degree

DOCTOR OF PHILOSOPHY

in

CHEMISTRY

2011

Approved
Dr. Shubhen Kapila, Advisor
Dr. Paul Nam
Dr. Prakash Reddy
Dr. Philip Whitefield
Dr. Virgil Flanigan

ABSTRACT

The objective of research presented in this dissertation was to develop a readily deployable and environmentally benign obscurant system operating with a single liquid for the visible and near infrared regions. To achieve this objective, research efforts were directed in two areas:

- i. Evaluating suitable biogenic oils to replace the United States Army's "Fog Oil" as the obscurant fluid.
- ii. Design, fabrication and validation of a prototype man-portable / vehicle mountable modular obscurant aerosol generator.

Petroleum middle distillate - "Fog Oil" has been the material of choice for wide area obscuration for several decades. Large quantities (thousands gallons) of the oil have been released into the environment during a single obscurant training exercise, posing potential risks to human health and the environment. Therefore, it is desirable to find a suitable replacement which is benign to humans and the environment. However, the oil must possess physical characteristics required for obtaining a desired obscurant plume. Various monoesters of biogenic oils were evaluated, methyl esters of soybean oil were found to be the most suitable oil from the availability, cost and performance points of views.

The current wide area obscurant generator in US Army's inventory is M-56, a large generator mounted on a dedicated vehicle. This generator suffers from logistic and portability limitations. The smaller man-portable generator designed and fabricated as part of this dissertation overcame limitations of M-56 while delivering same obscuration capabilities in the visible region and enhanced capability in the near infrared (NIR) region.

ACKNOWLEDGEMENTS

I would like to thank my parents William and Nancy Schaub for giving me a lifetime of advice and memories that helped shape my personality and provided me with a good moral foundation. Gratitude must also be shown to my wife Jennifer and our daughter Madison who has recently joined our home. I have found a new sense of pride and joy with you both.

A special thank you goes out to my friends, Kyle Anderson and Balaji Viswanathan for helping me unwind with conversation and hobbies.

At S&T I must also thank my adviser, Dr. Shubhen Kapila, for everything he has done to help me succeed. He believed in me when most probably would not have. He gave me a wealth of knowledge about instrumentation and chemistry in general. Gratitude is also extended to Dr. Virgil Flanigan for his assistance as one of the project's leaders. I give thanks to Dr. Paul Nam for giving me support along the way and helping me overcome instrumental difficulties. Appreciation is also given to my other committee members for their time and assistance, Dr. Prakash Reddy and Dr. Philip Whitefield. Also, Rusty Carlile and Max Trueblood for their help in making everything work.

I also thank past students whose work was included to help form the broader picture of this research: Shilpa Mathkar, Rachadaporn Seemamahannop, and Maj. Daniel Bahaghighat.

Finally I must thank the project sponsor, Edgewood Chemical Biological Center, RDE-COM, U.S. Army, without which this research could not have been conducted.

TABLE OF CONTENTS

	Page
ABSTRACT.....	iii
ACKNOWLEDGEMENTS.....	iv
LIST OF FIGURES.....	viii
LIST OF TABLES.....	xiv
NOMENCLATURE.....	xv
 SECTION	
1. INTRODUCTION.....	1
1.1. HISTORICAL APPLICATIONS.....	1
1.2. CURRENT GENERATION TECHNIQUE.....	2
1.3. LIMITATIONS OF EXISTING SYSTEMS.....	3
1.4. CURRENT NEEDS.....	4
2. LABORATORY TESTING OF BIOGENIC OILS.....	6
2.1. EQUIPMENT USED.....	6
2.2. EQUATIONS AND CALCULATIONS.....	18
2.3. PROPERTIES AND COMPARISONS OF OILS.....	19
2.3.1. Fog Oil.....	19
2.3.2. Methyl Soyate.....	23
3. DEVELOPMENT OF HIGH-OUTPUT MAN-PORTABLE GENERATOR.....	28
3.1. SWB-11 TURBOJET ENGINE.....	28
3.1.1. Specifications.....	28

3.1.2. Design.....	29
3.1.3. Obscurant Oil Sprayer Nozzle Designs.....	30
3.1.4. Performance.....	32
3.2. SWB-25 TURBOJET ENGINE.....	34
3.2.1. Specifications.....	34
3.2.2. Design.....	35
3.2.3. Performance.....	35
3.3. JetCat P80 TURBOJET ENGINE.....	36
3.3.1. Specifications.....	37
3.3.2. Design.....	37
3.3.3. Performance.....	37
3.4. CONSTRUCTION OF MODULAR GENERATOR UNIT.....	38
3.4.1. Target Parameters.....	38
3.4.2. Design and Construction.....	38
3.4.3. Subassemblies.....	40
3.4.4. Operation of Generator.....	44
3.4.5. Limitations and Hazards of Operation.....	46
4. TESTING.....	50
4.1. LABORATORY TESTING.....	50
4.1.1. Obscurant Oils.....	50
4.1.2. Effects of Generation Parameters.....	84
4.1.3. Environmental Temperature Fluctuation.....	85
4.1.4. Addition of Polymers.....	86

4.1.5. Copper Nanoparticles in Solution.....	87
4.1.6. Addition of Copper Nanoparticles as Powder.....	91
4.2. FIELD TESTING.....	97
4.2.1. Test Layout and Inherent Variables.....	97
4.2.2. Flow Rates.....	99
4.2.3. Comparison Between Oils.....	99
4.2.4. Comparison with M56.....	106
4.2.5. Addition of Polystyrene.....	107
4.2.6. Aerosol Deposition and Chemical Transformation Data.....	129
4.2.7. Performance at Simulated Urban Warfare Area.....	131
4.2.8. Remote Operation on ROV.....	131
4.2.9. Single Fluid Test.....	140
4.2.10. Discussion of Performance Evaluations.....	141
5. CONCLUSIONS.....	145
APPENDICES	
A. PORTABLE GENERATOR TECHNICAL DRAWINGS.....	147
B. COMPACT MAN-PORTABLE OBSCURANT SYSTEM OPERATIONAL MANUAL.....	159
BIBLIOGRAPHY.....	192
VITA.....	194

LIST OF FIGURES

Figure	Page
Figure 2.1 – Photograph of Particle Monitoring Instrumentation Cart.....	7
Figure 2.2 – Laser Source and Detector Layout and Specifications.....	12
Figure 2.3 – Photograph of Laser Source and Detector Units Mounted on Field-Deployable Tripods.....	13
Figure 2.4 – Photograph of Laboratory Climate-Controlled Aerosol Testing Chamber with Tubular Furnace-Based Obscurant Aerosol Generator.....	15
Figure 2.5 – Diagram of Climate-Controlled Aerosol Testing Chamber Layout.....	16
Figure 2.6 – Photograph and Diagram of Tubular Furnace-Based Obscurant Aerosol Generator.....	17
Figure 2.7 – Photograph of Fog Oil.....	20
Figure 2.8 – GC-FID Chromatogram of Fog Oil with Labeled Internal Standard Peaks.....	22
Figure 2.9 – Photograph of Methyl Soyate.....	24
Figure 2.10 – GC-FID Chromatogram of Methyl Soyate with Labeled Internal Standard Peaks.....	25
Figure 2.11 – Structures of the Fatty Acid Methyl Esters in Methyl Soyate.....	26
Figure 3.1 – Photograph of SWB-11 Turbojet Engine.....	29
Figure 3.2 – Photograph of Obscurant Oil Sprayer Nozzle Ring Designs.....	32
Figure 3.3 – Photograph of Obscurant Plume Generated in Urban Environment.....	33
Figure 3.4 – Photograph of SWB-25 Turbojet Engine.....	34
Figure 3.5 – Photograph of JetCat P80 Turbojet Engine.....	36
Figure 3.6 – Photograph of Engine Fuel Components Mounted on Prototype Generator Fuel Tank.....	41

Figure 3.7 – 3D Rendering of Dual Obscurant Sprayer Pump Assembly for Prototype Generator.....	42
Figure 3.8 – Photograph of Early Design of Prototype Generator Fuel Tank with Single Nozzle Obscurant Sprayer Pump Assembly.....	43
Figure 3.9 – 3D Rendering of Custom Radio Control Switch Assembly for Obscurant Oil Spraying and Line Purging Functions.....	43
Figure 3.10 – Prototype Generator Onboard Power Converter Schematic.....	45
Figure 3.11 – Photograph of Prototype Obscurant Generator In Use.....	46
Figure 4.1 – Layout of Biodegradation Experiment for Aquatic Systems.....	52
Figure 4.2 – Rates of Oil Biodegradation in Aqueous Systems.....	54
Figure 4.3 – Particle Size Distribution for Fog Oil at Different Generation Temperatures Obtained using Lasair OPC.....	60
Figure 4.4 – Particle Size Distribution for Fog Oil at Different Generation Temperatures Obtained using Spectro OPC.....	61
Figure 4.5 - Particle Size Distribution for Fog Oil at Different Generation Temperatures Obtained using Spectro OPC, Lower Size Ranges.....	62
Figure 4.6 – Percent Transmittance of Visible Radiation through Fog Oil at Different Generation Temperatures.....	63
Figure 4.7 – Photograph of Visible Wavelength Laser Attenuation in Climate-Controlled Aerosol Testing Chamber.....	64
Figure 4.8 - Particle Size Distribution for Methyl Soyate at Different Generation Temperatures Obtained using Lasair OPC.....	65
Figure 4.9 - Particle Size Distribution for Methyl Soyate at Different Generation Temperatures Obtained using Spectro OPC.....	66
Figure 4.10 - Particle Size Distribution for Methyl Soyate at Different Generation Temperatures Obtained using Spectro OPC, Lower Size Ranges.....	67
Figure 4.11 – Percent Transmittance of Visible Radiation through Methyl Soyate at Different Generation Temperatures.....	68
Figure 4.12 – Comparison of Particle Size Distribution Data for Methyl Soyate and Fog Oil at Different Generation Temperatures Obtained using Lasair OPC.....	70

Figure 4.13 - Comparison of Particle Size Distribution Data for Methyl Soyate and Fog Oil at Different Generation Temperatures Obtained using Spectro OPC.....	71
Figure 4.14 - Comparison of Particle Size Distribution Data for Methyl Soyate and Fog Oil at Different Generation Temperatures Obtained using Lasair OPC, Lower Size Ranges.....	72
Figure 4.15 – Particle Size Distribution for Fog Oil at Different Ambient Temperatures.....	73
Figure 4.16 - Particle Size Distribution for Methyl Soyate at Different Ambient Temperatures.....	74
Figure 4.17 – Particle Size Distribution of Methyl Soyate Blended with Polymers.....	75
Figure 4.18 – Transmittance of Visible Radiation through 0.5% Polystyrene-Methyl Soyate Blend Over Time.....	76
Figure 4.19 – Transmittance of Visible Radiation through 1.0% Polystyrene-Methyl Soyate Blend Over Time.....	77
Figure 4.20 - Transmittance of Visible Radiation through 1.0% EAS-Methyl Soyate Blend Over Time.....	78
Figure 4.21 – Particle Size Distribution Obtained using Lasair Comparing Fog Oil, Methyl Soyate, and PS-MS When Generated at 450 C.....	79
Figure 4.22 - Particle Size Distribution Obtained using Lasair Comparing Fog Oil, Methyl Soyate, and PS-MS When Generated at 500 C.....	80
Figure 4.23 - Particle Size Distribution Obtained using Spectro Comparing Fog Oil, Methyl Soyate, and PS-MS When Generated at 450 C.....	81
Figure 4.24 - Particle Size Distribution Obtained using Spectro Comparing Fog Oil, Methyl Soyate, and PS-MS When Generated at 500 C.....	82
Figure 4.25 – Particle Size Distribution Obtained using Lasair for Methyl Soyate Aerosolized at Different Generation Conditions.....	83
Figure 4.26 – Diagram of Aqueous Solutions Sprayer Assembly for Formation of Copper Nanoparticles.....	89
Figure 4.27 – Photograph of Aqueous Solutions Copper Nanoparticle Reaction Sprayer Mounted on JetCat P80 Generator System.....	90

Figure 4.28 – Scanning Electron Microscope Image of Copper Nanoparticles on Filter Fibers.....	91
Figure 4.29 – Scanning Electron Microscope Image of Needle and Agglomerate Structures in Dry Copper Nanoparticle Powder.....	93
Figure 4.30 – Transmittance Measurements through Copper Nanoparticle Powder.....	94
Figure 4.31 – Extinction Coefficient Measurements for Copper Nanoparticle Powder...95	
Figure 4.32 – Photograph of Brass Screen Faradic Cage.....	96
Figure 4.33 – Diagram of Field Testing Instrument Layout.....	98
Figure 4.34 – Particle Size Distribution for Fog Oil from SWB-11 Based Obscurant Aerosol Generator.....	100
Figure 4.35 - Particle Size Distribution for Methyl Soyate from SWB-11 Based Obscurant Aerosol Generator.....	101
Figure 4.36 - Particle Size Distribution Obtained using Lasair OPC for Fog Oil and Methyl Soyate from SWB-25 Based Obscurant Aerosol Generator.....	102
Figure 4.37 - Particle Size Distribution Obtained using Spectro OPC Comparing Methyl Soyate Aerosols from Modular versus Exposed SWB-11 Based Obscurant Aerosol Generator.....	103
Figure 4.38 – Particle Size Distribution Obtained using Lasair OPC for Methyl Soyate using Different Oil Flow Rates.....	104
Figure 4.39 - Particle Size Distribution Obtained using Spectro OPC for Methyl Soyate using Different Oil Flow Rates.....	105
Figure 4.40 – Percent Transmittance of Visible and Near Infrared Radiation through Methyl Soyate at Different Oil Flow Rates.....	106
Figure 4.41 – Percent Transmittance Comparison of Visible and Near Infrared Radiation of SWB-11 Based Obscurant Aerosol Generator versus M56 Generator.....	108
Figure 4.42 – Particle Size Distribution Comparison for Fog Oil from SWB-11 Based Obscurant Aerosol Generator versus M56 Generator.....	109
Figure 4.43 – Photograph of Relative Size Comparison of SWB-11 Based Obscurant Aerosol Generator versus M56 Generator.....	110

Figure 4.44 – Particle Size Distribution Data Obtained using Lasair OPC for Methyl Soyate and Fog Oil Comparing Different Numbers of Sprayer Nozzles.....	111
Figure 4.45 - Particle Size Distribution Data Obtained using Spectro OPC for Methyl Soyate and Fog Oil Comparing Different Numbers of Sprayer Nozzles.....	112
Figure 4.46 – Photograph of Laboratory High-Throughput Obscurant Aerosol Characterization Facility.....	113
Figure 4.47 – Particle Size Distribution Data Obtained using Spectro OPC for Methyl Soyate with 0.0-10.0% Dissolved Polystyrene.....	116
Figure 4.48 - Particle Size Distribution Data Obtained using Spectro OPC for Methyl Soyate with 0.0-5.0% Dissolved Polystyrene from SWB-11 Based Obscurant Aerosol Generator.....	117
Figure 4.49 – Percent Transmittance Comparisons of Visible and Near Infrared Radiation through Fog Oil, Methyl Soyate, and 0.0-10.0% Polystyrene-MS Blends.....	118
Figure 4.50 – Particle Size Distribution Data Obtained using Lasair OPC for Methyl Soyate with 0.0-4.0% Dissolved Polystyrene.....	119
Figure 4.51 - Particle Size Distribution Data Obtained using Spectro OPC for Methyl Soyate with 0.0-4.0% Dissolved Polystyrene.....	120
Figure 4.52 – Percent Transmittance of Visible and Near Infrared Radiation through Methyl Soyate with 0.0-4.0% Dissolved Polystyrene.....	121
Figure 4.53 – Particle Size Distribution Obtained using Lasair OPC for Methyl Soyate with 0.0-2.0% Dissolved Polystyrene.....	122
Figure 4.54 - Particle Size Distribution Obtained using Spectro OPC for Methyl Soyate with 0.0-2.0% Dissolved Polystyrene.....	123
Figure 4.55 – Photograph of Obscurant Aerosol Passing Through the Laboratory High-Throughput Aerosol Characterization Facility.....	124
Figure 4.56 - Particle Size Distribution Obtained using Lasair OPC for Methyl Soyate with 0.0-5.0% Dissolved Polystyrene.....	125
Figure 4.57 - Particle Size Distribution Obtained using Spectro OPC for Methyl Soyate with 0.0-5.0% Dissolved Polystyrene.....	126
Figure 4.58 – Percent Transmittance of Near Infrared Radiation through Methyl Soyate with 0.0-4.0% Dissolved Polystyrene.....	127

Figure 4.59 – Photograph of Field Testing in Progress.....	128
Figure 4.60 – Diagram of Aerosol Deposition Field Test Layout.....	130
Figure 4.61 – Photograph of Fort Leonard Wood Simulated Urban Combat Site Before Obscuration with JetCat P80 Based Obscurant Aerosol Generator.....	132
Figure 4.62 - Photograph of Fort Leonard Wood Simulated Urban Combat Site During Obscuration with JetCat P80 Based Obscurant Aerosol Generator.....	133
Figure 4.63 - Photograph of Fort Leonard Wood Simulated Urban Combat Site After Obscuration with P80 Based Obscurant Aerosol Generator.....	134
Figure 4.64 – Photograph of Radio Controlled Prototype Modular Obscurant Aerosol Generator Mounted to Radio Controlled Amphibious Vehicle.....	135
Figure 4.65 – Photograph of Obscuration of a Farm in a Valley Using Prototype Modular Obscurant Aerosol Generator.....	136
Figure 4.66 - Photograph of Obscuration of a Farm in a Valley Using Prototype Modular Obscurant Aerosol Generator, After Plume Dissipation.....	137
Figure 4.67 – Photograph of Simultaneous Obscuration by Prototype Modular Obscurant Aerosol Generator on Amphibious Vehicle and Exposed Obscurant Generator.....	138
Figure 4.68 – Photograph of Obscuration of a Farm in a Valley with Simultaneous Application of Two JetCat P80 Based Generators.....	139
Figure 4.69 – Photograph of Demonstration of Methyl Soyate Plume from Prototype Modular Obscurant Aerosol Generator Remaining Dense and Near the Ground.....	143
Figure 4.70 – Photograph of Methyl Soyate Plume Density Obscuring a Fence.....	144

LIST OF TABLES

Table	Page
Table 2.1 – Physical and Chemical Properties of Fog Oil.....	21
Table 2.2 – Polyaromatic Hydrocarbon Content of Neat and Aerosolized Fog Oil.....	21
Table 2.3 – Physical and Chemical Properties of Methyl Soyate.....	23
Table 2.4 – Polyaromatic Hydrocarbon Content of Neat and Aerosolized Methyl Soyate.....	25
Table 4.1 – Kinematic Viscosities of Biogenic Oils and Comparison with Fog Oil.....	51
Table 4.2 – Recovered Oil after Biodegradation in Terrestrial Systems, Oil on Top.....	56
Table 4.3 - Recovered Oil after Biodegradation in Terrestrial Systems, Oil in Middle...	57
Table 4.4 – Mutagenicity Tests on Neat Obscurant Oils.....	58
Table 4.5 – Mutagenicity Tests on Obscurant Oil Condensates.....	59

NOMENCLATURE

Symbol	Description
FO	Fog Oil, SGF-2, Specification Revision E: MIL-PRF-12070E
MS	Methyl Soyate biodiesel, B100
PS	Polystyrene
PS-MS	Methyl Soyate containing dissolved Polystyrene
EAS	Epoxidized Allyl Soyate
RPM	Revolutions Per Minute
CCF	Counts Per Cubic Foot
CCM	Counts Per Cubic Meter
cSt	Centistokes
OPC	Optical Particle Counter/Classifier
GC-FID	Gas Chromatography with Flame Ionization Detector
GC-MS	Gas Chromatography with Mass Spectrometry

1. INTRODUCTION

1.1. HISTORICAL APPLICATIONS

It has long been recognized that clouds of smoke obstruct the sense of sight. It is unclear when this property of smoke was first utilized on battlefields, but a source cites that smokes have been associated with obscuration since at least 1565.^[1] The easiest way to produce smoke is to burn vegetation such as wet leaves. The clouds of smoke, composed of combustion products, could help obscure visual detection of soldiers retreating. However, this method is not without drawbacks: the smoke is irritating to soldiers that must be in contact with the cloud, the haze tends to rise in the air quickly requiring many sources of smoke to be used, and igniting wet vegetation takes time that retreating soldiers may not have at their disposal.

Around World War I there were significant advances in the technologies of warfare. Smokescreens transitioned from the combustion of natural resources to the combustion of chemical compounds. Substances such as hexachloroethane blended with zinc oxide and powdered aluminum (designated "HC") burn to produce zinc chloride which absorbs humidity from the environment to produce a corrosive smoke. White (WP) and red phosphorus (RP) are incendiary substances which can burn to give a thick smoke. White phosphorus in particular combusts to give phosphorus pentoxide which absorbs humidity from the environment to produce phosphoric acid. Another substance is sulfur trioxide-chlorosulfonic acid (FS) which again absorbs moisture from the air to form a fog containing hydrochloric acid and sulfuric acid. However these substances were also not without problems. Common products were corrosive acid gases that would

cause pain and tissue damage to the eyes and respiratory system, posing hazards to friendly forces. White phosphorus artillery shells are designed to explode above a target, releasing ignited pieces of white phosphorus which would rain down on an area. However, white phosphorus burns extremely hot and is difficult to extinguish and burns into flesh upon contact. Once within the body, the phosphorus can react with water in the bloodstream to produce phosphoric acid that can spread throughout the body, causing significant pain and damage.^[2,3]

In World War II these same chemicals were still used, but smoke generator designs had become more numerous. Portability and smoke on demand were recognized as valuable assets to smokescreen systems. Combustion-based generators began to be found on aircraft, ground vehicles and naval vessels. However, another technique came into play as well. Fuel oil was applied to combustion cylinders in engines of tanks and ships to produce a smoke, but the old limitations still applied. Despite the drawbacks, the large scale usage of smokescreens had evident benefits in that it could obscure targets of interest such as munitions plants and vehicle production lines from the sights of bomber aircraft passing overhead.

1.2. CURRENT GENERATION TECHNIQUE

In the decades following World War II obscurant generation began to shift away from combustion-based smokes and toward obscurant aerosols for large scale obscurations. This was largely necessitated by the drawbacks of prior smoke generation techniques, chiefly the formation of corrosive acid gases that could be inhaled. The technique used in recent decades for large scale continuous smokescreens is to use

obscurant aerosols. In this process an obscurant fluid, namely the middle petroleum distillate SGF-2 “Fog Oil,” is sprayed into a heat source to provide enough thermal energy to cause vaporization of the oil.^[4] Coupled to this is a need for sufficient air flow to remove the vaporized oil from the heat source before ignition can occur. The vaporized oil is ejected from the generator where it contacts relatively cool ambient air in the environment and condenses into tiny droplets, essentially creating the equivalent of fog, which are small enough to remain airborne for substantial durations and have a diameter conducive to the Mie scattering of visible light.^[5] One such generator is the M56 Coyote which is a large engine mounted onto a HUMVEE vehicle. Capable of aerosolizing up to 4.9 liters (1.3 gallons) of fog oil per minute with up to 90 minutes of runtime using around 45 liters (12 gallons) of turbine fuel per hour a single M56 can obscure a large area of terrain in a short time, with standard practice having six M56 generators comprising a smoke platoon.^[6]

The effective requirements for creating an obscurant aerosol are therefore: a fluid with a vapor pressure low enough it can condense after being vaporized, a heat source to cause vaporization, and an air flow to push the vaporized substance away from the heat to prevent ignition.

1.3. LIMITATIONS OF EXISTING SYSTEMS

Systems such as the M56 can produce large obscurant plumes in a short time, but not without some drawbacks. The system is complex with numerous electronic and mechanical controls that can cause the generator to malfunction. It is also a very large, heavy system with a modified helicopter turbine engine mounted onto a dedicated

vehicle, limiting its usage to areas where a full vehicle may be maneuvered into position. The operators must also remain with the vehicle during operation which makes them more vulnerable to enemy fire since the generator unit becomes the target if the enemy tries to eliminate the obscurant source. By having the limited number of obscurant generators in the military inventory organized as 6-unit smoke platoons with trained operators the application of these generators is more limited. Each unit costs over \$150,000 and has a poor ratio of fuel consumption to obscurant output at about 1 gallon of fuel used to aerosolize one gallon of fog oil. The M56 is also logistically intensive in that it requires three separate fluids for operation: the obscurant fluid, the turbine fuel, and the vehicle fuel. There are also environmental and human health concerns associated with the large scale release of petroleum-based fog oil since its composition is not fully characterized but is known to contain polyaromatic hydrocarbons.

1.4. CURRENT NEEDS

The benefits of smokescreens will remain relevant for as long as visually-aimed weapons and intelligence gathering methods remain in use. In order to combat the ill reputations of continuous obscurant generators, newer generators must be smaller to be attached to virtually any vehicle in the military, lightweight enough to be carried by one or two soldiers for placement in remote locations, simple enough that any soldier can operate it regardless of the amount of training, and relatively inexpensive so many such generators can be available for immediate use on demand. Additionally, it is desired to have a generator that can operate on one fluid as both the fuel and the obscurant fluid to reduce the logistical needs of fluid transport into battle zones.

The two main areas of interest in this research are: 1) find a fluid to suitably replace fog oil in regards to obscurant performance and environmental and health impacts which can serve dual roles as a fuel and obscurant fluid, and 2) create a prototype modular obscurant aerosol generator that is the approximate size of two face-to-face jerry cans, lightweight enough for two soldiers to manually transport, have an obscurant output directly comparable to the M56 generator, and be able to provide five to ten minutes of continuous cover. Additional objectives were to investigate whether the addition of polymeric materials could shift aerosol particle diameters to more effectively attenuate infrared targeting wavelengths, and whether copper nanoparticles could effectively replace brass flakes in scrambling radio frequencies

2. LABORATORY TESTING OF BIOGENIC OILS

2.1. EQUIPMENT USED

Evaluating the effectiveness of obscurant aerosols requires an assortment of instruments and other devices as shown in Figure 2.1. In order to better understand the nature of the aerosols it is necessary to know the chemical and physical properties of the substances used, effects of generation conditions, resultant particle size distributions, effects of ambient temperatures, and their light scattering properties.

Though there are a variety of techniques available to determine particle size distributions in air, the systems at use here are optical particle classifiers (OPCs). These OPCs use a laser beam to shine across the sample inlet path, with a wavelength beyond that affected by scattering principles. The laser beam strikes a quartz crystal designed to oscillate at different frequencies, thereby changing the wavelength of the electromagnetic radiation. These new wavelengths are on the order of the particle diameters and can be affected by scattering theories. This altered laser radiation is reflected back into the sample stream where it interacts with incoming aerosolized particles, causing light scattering. A layout of mangin mirrors directs the scattered light to a photodiode detector. The relationship between scanning the quartz crystal frequency oscillations and the intensity of scattered light at the collecting photodiode detector provides a measure of the number of particles per volume of air sampled and the relative sizes of particles.

This research used two OPCs. The first is a Lasair Model 1003 from Particle Measuring Systems. It has a programmable collection cycle that is usually set to a ten second duration. It has eight channels on which it collects data, broken down into

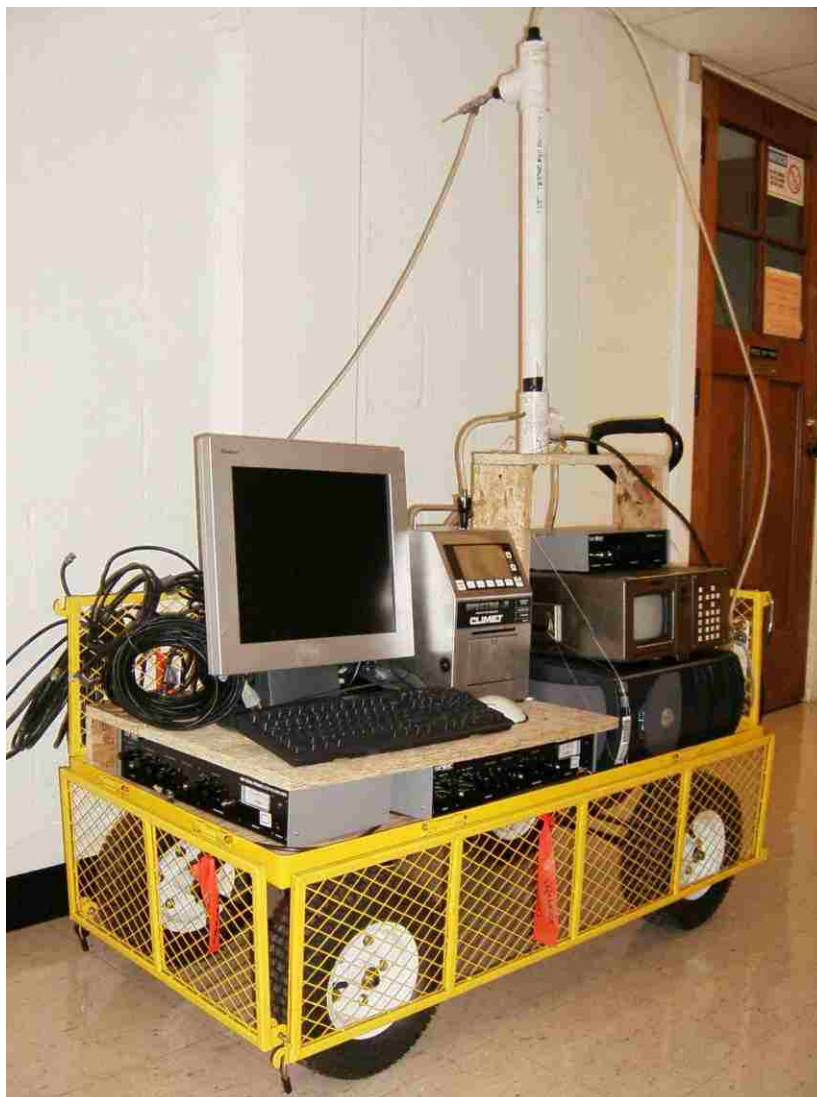


Figure 2.1 – Photograph of Particle Monitoring Instrumentation Cart

specific particle size ranges covering 0.1-0.2 μm , 0.2-0.3 μm , 0.3-0.4 μm , 0.4-0.5 μm , 0.5-0.7 μm , 0.1-1.0 μm , 1.0-2.0 μm , and diameters greater than 2.0 μm , respectively.

Data from this instrument is sent at the end of each sampling cycle via a RS232 connection to a PC for tabulation within the Facility Net software, and is then transcribed into Microsoft Excel for further data manipulation.

The second OPC is the Spectro .3 from CLiMET Instruments Company. This system has a set sampling flow rate of one liter per minute (LPM) and operates on sixteen channels covering particle size ranges of 0.3 μm , 0.4 μm , 0.5 μm , 0.6 μm , 0.7 μm , 1.0 μm , 1.3 μm , 1.6 μm , 2.0 μm , 2.5 μm , 3.0 μm , 4.0 μm , 5.0 μm , 6.0 μm , 7.0 μm and 10.0 μm , respectively. Data from this instrument was originally printed using the onboard printer option then transcribed into Microsoft Office, but later tests exported the data to a file on the PC through the use of an RS232 serial port and the National Instruments LabView software for further manipulation with Microsoft Excel.

The OPCs were not designed to sample particle number densities on the magnitude at which they are created in this research, so a dilution system was constructed to equally reduce the numbers of particles reaching the OPCs at each size range. The dilution tube consists of a 3.81 cm (1.5 in) diameter PVC pipe with a length of 60.96 cm (24 in) with 3.81 cm (1.5 in) PVC slip socket T fittings on either end with the center port oriented perpendicular to the dilution tube axis. This assembly is mounted vertically in regard to the dilution tube axis.

The upper slip socket T fitting has a 0.635 cm ($\frac{1}{4}$ in) diameter plastic air line coming into the top port. This line is fed by a 49.2 L (13 gal) air compressor with a maximum pressure rating of 8.5 atm (125 PSI), with the line being passed through a HEPA capsule filter followed by an adjustable 40 LPM maximum flow regulator. The center port of the upper T is fitted with a venturi sample inlet system. The venturi's sheath air flow is fed from the same air compressor and HEPA filter, but then routed through a digital air flow controller before introduction into the venturi setup. The sample inlet tube on the venturi is 0.3175 cm ($\frac{1}{8}$ in) diameter stainless steel tubing.

The lower slip socket T fitting houses the OPC sampling inlet tubes. The bottom port is blocked due to the mounting arrangements, while the center port is kept open as the exhaust of the dilution tube apparatus.

The data acquisition board in use on the PC is a National Instruments brand BNC-2110. This is internally connected to the PC motherboard using a National Instruments brand 6034E PCI card rated at 200 kS/s (kilosamples per second) with 16 inputs and 16 bits. The analog channels ACH0 and ACH1 were both used on the floating source (FS) mode as opposed to the ground reference source (GS) mode.

A pair of dual-phase lock-in amplifiers were used in conjunction with laser light transmittance tests. The Model 420 amplifiers were produced by Scitec Instruments Ltd. of the United Kingdom and distributed in the United States by Boston Electronics Corporation. The settings varied for each test to optimize the signal, but the input sensitivity was usually near 300 μV and the output time constant near 3 ms. Offset controls and phase shifts were all maintained at zero. The output offset was disabled (off) and the output select switch was set to 'R' as opposed to 'X' or 'Y.' 'X' mode output uses the first of two internal demodulator circuits to multiply the input with the reference signal to give an in-phase signal, whereas 'Y' uses a second internal demodulator to multiply the input with a 90 degree phase shifted reference to give an out of phase signal. 'R' mode calculates the signal amplitude independent of phase relationships between the input and reference signals and is the square root of the sum of squares for 'X' and 'Y.'

Signals from the laser photodiode detectors are directed into the amplifiers before being passed on to the data acquisition board. All connections between the photodiode

and the data acquisition board are made using coaxial cables with BNC connectors. A reference signal is provided by the beam chopper control unit to provide signal modulation for the elimination of contributing errors from environmental lighting variations encountered throughout the testing process. The reference signal is also sent to the amplifiers through use of a coaxial cable with BNC connectors. The reference signal frequency selector was kept on '1F.'

The laser photodiode detectors are not wavelength-specific and have no selection filters attached. Therefore they are prone to signal disturbances from environmental sources such as indoor lighting and outdoor sunlight, as well as variations in the amount of light striking the detectors from these sources from angle of orientation relative to the detectors and shadows or reflective occurrences in the proximity of the detectors. This source of error requires the use of a beam chopper for modulation. The chopper in use is manufactured by Scitec Instruments Ltd. of the United Kingdom and distributed in the US through Boston Electronics Corporation, and is a Model 300CD Variable Frequency Optical Chopper package with digital frequency readout. The 300CDU control unit connects to the 300H chopping head using the provided 300I cable. The chopping disc used is the two slot 300D2. The frequency was adjusted as necessary to provide the best signal, and was normally around $60 \text{ Hz} \pm 10 \text{ Hz}$. The frequency control was set to internal for adjustment by the onboard dial rather than using an external control source, and the frequency selector switch was set on '1S' rather than '10S.'

Two lasers were used for light transmittance measurements. Both are manufactured by B&W Tek Inc. as Class IIIA lasers. The first, a model BWT-20-E/54168 has a wavelength of 532 nm and a maximum power output of 30 mW. The

second is a model BWR-50E/55870 with a wavelength of 1064 nm and a maximum power of 80 mW. These wavelengths were chosen due to 532 nm being in the middle of the visible spectrum and 1064 nm being a near-infrared wavelength used for some military laser targeting systems. Attenuation at these wavelengths is an approximation for relative quantitative determination of the effectiveness of the different aerosolized oils as obscurants. Detection relies on using two photodiode sensors. Specifications for the lasers with chopper assembly are shown in Figures 2.2 and 2.3.

The first testing chamber used in the lab for particle size and number density measurements is a 1 m³ cube made of laminated plywood 1.9 cm (0.75 in) thick. The front door has four hinges along the left side for access to the chamber's interior, and has a rubber gasket installed around its mating surface to improve the seal. Each edge is glued and screwed together for strength as well as to help contain the aerosols within. Centered in the left and right side panels are 6.67 cm (2.625 in) diameter holes for the placement of mounted quartz window units for light transmittance measurements across the chamber. There is an internal copper tubing of 0.635 cm (0.25 in) outer diameter and 0.3175 cm (0.125 in) inner diameter carrying air to provide a sheath flow over the quartz windows to prevent deposition of oil particles. The top panel of the chamber has five copper sampling tubes installed, each with a diameter of 1.59 cm (0.625 in) and length of 60.96 cm (24 in) with approximately 44.45 cm (17.5 in) of the length contained within the chamber. With a constant depth within the chamber, the sampling tubes are arranged at equidistant intervals along an axis between the sides, following near the path between the light transmittance quartz windows. Spacing between sampling tube centers is 17.15 cm (6.75 in). Mounted on the center of the floor panel is an electrical fan for circulating

the stream of obscurant entering the chamber. It has an operating diameter of 11.43 cm (4.5 in), overall width and height of 11.75 cm (4.625 in) and a depth of 3.81 cm (1.5 in).

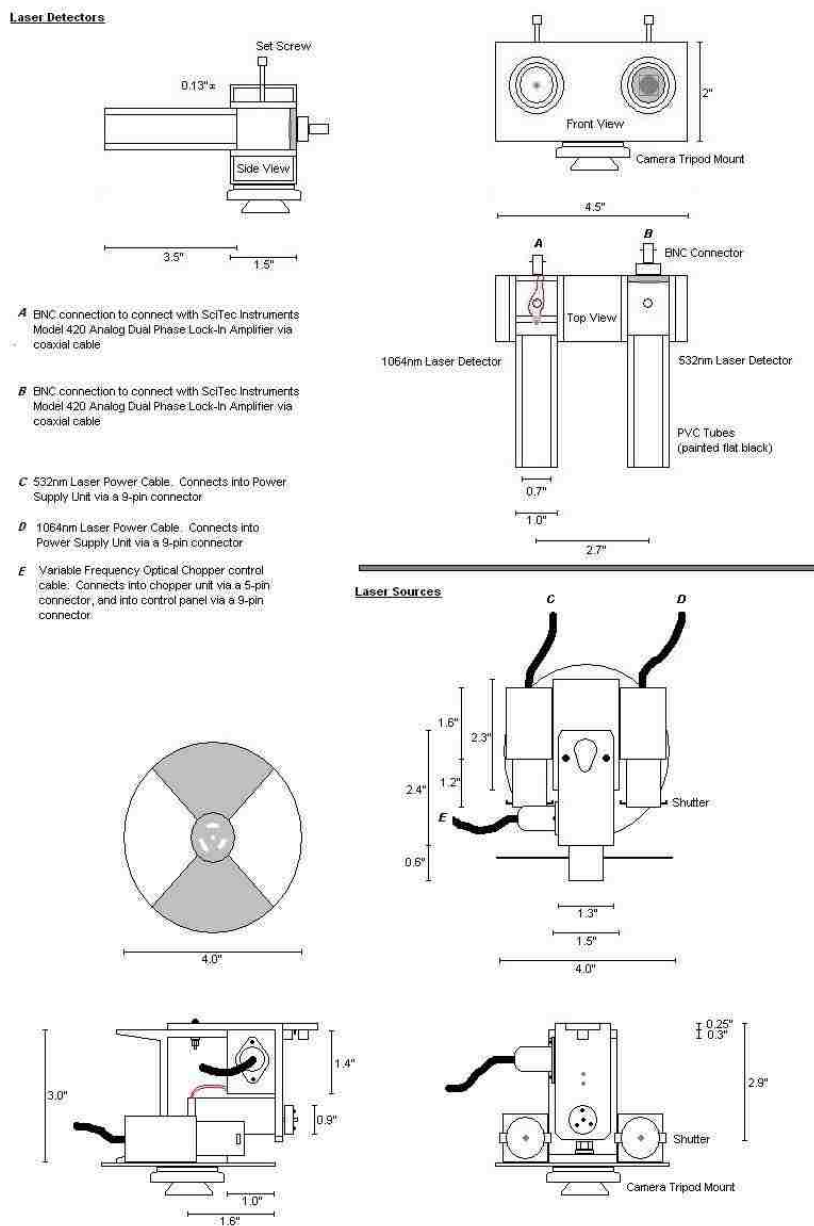


Figure 2.2 – Laser Source and Detector Layout and Specifications



Figure 2.3 – Photograph of Laser Source and Detector Units Mounted on Field-Deployable Tripods

The fan is mounted on some right-angle brackets and has a space of 5.72 cm (2.25 in). The right side wall has a copper tube installed with the same diameter as the sampling tubes which extends 48.90 cm (19.25 in) inside the chamber for the introduction of obscurant aerosol plumes.

The second aerosol testing chamber is a modular industrial refrigerated room manufactured by Norlake Scientific. It is capable of temperatures ranging from 4°C to 50°C using a digitally controlled heating and cooling unit mounted on the top. The walls are four inches thick, filled with insulating foam, with stainless steel sheeting as the exterior surfaces. Circular openings were made in the center of both sides to mount the

quartz windows for passing visual or laser light through the chamber for transmittance testing. A small six inch diameter desk fan was placed inside the chamber to generate a small internal circulation to ensure adequate mixing of the aerosol samples once introduced to the chamber. Aerosol samples enter the chamber through a 1.27 cm (0.5 in) diameter copper tube fitted with a commercial plastic valve which allows precise control over aerosol introduction times into the chamber. The rear wall of the chamber has four additional copper tubes midway up the height of the wall which penetrate into the chamber and provide sampling port access. At the top rear of the right side wall is a 6.35 cm (2.5 in) exhaust port with a plastic valve, and at the bottom center of the left side wall is another port through which ambient room air can enter during chamber evacuations. The testing chamber is shown in Figures 2.4 and 2.5.

A small scale aerosol generator, as seen in Figure 2.6, was constructed for laboratory testing. A 1.27 cm (0.5 in) steel aerosol generation tube was placed inside a 2.54 cm (1 in) steel tube with fine grade steel wool packed in the void between the tubes to serve as the heat conductor, and a thermocouple probe placed alongside the inner tube. This tube assembly, with Swagelok fittings and nuts on the ends of the inner generation tube, was placed through the center of the tube furnace and protruded from both ends of the furnace. The thermocouple probe was connected to a digital temperature programmer installed on the front side of the tube furnace to control heat cycling. Glass wool was placed around the outer tube where it protruded from the furnace to fill a small void space and prevent unnecessary heat loss.



Figure 2.4 – Photograph of Laboratory Climate-Controlled Aerosol Testing Chamber with Tubular Furnace-Based Obscurant Aerosol Generator

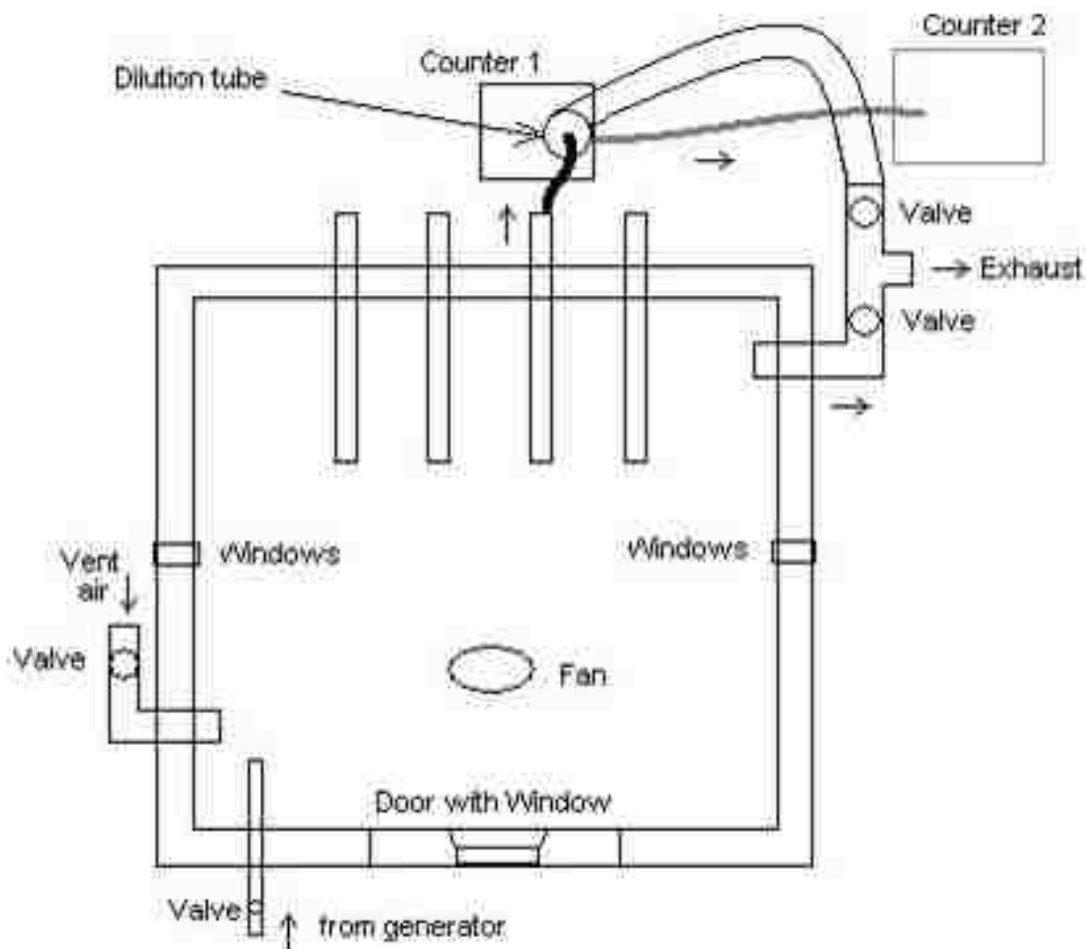


Figure 2.5 – Diagram of Climate-Controlled Aerosol Testing Chamber Layout

On the inlet side of the generation tube was a stainless steel T-fitting, which allowed a 0.159 cm (0.0625 in) stainless steel tube to carry sample oil from the oil pump to a thick-walled 1/8 in stainless steel probe which runs coaxially within the generation tube and drips oil sample into the front heated portion, ranging from 400°C to 650°C, of the generation tube. An air flow controlled by a flow regulator brings air into the generation tube from the perpendicular access port of the T-fitting. It is through this method that sample oil and air flow combine in a heated region of the generation tube to allow subsequent oil vaporization and aerosolization. The oil pump was set to deliver 0.5

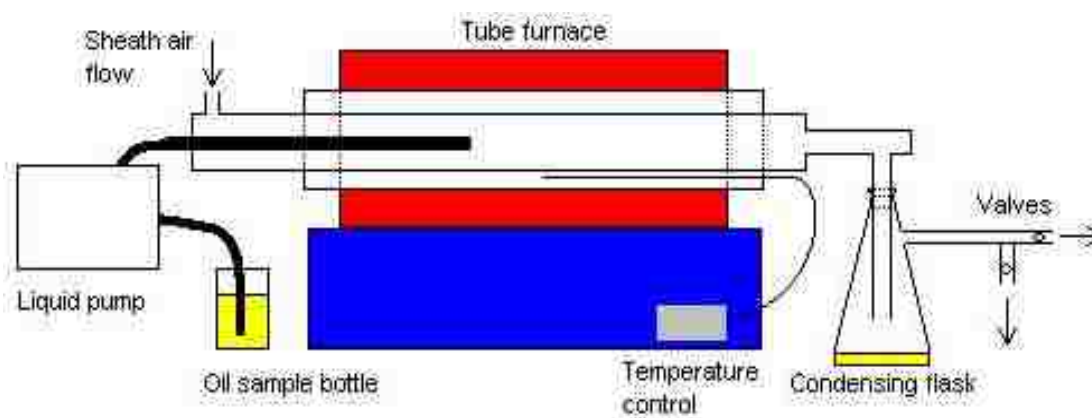


Figure 2.6 – Photograph and Diagram of Tubular Furnace-Based Obscurant Aerosol Generator

mL/min of oil flow to the generator, and the air flow was varied in experiments from 5 L/min to 10 L/min.

On the outlet side of the generation tube was another stainless steel T-fitting, through which a second temperature probe was placed into the steam of aerosol exiting the generator. The aerosol exited the generation tube perpendicularly where it entered a vacuum flask which served as a collection point for unaerosolized and condensed oil. Remaining aerosol samples exited the flask through a tube connecting the flask's vacuum line port to the chamber's front access tube valve.

2.2. EQUATIONS AND CALCULATIONS

In order to analyze the effectiveness of the obscurant aerosols for attenuating wavelengths of interest, the principal equation of interest is the Beer-Lamber Law:

$$A = \epsilon \iota c$$

for A = absorbance, ϵ = molar extinction coefficient, ι = path length,

and c = concentration

Using this equation, the absorbance should be proportional to the concentration of airborne particles and the path length across the plume assuming a constant molar extinction coefficient, also known as molar absorptivity, for a given obscurant oil type. The molar extinction coefficient is a measured value expressing the degree of absorption by a given substance at a given wavelength. This value is directly attributed to the properties of the substance and should therefore be a constant for a fixed wavelength.

It may also be noted that when testing obscurant oil samples in the laboratory, the path length is a fixed value. Additionally, the concentration of particles occupying a

space may be controlled to give equal concentrations between oil types, therefore rendering the concentration variable to serve as a constant as well. Therefore, in laboratory environments the absorption should generally follow the extinction coefficient and vary with the type of oil being tested.

Additional calculations come in determining the particle number densities and size distributions. Data for the numbers of particles in a given volume are found and recorded by the OPCs. These values are given in either counts per cubic foot (CCF) or counts per cubic meter (CCM). These values are determined by the number and intensity of signals received at a photodiode detector after a laser beam shining through the sample stream reflects off of the airborne particles present. The volume of air sampled is calculated internally using the flow rate and run time of a sampling pump.

2.3. PROPERTIES AND COMPARISONS OF OILS

2.3.1. Fog Oil. Fog Oil, shown in Figure 2.7, is the name given to a light yellow petroleum middle distillate used by the military as substance designation SGF-2 (Standard Grade Fuel), with required substance specifications outlined in MIL-F-12070E.^[8] Physical and chemical properties may be seen in Table 2.1.

Originating from naphthenic petroleum, fog oil inherently contains carcinogenic compounds in its complex composition of around 1000 different chemical constituents, including polyaromatic hydrocarbon compounds (PAHs) until 1986 when revised specifications called for their removal.^[5] Under the current manufacturer specifications, fog oil must contain no detectable amounts of carcinogenic or possible carcinogenic



Figure 2.7 – Photograph of Fog Oil

compounds, so these substances are hydrogenated to render them less toxic and then extracted, leaving behind alkane molecules that can have between 10 and 40 carbons in a variety of structural arrangements.^[7] However, being below detection limits does not mean these compounds are completely absent. Information about relative levels of common polycyclic aromatic hydrocarbons (PAHs) found in neat fog oil as well as fog oil aerosolized at different temperatures was previously performed and reported, with

samples aerosolized at oil flow rates of 0.5 mL/min with air flows of 10 L/min, and is seen in Table 2.2.^[5]

Table 2.1 – Physical and Chemical Properties of Fog Oil

Color	Lt Yellow
Biogenic	No
PAH Presence	Yes
Pour Point, °C	-4
Kinematic Viscosity (cst) 100°C	3.4 to 4.17
Average Boiling Point, °C	300 to 600
Flash Point, °C	>160

Table 2.2 – Polyaromatic Hydrocarbon Content of Neat and Aerosolized Fog Oil

Compound Name	Neat	350°C	400°C	450°C	500°C	550°C	600°C	650°C
Naphthalene (ppm)	4	4	5	6	6	10	12	15
Fluoranthene	5	4	5	4	6	3	3	7
Pyrene	11	21	28	17	32	18	25	22
2,6-Dimethyl Naphthalene	2	1	2	1	7	4	4	5
3,6-Dimethyl Phenanthrene	5	6	7	11	8	6	8	10
Dimethyl Phenanthrene	7	7	8	11	9	8	8	11
Dimethyl Phenanthrene	7	7	8	11	9	10	10	10
Dimethyl Phenanthrene	42	40	39	47	44	44	48	52
Dimethyl Phenanthrene	14	15	16	20	18	19	17	23
Dimethyl Phenanthrene	7	7	8	11	9	9	8	11
Other	32	25	42	41	48	70	69	112
Total (ppm)	136	137	168	180	196	201	212	278

The chromatogram of fog oil, as previously analyzed by Maj. Daniel Bahaghighat, seen in Figure 2.8, showed a broad hump with few distinguishing characteristics due to the composition of this petroleum-based oil containing around a thousand different individual chemical species. GC-FID chromatograms of fog oil and

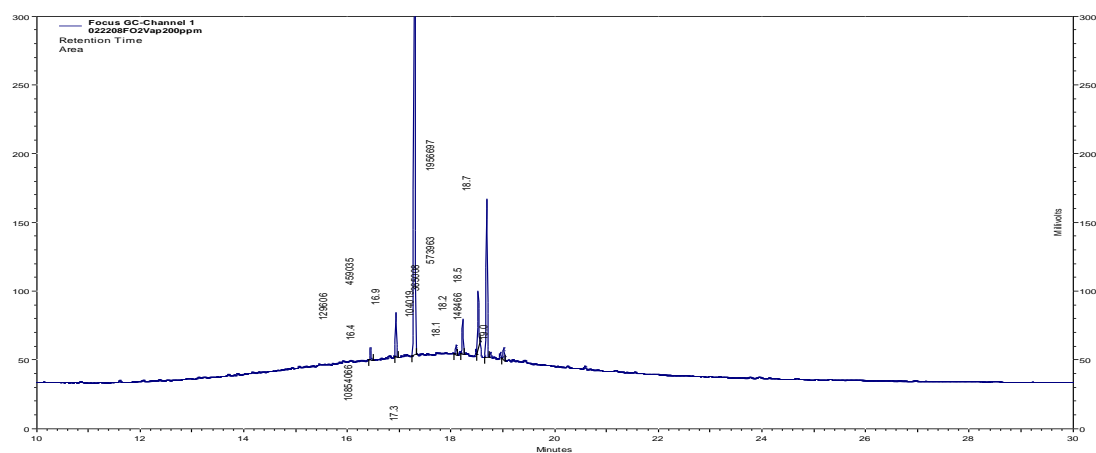


Figure 2.8 – GC-FID Chromatogram of Fog Oil with Labeled Internal Standard Peaks

methyl soyate were obtained by placing 5 mg oil sample into a 7 mL amber vial and adding 5 mL isooctane. A 0.1 mL sample was taken and added to another 0.9 mL isooctane and blended with 10 μ L C17:0 internal standard. Conditions of the GC-FID experiment are as follows: 1 μ L injection volume in splitless injection mode using a 15m x 0.25mm i.d. J&W Scientific DB-225 cyanopropyl siloxane column with a 0.15 μ m film thickness. The column oven was initially held at 50 $^{\circ}$ C for one minute, then ramped at 10 $^{\circ}$ C/min to a final temperature of 220 $^{\circ}$ C then held for 12 minutes. Helium at a flow rate

of 1.20 mL/min was used as the carrier gas, and the FID hydrogen flow rate was 25 mL/min.^[9]

2.3.2. Methyl Soyate. Methyl Soyate is the methyl ester of soybean oil and is currently used as commercial biodiesel. Some testing used B100 biodiesel (100% methyl soyate, 0% standard diesel fuel) while other testing used commercially available B99 biodiesel (99% methyl soyate, 1% standard diesel fuel). Soybean oil is composed of triglycerides that are reacted with methanol in the presence of a base catalyst to produce monoesters and glycerol. The fatty acid methyl esters (monoesters) and relative abundances comprising methyl soyate are methyl palmitate (C16:0, 10%), methyl stearate (C18:0, 7%), methyl oleate (C18:1, 21%), methyl linolate (C18:2, 52%), and methyl linolenate (C18:3, 10%). Some properties of B100 methyl soyate are seen in Table 2.3.

Table 2.3 – Physical and Chemical Properties of Methyl Soyate

Color	Lt Yellow
Biogenic	Yes
PAH Presence	No
Pour Point, °C	-1
Kinematic Viscosity (cst) 100°C	3.8
Average Boiling Point, °C	>350
Flash Point, °C	>260

MS, seen in Figure 2.9, is a light yellow oil as well, though its color intensity can vary with age. Pure MS (B100) contains no detectable amounts of polyaromatic

hydrocarbons, and has no inherent concerns about carcinogenic constituents in its makeup. The analysis of polyaromatic hydrocarbon content for MS may be found in Table 2.4.^[5]

Methyl soyate was observed to contain five different fatty acid methyl ester chains in its GC-FID chromatogram, shown in Figure 2.10, which are methyl palmitate, methyl stearate, methyl oleate, methyl linoleate, and methyl linolenate, with C17:0 added as an internal standard since it is not naturally occurring. Structures of these fatty acid



Figure 2.9 – Photograph of Methyl Soyate

Table 2.4 – Polyaromatic Hydrocarbon Content of Neat and Aerosolized Methyl Soyate

Compound Name	Neat	350°C	400°C	450°C	500°C	550°C	600°C	650°C
Naphthalene (ppm)	<0.1	<0.1	<0.1	<0.1	<0.1	<0.1	<0.1	<0.1
Acenaphthylene	<0.1	<0.1	<0.1	<0.1	<0.1	<0.1	<0.1	<0.1
Phenanthrene	<0.1	<0.1	<0.1	<0.1	<0.1	1	6	6
2-Methyl Naphthalene	<0.1	<0.1	<0.1	<0.1	<0.1	<0.1	<0.1	<0.1
2,6-Dimethyl Naphthalene	<0.1	<0.1	<0.1	<0.1	<0.1	<0.1	<0.1	<0.1
3,6-Dimethyl Phenanthrene	<0.05	<0.05	<0.05	<0.05	<0.05	<0.05	<0.05	<0.05
Total (ppm)	0	0	0	0	0	1	6	6

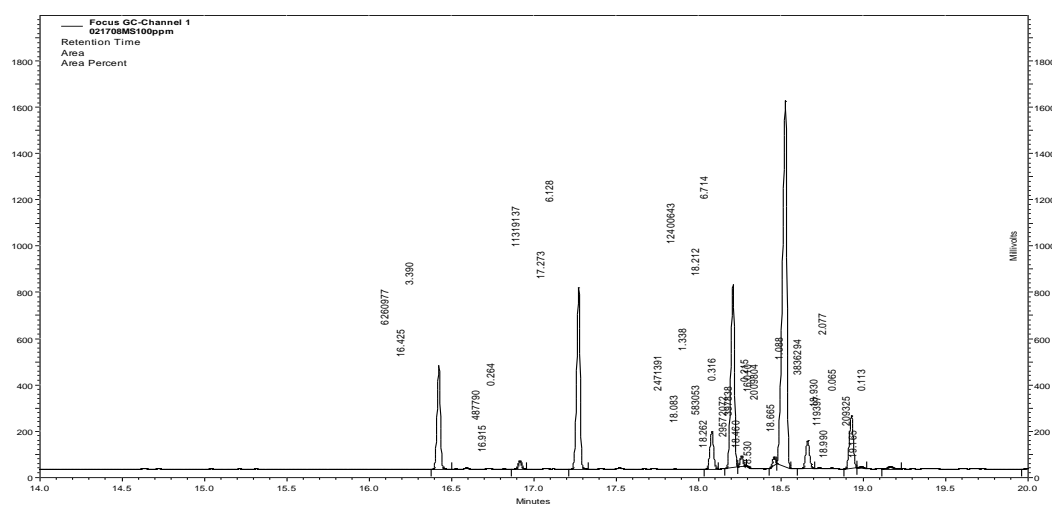


Figure 2.10 – GC-FID Chromatogram of Methyl Soyate with Labeled Internal Standard Peaks

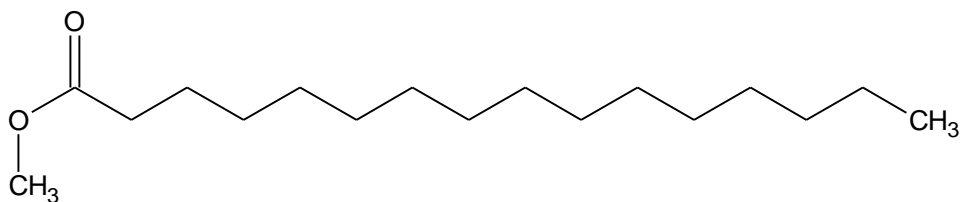
methyl esters are shown in Figure 2.11. Conditions of the GC-FID experiment are as

follows: 1 μ L injection volume in splitless injection mode using a 15m x 0.25mm i.d.

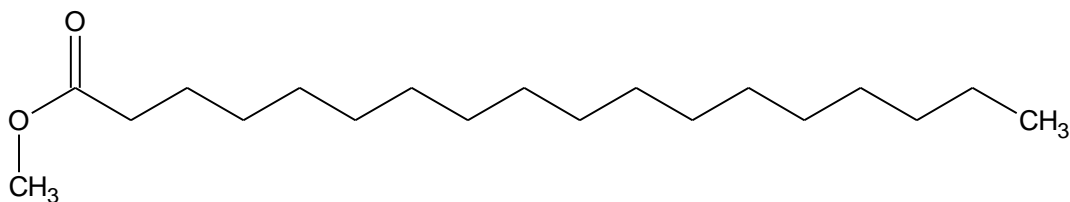
J&W Scientific DB-225 cyanopropyl siloxane column with a 0.15 μ m film thickness.

The column oven was initially held at 50 $^{\circ}$ C for one minute, then ramped at 10 $^{\circ}$ C/min to

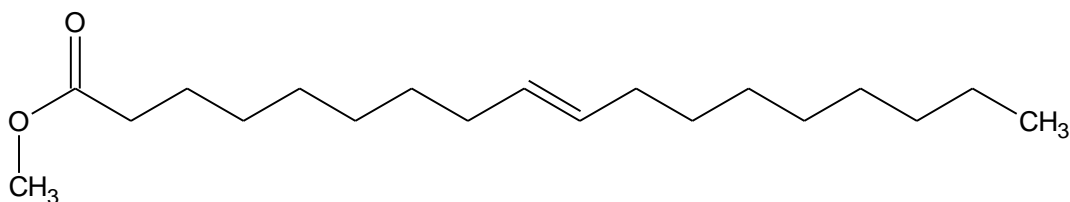
a final temperature of 220 °C then held for 12 minutes. Helium at a flow rate of 1.20 mL/min was used as the carrier gas, and the FID hydrogen flow rate was 25 mL/min.^[9]



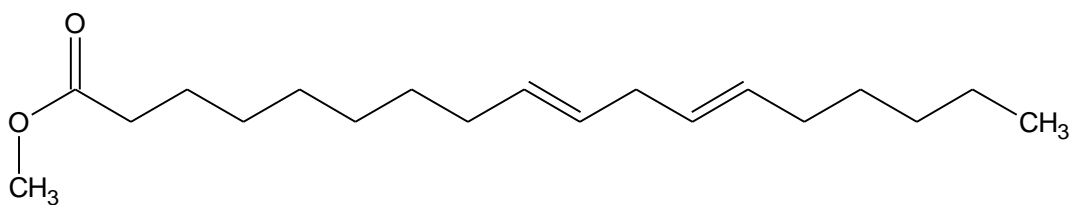
(a) Methyl Palmitate, C16:0



(b) Methyl Stearate, C18:0

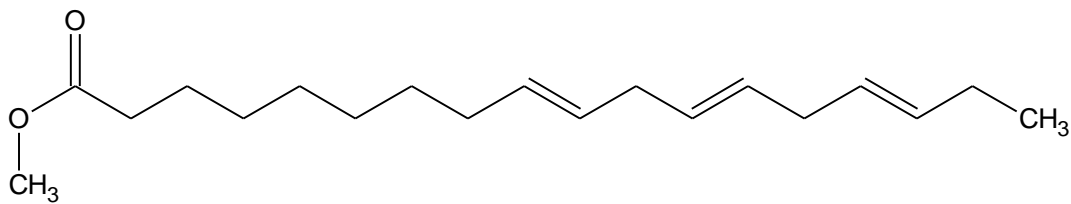


(c) Methyl Oleate, C18:1



(d) Methyl Linolate, C18:2

Figure 2.11 – Structures of the Fatty Acid Methyl Esters in Methyl Soyate



(e) Methyl Linolenate, C18:3

Figure 2.11 – Structures of the Fatty Acid Methyl Esters in Methyl Soyate (cont.)

3. DEVELOPMENT OF HIGH-OUTPUT MAN-PORTABLE GENERATOR

3.1. SWB-11 TURBOJET ENGINE

In recent decades the U.S. Army has used a continuous obscurant aerosol generator known as the M56 Coyote. This generator uses a large turbine engine as the source of heat and air flow to allow vaporization and condensation of obscurant oils to form aerosols. With this idea in mind, the decision was made to test a small scale turbojet engine as used in model radio controlled aircraft since this would again have high heat and air flow output in a small size and weight. The first small scale turbojet engine tested for application in a high-output man-portable obscurant generator was the SWB-11 “Mamba” built by SWB Turbines of Neenah, Wisconsin.

3.1.1. Specifications. The SWB-11 “Mamba” was the smallest turbojet engine tested in this research project, shown in Figure 3.1. It had a diameter of 8.89 cm (3.5 in), length of 18.42 cm (7.25 in) and a weight of 0.86 kg (1.9 lb). Exhaust gas temperatures could reach 650°C (1202°F) and the engine had a thrust rating of 5.17 kg (11.4 lb) at full speed. The number of revolutions ranged from 60,000 at an idle to 150,000 at full throttle. At full RPM the engine consumed 0.20 L/min of commercial Jet-A fuel mixed with 5% turbine lubricating oil. However, the engine had to be started using a small propane cylinder and then switched over to Jet-A after reaching a minimum RPM.



Figure 3.1 – Photograph of SWB-11 Turbojet Engine

3.1.2. Design. A test platform was constructed of angle iron so the SWB-11 turbine could be mounted approximately four feet above the ground level to facilitate access to all parts of the system for optimization. The engine was bolted onto an aluminum pan so if any fluids leaked they would be less likely to spread onto other components mounted below, including the control modules and fuel systems. Below the engine tray was a shelf onto which the electronic engine control module, fuel pumps, throttle control and battery could be mounted. Below this was a second shelf which had the engine fuel tank and a fuel filter attached.

The obscurant system consisted of a sprayer nozzle mounted directly behind the engine exhaust, connected to a metal Jerry Can fitted with a 12 V DC fuel pump

submerged in obscurant fluid. The pump was powered by a 12 V DC battery placed on the ground beside the Jerry Can, and controlled by a three-position toggle switch that could turn the fuel pump on and off and also control a small air compressor mounted on the Jerry Can lid to purge the obscurant oil lines at the end of a test. Other models of turbojet engines were also tested on identical stands.

3.1.3. Obscurant Oil Sprayer Nozzle Designs. A few designs were tested in pursuing the ideal configuration of obscurant oil nozzles for the miniature turbojet based generator. The first configuration pumped the obscurant oil into a 0.3175 cm (0.125 in) diameter stainless steel tube that entered the engine exhaust area perpendicular to the exhaust flow, then bent 90° to face upstream in the center of the exhaust flow to spray a stream of oil toward the heat of the exhaust. It was predicted that the exhaust flow would impact this flow and help to generate a spray that would be heated, vaporized and pushed downstream to condense in the cooler air farther away from the engine. However, this design was unsuccessful even after some modifications because the tube became heated past the combustion and decomposition points and clogged the sprayer nozzle tubing with combustion and decomposition products.

The second design tested used 0.635 cm (0.25 in) copper tubing and Swagelok T-fittings to construct a ring larger than the diameter of the exhaust with three short segments of brass fittings with restricted openings directing oil into the exhaust from the sides. The problem with this design was that the oil spraying into the exhaust was too localized for the amount of heat available and therefore could not be adequately vaporized. Diameter restrictions were placed on the sprayer outlets but these were also unsuccessful for the same reason. This design was also tested by coupling it with an air

flow to encourage spray formation, but this was also unsuccessful. The oil needed to be sprayed as a finer mist rather than the larger streams that resulted from these nozzle designs.

The third sprayer nozzle design used on the SWB-11 had a single piece of 0.48 cm (0.1875 in) diameter stainless steel tubing bent to a 6.35 cm (2.5 in) diameter circle, then had the engine-facing side of the tubing thinned in approximately ten locations using a hack saw blade which was punctured by tapping the tip of a hobby knife blade through the thinned metal walls. This gave approximately ten sprayer ports facing 45° upstream into the engine exhaust, providing a finer spray with oil distributed over a greater area of the exhaust to maximize the heat to oil volume ratio while keeping the oil sprayer nozzles away from the heat to prevent in-tube combustion and decomposition product formation and thus prevent blockages. This sprayer nozzle provided finer sprays of obscurant oil in multiple locations within the exhaust stream so there was greater accessibility to the heat for purposes of vaporizing the oil, creating less unvaporized oil “dribble” on the aluminum pan the engine is mounted on.

With the success of the third sprayer design, a fourth design was made closely representing the third but with a few size changes to be used with the higher thrust engines. The tubing was upgraded to a larger 0.635 cm (0.25 in) diameter stainless steel tube bent into a 8.89 cm (3.5 in) diameter circle, with approximately 16 sprayer ports punched into thinned locations around the ring. This design was used on the larger engines tested after being found successful on the SWB-11, and in some cases testing was performed using two sprayer nozzles placed next to each other both facing upstream. Figure 3.2 shows the SWB-25 engine with both the second and fourth types of sprayer

nozzles mounted behind the engine (engine at left, followed by fourth type and second type nozzles).



Figure 3.2 – Photograph of Obscurant Oil Sprayer Nozzle Ring Designs

3.1.4. Performance. The SWB-11 “Mamba” engine had some difficulties in creating a successful obscurant generator. It used propane to start the engine to a required minimum RPM before the ECM switched over to the Jet-A fuel source. However, the propane proved difficult in that the small commercial propane cylinders had to be shaken during this portion of the startup procedure to get enough flow to the engine. The engine seldom started properly and would misfire frequently. The necessity for multiple fuel sources also posed a problem since the final design needed to minimize

the numbers of required fluids. Additionally, the engine was small enough that it could not vaporize enough oil to be truly comparable to the M56 generator and was difficult to use with manual engine controls.

Despite the drawbacks, the SWB-11 was successful at aerosolizing both fog oil and methyl soyate in a continuous manner, as shown in Figure 3.3. Both oils produced thick white plumes that persisted for satisfactory durations.



Figure 3.3 – Photograph of Obscurant Plume Generated in Urban Environment

3.2. SWB-25 TURBOJET ENGINE

The SWB-11 proved successful at aerosolizing obscurant oils, yet was undersized to provide a unit directly comparable to the output of the M56 and required both jet fuel and liquid propane. A second turbine was chosen for testing, which was the larger SWB-25 turbojet engine produced by SWB Turbines of Neenah, Wisconsin, shown in Figure 3.4.



Figure 3.4 – Photograph of SWB-25 Turbojet Engine

3.2.1. Specifications. The SWB-25 was the largest turbojet engine tested in this research. It measured 11.43cm (4.5 in) diameter with a length of 29.99 cm (10.625 in)

and a weight of 1.68 kg (3.7 lb). It could range from 35,000 RPM at idle to 120,000 RPM at full throttle. At full throttle, the thrust was rated at 11.34 kg (25 lb) and consumed 0.30 L/min (10.1 oz/min) of Jet-A mixed with 5% turbine lubricating oil. The exhaust gas temperature was rated at 696°C (1284°F). This engine was designed to start and run on Jet-A, eliminating the need for propane and thus provided a beneficial reduction in the number of fluids required to operate the system, but the engine retained the manual throttle controls.

3.2.2. Design. An identical angle iron test platform was used for testing the SWB-25 as for the SWB-11, and all component locations remained the same with the exception of eliminating the propane canister. However, the SWB-25 had a higher heat output volume so the obscurant oil sprayer nozzle tubing was rebuilt in a larger diameter tubing and conformed to the specifications previously mentioned for the fourth nozzle design. With the larger engine and larger obscurant oil nozzles the upper aluminum tray on the engine stand was enlarged, and the engine mounting brackets were strengthened to withstand the additional forces.

3.2.3. Performance. The SWB-25 performed well at producing a thick white plume of obscurant aerosol from both fog oil and methyl soyate, but the overall engine system had drawbacks. The system, like the SWB-11, was still difficult to start despite being started on Jet-A over propane, and the manual throttle controls contributed to this difficulty. If the fuel controls were changed too quickly or slowly during startup the engine would not fire properly by the requirements pre-programmed into the ECU. However, the engine gave promising results to continue along this path of research.

3.3. JetCat P80 TURBOJET ENGINE

The third choice of turbojet engine was a 9.53 kg (21 lb) thrust engine (at full RPM) produced by JetCat USA of Van Nuys, California, given the designation of the JetCat P80, shown in Figure 3.5. It offered a relatively high thrust output for its size, as well as digital engine controls, Jet-A starts, and a strong company reputation built around radio controlled applications.



Figure 3.5 – Photograph of JetCat P80 Turbojet Engine

3.3.1. Specifications. The JetCat P80 engine was 30.48 cm long (12 in), had a diameter of 11.18 cm (4.4 in) and a weight of 1.32 kg (2.9 lb) including the electric starter motor mounted in the center of the air intake. The engine idled at 30,000 RPM and had a maximum of 123,000 RPM at which it reached its thrust rating of 9.53 kg (21 lb) while consuming 0.27 L/min (9.0 oz/min) of Jet-A mixed with 5% turbine lubricating oil. The exhaust gas temperatures ranged between 580°C and 690°C.

3.3.2. Design. This engine again used the fourth obscurant oil sprayer nozzle design, and in some applications used two of these nozzles mounted in tandem to double the amount of obscurant oil entering the exhaust. Another angle iron stand was built and lightly modified to house one of these engines, and two prototype modular man-portable generator units were also constructed based on these engines.

3.3.3. Performance. The JetCat P80 engine was by far the superior choice of engine for this research work. It offered an easy to use, lightweight, cheaper alternative to the SWB-25 with a much heightened sense of reliability. The engine featured a digital pushbutton control unit which offered simplified startups, and decreased the chance of operator error. Additionally, these engines were already designed for radio controlled aircraft applications and were therefore easily modified to be radio controllable as an obscurant aerosol generation device. The aerosol plumes were again thick, fluffy white plumes of fog, and the engine had sufficient heat and air flow to aerosolize around a gallon of fog oil or methyl soyate per minute. Another improvement with this brand was a close working relationship with JetCat representatives who were willing to entertain our questions and problems during the development stages. The JetCat P80 was so notably

reliable that four P80 engines were purchased for this research, and all four were still performing reliably at the conclusion of the project.

3.4 CONSTRUCTION OF MODULAR GENERATOR UNIT

3.4.1 Target Parameters. There were several goals associated with this research project. Prototype continuous obscurant aerosol generators had to be constructed which were lightweight enough for one to two soldiers to carry the device when fully loaded with fuel and obscurant oil. Additionally, the unit had to physically be small, approximately the size of two face-to-face “Jerry Cans” so they could fit onto any existing and future military vehicle. They also needed to provide an obscurant output comparable to that of the M56 Coyote generator, and have a runtime of around ten minutes. It was also preferable for the unit to be radio controllable and minimize the number of fluids required for usage. Ideally, the generator’s engine should be able to operate on the same substance as produces the obscurant aerosol.

3.4.2 Design and Construction. The prototype design stage began by organizing its layout similarly to that of the angle iron test stands. The engine needed to be on top to keep the heat and obscurant oil away from whatever the prototype was resting on, whether it be ground or vehicle bodies. There is sufficient heat to cause ignition of dry vegetation and damage to paints. It also allows the engine to receive maximum air flow, while keeping it above ground level enough to minimize the likelihood of debris reaching the air intake. To further reduce the risk of debris intake,

filters surrounded by stainless steel woven screens were installed around the sides, intake end of the engine, and above the engine to allow maximum air flow while reducing the chance of solid particulate entry. Additionally, aluminum louvers were installed over all air openings to reduce the risk of rain water from entering the system when mounted onto a vehicle. A section of steel pipe is installed behind the engine to direct the heated aerosolized oil and exhaust away from the engine compartment to reduce both the heat buildup within the engine area and the fire risk of accumulated unaerosolized oil within the engine area. The top of the box was hinged to allow for access to the engine and obscurant oil sprayer nozzles.

The middle compartment of the prototype generator box was meant to house the electronic control modules and the fuel pump systems. This is lightweight and a poor choice to put on the lowest level, since the box had a sideways force acting upon it with the engine running. Two access doors, located on either side of the box, provided the means to reach the batteries and control units.

The lowest level of the smokescreen generator prototype has a detachable fuel and obscurant oil tank. This was made detachable so it could be more readily cleaned and maintained since there are pump assemblies located within the sections of the tank. A larger portion of the tank is dedicated to obscurant oil storage, and the smaller side for Jet-A. Additionally, both portions of the tank have flameproof filler necks and vented caps.

Most of the prototype unit was constructed of 0.3175 cm (0.125 in) thick aluminum, chosen for its strength and density. Some smaller portions were manufactured from

different thicknesses of metal, as in the case of the louvers which were pressed from thin aluminum but readily available in the local area.

The original design had hinged handles on the front and back end of the obscurant generator unit, but this became problematic due to the engine exhaust being directly above a handle so the design was modified to have rugged handles integrated into the sides of the box. These handles ran the full length of either side and could serve to move the generator when running while keeping the operators safely at the sides. These newer handles were also designed to swing down into recessions made in the sides of the box for storage so there would be no additional length and could thereby preserve a smaller storage and vehicle mounting footprint.

3.4.3 Subassemblies. Many subassemblies had to be custom built for this unit to operate, from the fuel and obscurant oil pickups to the radio control switches and power converter unit. The fuel tank had float style fluid level indicators installed on each side, modified slightly to show when the tank was full and slightly above empty. These gauges could be viewed through an electronics bay side access panel, and were the last addition to the prototype systems. Some engine fuel system components are shown on the fuel tank in Figure 3.6.

Other fuel tank subassemblies included the fuel pickup and the obscurant oil pickups. The fuel pump is external from the fuel tank, but there is a bulkhead penetrator installed into the top of the fuel tank for the inlet of the pickup line. A more complex subassembly was made for the obscurant oil pumps, as shown in Figure 3.7. The obscurant oil sprayer system utilized two standard 12V automotive fuel pumps rated at



Figure 3.6 – Photograph of Engine Fuel Components Mounted on Prototype Generator Fuel Tank

100 psi each. These pumps were mounted within the obscurant oil tank, and had to be mounted near the bottom for proper function. A detachable plate was manufactured to bolt onto an opening in the top of the tank to allow access to the pumps for maintenance, seen in Figure 3.8. The plate had an aluminum arm welded perpendicularly onto the end of which the two fuel pumps were mounted. On the opposite side of the plate, the pickup lines were routed through T-fittings. One side of the T was the outlet to the obscurant oil sprayer nozzles, and the other side of the T connected to a small air compressor which could be engaged to purge the obscurant oil sprayer lines and sprayer nozzles after a run to prevent line blockage and oil leaks.

In order to use the generator as a radio controlled unit, custom radio controlled switches had to be manufactured to control the obscurant oil pumps and purge

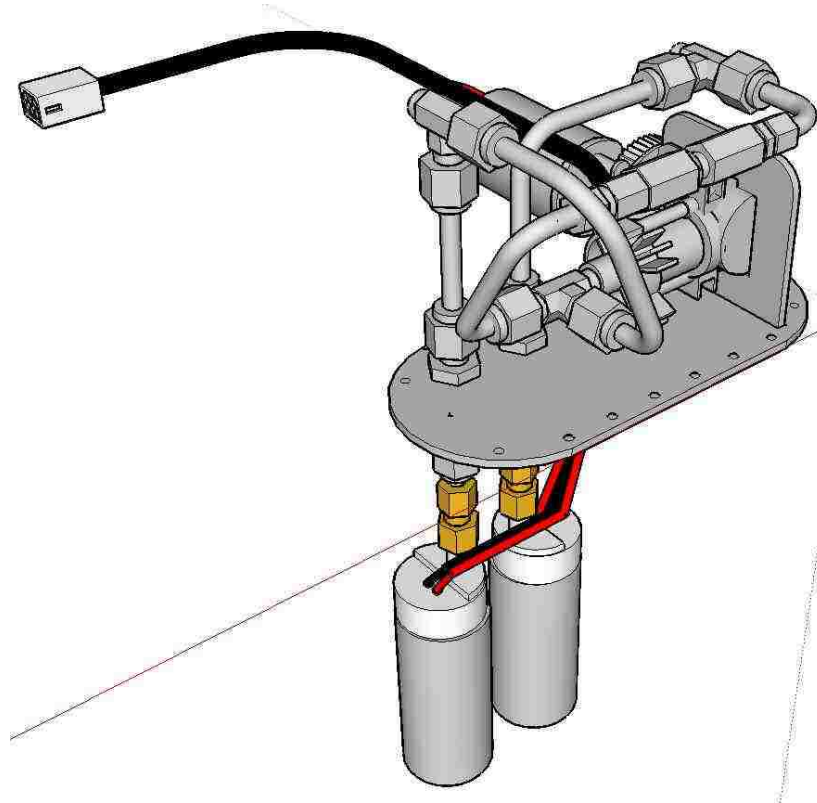


Figure 3.7 – 3D Rendering of Dual Obscurant Sprayer Pump Assembly for Prototype Generator

compressors, shown in Figure 3.9. These switches were based on standard radio control aircraft servo motors housed in a block of Teflon. Each servo motor had a round disc attached which was fit with a metal contact plate connected to the main power source. On the Teflon block were four other metal contact points, two for each servo motor, to provide switch contacts for routing the power to the obscurant oil pumps or to the line purge air compressors. Each servo could rotate clockwise or counterclockwise independently from each other to connect the main power contact to a function contact. One set of wires bundled into a connector led to a connector on the obscurant oil pumps. Another pair of wires led from the servo discs to a connector for the main power. Two other sets of wires led to connectors which connected to the radio control receiver



Figure 3.8 – Photograph of Early Design of Prototype Generator Fuel Tank with Single Nozzle Obscurant Sprayer Pump Assembly

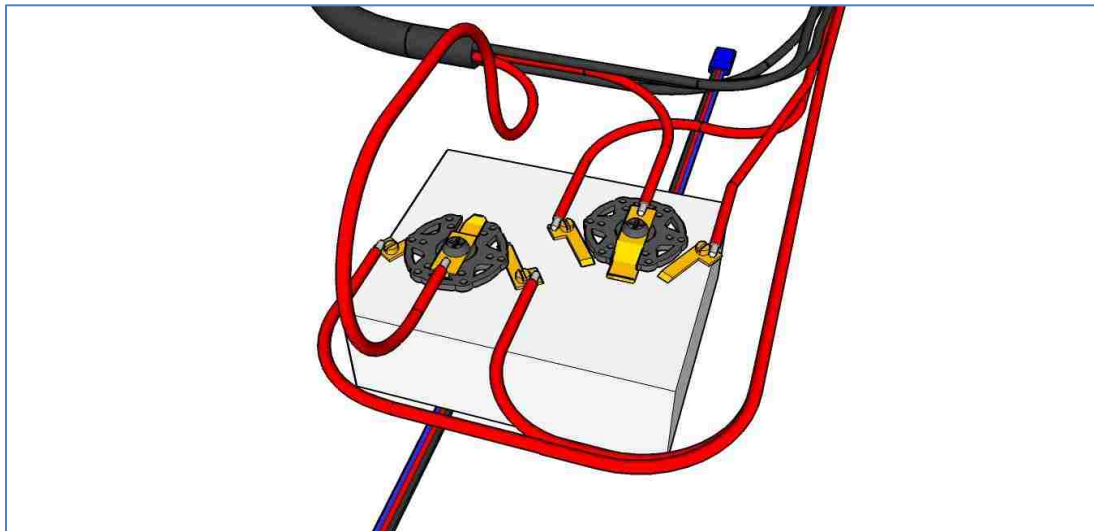


Figure 3.9 – 3D Rendering of Custom Radio Control Switch Assembly for Obscurant Oil Spraying and Line Purging Functions

module on two separate channels so they could be controlled independently by a stick on the radio control transmitter which is normally used in radio control aircraft applications as the aileron and elevator control stick.

Originally the prototype modular generator used three separate batteries. The radio control functions used a rechargeable 4.5 V DC battery pack, the engine used a rechargeable 7.6 V DC battery, and the obscurant oil sprayers used a rechargeable 12 V DC battery. It became problematic to have three different battery voltages to keep charged, and with the potential application on military vehicles which frequently use 24 V DC systems, the choice was made to create a power supply for the modular generator that used 24 V DC as the main input voltage. Two lines ran from the power supply unit for connection to two standard 12 V DC automotive batteries. Within the power supply were a 24 V DC to 8 V DC power converter and a 24 V DC to 5 V DC power converter. One master switch allowed power control to the engine control modules and engine fuel pumps as well as the radio control receivers. The schematic for the power converter unit is shown in Figure 3.10.

3.4.4 Operation of Generator. Although the generator may be controlled manually using tethered controls, the preferred mode of operation is radio control. The two 12 V DC batteries must be connected to the power supply unit, and the radio control transmitter turned on first to avoid erratic behavior of the obscurant oil sprayer nozzle pumps. Then the generator's power supply master switch can be turned on. The three-position switch on the transmitter can be turned to the "run" position, and after a few seconds the throttle lever may be pushed to the top. The generator should undergo its

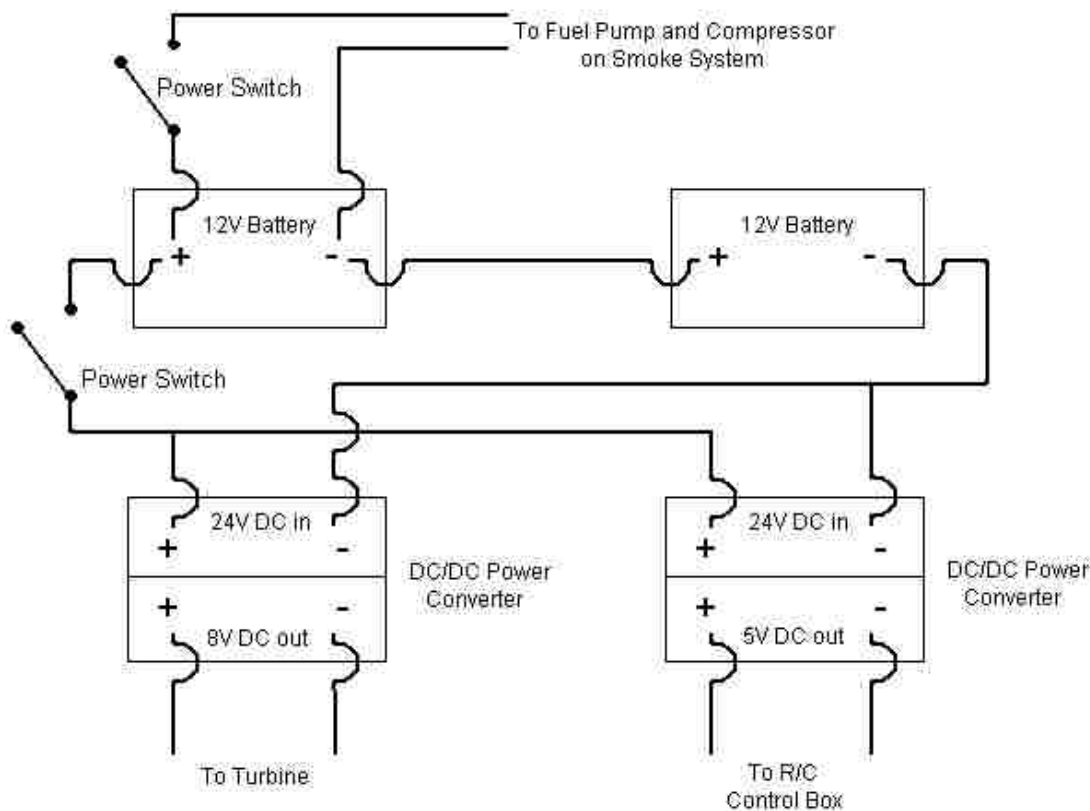


Figure 3.10 – Prototype Generator Onboard Power Converter Schematic

startup procedure, ramp up to a medium RPM, then settle back to its idle RPM. Once settled to an idle the control is transferred to the user. The throttle lever can be brought down to engage its control, then pushed back to the top to take the engine to full RPM. After the engine is running at 100% power the user may use the second control stick to engage one or both obscurant oil sprayers. After done with creating an obscurant plume, the user should engage both line purging air compressors for a few seconds to ensure all obscurant oil is cleared, and then bring the engine back down to an idle RPM. Then the three-position switch can be put on the automatic shutdown setting to complete the engine shutdown steps. Alternately, the three-position switch can be moved to the

immediate shutdown position for a manual override of the normal automated shutdown steps. After the engine is off, the main power switch on the generator power supply should be switched off and the transmitter is switched off. More detailed information can be found in Appendix B. A photograph of the generator in operation is shown in Figure 3.11.

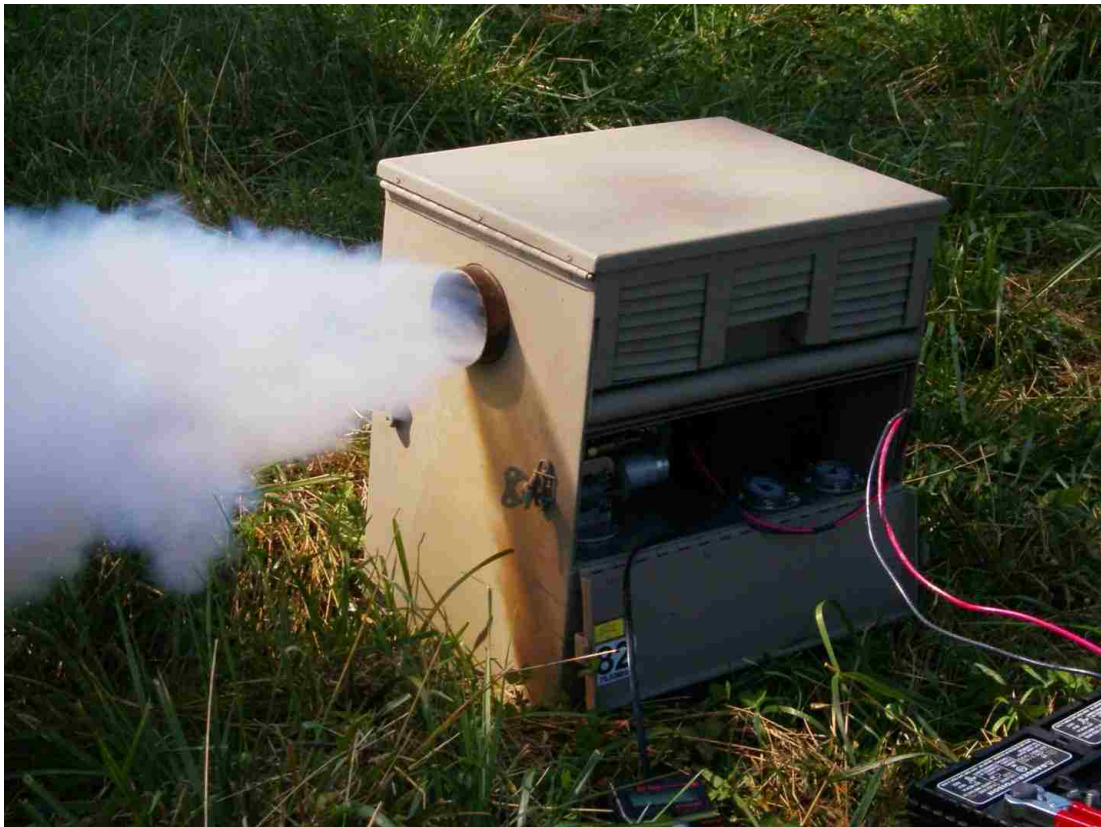


Figure 3.11 – Photograph of Prototype Obscurant Generator In Use

3.4.5 Limitations and Hazards of Operation. There are several safety considerations to remember when using a turbojet-based obscurant generator. One is to be aware of the high temperatures involved. The engine, exhaust tube and exhaust gases

are at high temperatures during and after operation, so users must be cautious not to come into contact with these materials to prevent burn injuries. Additionally, the exhaust gases are at high temperatures so no one should be within 4.6 m (15 ft) directly in line with the exhaust.

There are also hazards associated with the use of a turbojet engine operating at high RPMs. The high stresses on the moving components pose a risk of shrapnel if the engine bearings overheat or if any foreign bodies enter the engine air intake. The engines must be properly lubricated using turbine lubricating oil in the fuel, and proper maintenance schedules must be followed. Air filters and screens to prevent debris from entering the engine should also be used to prevent injury or death.

Another caution is from the exhaust air flow. No one should stand directly behind the exhaust in case anything should happen to be thrown by the force of the exhaust which could cause injury. Additionally, users must also be aware that the modular generator undergoes forces from the engine exhaust which push on the top portion of the unit, so the generator must be positioned on a level surface so it can not tip over.

Flammability of fuel and obscurant oils must also be respected. Any spilled fluids pose a risk of accidental fire and should be cleaned immediately. Related to this, the obscurant oil sprayers should not be engaged unless the engine is operating at a full RPM. The safe operation relies on the full air flow to move the vaporized oil away from the heat source before it undergoes combustion. If the engine is at an idle RPM while the obscurant oil sprayers are engaged there will be a strong likelihood of a dangerous flame exiting the exhaust due to the vaporized oil not leaving the heated region quickly enough.

A limitation of operation was the run time. Due to the onboard fluid capacities, the modular generator produced obscurant with dual nozzles for about three and a half minutes, or single nozzle for about seven minutes using fog oil. Using methyl soyate it operated for about two and a half minutes on dual nozzles or five minutes with a single nozzle. One possibility would be to have an external tank connection on the generator so it could be switched to draw obscurant oil and fuel from external tanks so it could be run indefinitely.

Another limitation was the tendency of methyl soyate to begin polymerizing after long term storage, which could cause blockages of the obscurant oil lines. Methyl soyate also has a tendency to gel at low temperatures, which could inhibit its usage as an obscurant oil and generator fuel source in some environments. This could most likely be prevented with additives or an onboard heating element.

The batteries also lost charge over time and required recharging. Some possibilities for keeping the batteries charged could be onboard solar panels on the top cover, or possibly a thermal recharging system that would use technology placed in the exhaust pipe to recharge the batteries during operation.

The maintenance schedule for the turbojet engines was considered 25 hours of run time. This may not be a long time in terms of military applications, but the relative inexpensiveness of the engines could allow backup units to be stored to simply replace engines as necessary to send back used engines for maintenance. Replacing an engine in this configuration involved removing two fuel lines and two control wire bundles. After that, it was a matter of loosening the mounting bolts.

One additional limitation of the generator was that it had difficulty starting when there was a strong wind moving backwards through the exhaust pipe. The engine had difficulty attaining its required RPMs, and the fuel-air mixture may have also been disturbed.

4. TESTING

4.1. LABORATORY TESTING

4.1.1. Obscurant Oils. Various obscurant oils were tested in the laboratory using a laboratory scale aerosol generator to generate obscurant plumes which were transferred to the obscurant chambers for analysis using the OPCs, light photodiode detectors and other instrumentation all previously described. Suitable biogenic oil candidates for the replacement of fog oil had to have low viscosities so they could be pumped and sprayed, low vapor pressures so the vaporized oil would condense into droplets in ambient air, a low pour point temperature so they could be free-flowing at lower temperatures, minimal (no) toxicity, be renewable with a high degree of biodegradability, and serve dual purposes as an effective obscurant and an engine fuel source.

Candidate oil kinematic viscosities, Table 4.1, and vapor pressures were previously investigated and compared against each other by Dr. Rachadaporn Seemamahannop. Soybean oil and sunflower oil had the more ideal viscosities for obscurant generation, and both of these oils were found to have similar pour points. It was decided to continue testing with soybean oil, specifically methyl soyate, for testing due to its availability as commercial biodiesel fuel since its properties were comparable to fog oil. Additional physical and chemical properties of methyl soyate and fog oil can be found in Section 2.3.1 Fog Oil and 2.3.2 Methyl Soyate.^[5]

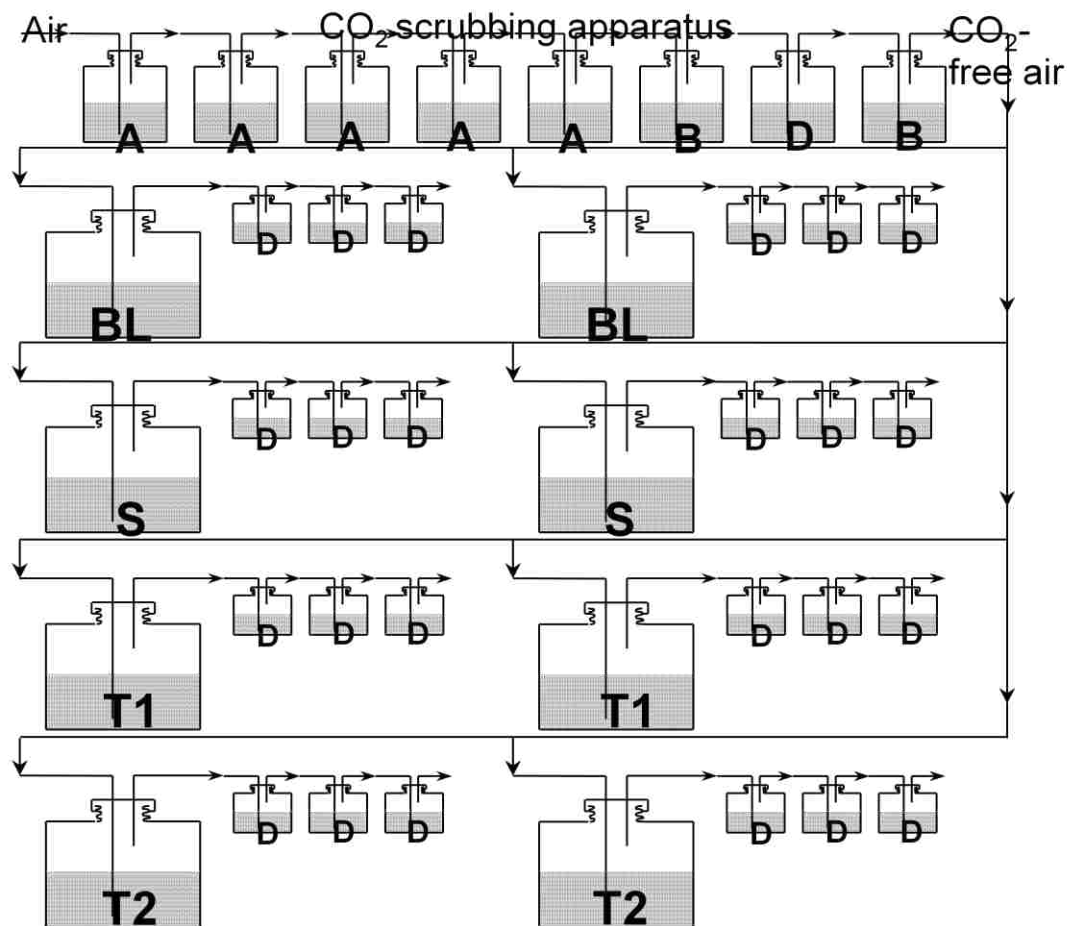
Table 4.1 – Kinematic Viscosities of Biogenic Oils and Comparison with Fog Oil

Fat and Oils	Viscosity of Methyl Ester, 25°C (cSt)	Viscosity of Iso-propyl Ester, 25°C (cSt)
Soybean oil	7.1252	8.4979
Low saturated soybean oil	7.0721	8.3507
High oleic soybean oil	10.5589	10.2637
Palm oil	8.6487	10.4307
Sunflower oil	7.0632	8.7148
Chicken fat	7.3427	18.7391
Canola oil	7.6482	9.5247

Substance	Viscosity, 100°C (cst)
Fog Oil	3.4 - 4.17
Methyl Soyate	3.8

Biodegradation studies were also previously conducted by Shilpa Mathkar and Kanisa Kittiratanapiboon to better assess environmental impacts of using fog oil and methyl soyate in continuous aerosol generation applications. Aquatic biodegradation testing was conducted in accordance with the standard test method ASTM D 5864-95 using the system shown in Figure 4.1, where relative biodegradations are calculated based on the production of carbon dioxide gas when acclimatized soil microbes consume the test samples.^[5]

Test organisms from soil samples were inoculated by suspending 100 g of soil in 1 L of water, followed by 30 minutes of equilibration time. The supernatant was filtered through coarse Whatman #4 filter paper, and the filtrate was continuously aerated. The inoculums were then pre-adapted by exposure to the test substances under the same conditions as used during testing stages, only done prior to actual experimental testing.



A = KOH
 B = empty bottle
 D = 0.0125N Ba(OH)₂
 BL = Blank Inoculums
 S = Standard (canola oil)
 T1 = Fog Oil
 T2 = Methyl Soyate

Figure 4.1 – Layout of Biodegradation Experiment for Aquatic Systems

To achieve this, 100 mL of inoculums were combined with 25 mg Difco vitamin-free casamino acids, 25 mg of yeast extract and 900 mL of test medium. The test medium consisted of 1 mL (NH₄)₂SO₄, MgSO₄·7H₂O, CaCl₂ with 10 mL phosphate buffer and 4

mL FeCl₂, then diluted to a total volume of 1 L with distilled water. The inoculum mixture was then added to the test substance (4.7 mg fog oil, approximately equal to 4 mg Carbon/L) and aerated with a stirrer for a 14 day incubation period, with 9.4 mg of FO added on day 7 and 10.4 mg MS added on day 11. The culture was then homogenized and re-filtered through glass wool, resulting approximately 1.5×10^7 cfu/mL inoculum for use in the actual test.^[5]

30 mL of pre-adapted test inoculum were then added to 2470 mL distilled water with 3 mL (NH₄)₂SO₄, MgSO₄·7H₂O, CaCl₂, 30 mL phosphate buffer, and 12 mL FeCl₂ in a 4 L flask. This was then aerated with carbon dioxide-free air for 24 hours, then the pH was measured and adjusted to 7 ± 0.5 . Samples were made with this test medium solution by blending with a sonicated mixture of 5 mL water with 40 mg Carbon/3L from fog oil (47 mg), methyl soyate (52 mg), or canola oil as the standard reference in respective bottles. This was added to 445 mL water to give a final volume of 3000 mL and connected to three carbon dioxide absorber bottles each containing 100 mL of 0.0125 N Ba(OH)₂. The tests were run at 20-25 °C in darkness to prevent any photodegradation, and carbon dioxide-free air was bubbled through the test solution at a rate of 100 mL/min in each flask. Any carbon dioxide liberated as a result of biodegradation was collected in the three bottles of barium hydroxide and analyzed.^[5]

Carbon dioxide content generated as a result of biodegradation was quantitated by removing the CO₂ absorber bottle nearest the test flask for titration with hydrochloric acid and phenolphthalein indicator every day for the first ten days, then every fifth day until reaching a plateau on the evolution of CO₂. After either 28 days or until the CO₂ reached a plateau, the solution pH was measured and then followed by the addition of 1 mL

concentrated HCl to decompose inorganic carbonate and to release any trapped carbon dioxide. This was allowed to aerate overnight to collect any released carbon dioxide for quantitation.^[5]

The results, Figure 4.2, show that methyl soyate degrades more rapidly than the canola oil standard reference material in aqueous environments, and that fog oil degrades more slowly than the reference oil in aqueous conditions. Diesel I, Diesel II and the military equivalent JP-8 were also tested for comparison, and showed very poor rates of degradation, though some of this may be attributed to their higher vapor pressures and volatility which caused the loss of some test substance from the solution.^[5]

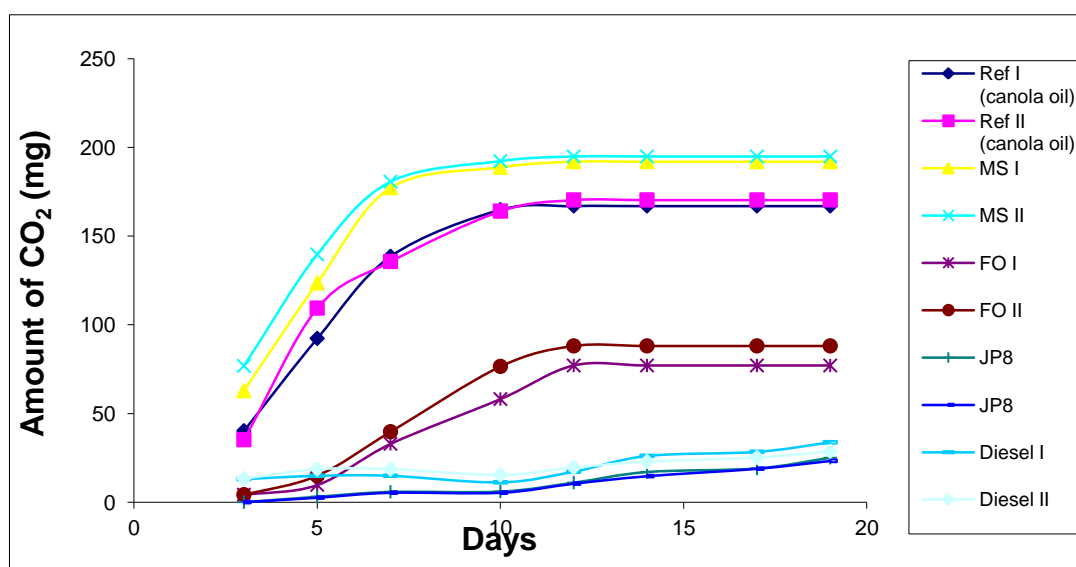


Figure 4.2 – Rates of Oil Biodegradation in Aqueous Systems

Additional biodegradation tests were conducted at the same time to compare the relative rates of decomposition in terrestrial environments. Testing used a 7 cm i.d.

aluminum tube and a slicing apparatus, and was divided into two sets of experiments. Set I applied oil to the surface of a soil sample, and Set II placed the oil in a layer in the middle of the soil sample.^[5]

Set I experiments were packed with 500 g of dry sieved yard soil and 13.5 g of test oil was sprayed on the surface. This oil was allowed to migrate downward through the soil, kept at 25 °C, provided with daily aliquots of 10 mL water to simulate rainfall, and monitored for three months. At 2 weeks, 4 weeks and 12 weeks soil slices were collected for analysis. The details of this analysis can be seen in Table 4.2. Methyl soyate and fog oil had both spread throughout the soil during each time period, but methyl soyate consistently was found to have degraded significantly. After only 2 weeks there was 2 g of recovered MS in the soil sample out of a 13.5 g starting weight. Fog oil still had a recoverable mass of 11.85 g after all 12 weeks of testing, showing the immense difference in biodegradation when oil is applied to the surface of a soil sample, as is the case in obscurant aerosol deposition in the environment.^[5]

Set II experiments put 225 g of dry sieved yard soil on the bottom layer, followed by 50 g of soil mixed with 13.5 g of sample oil in the middle, and topped with another 225 g of dry sieved yard soil. Temperature, water addition, and sampling times were the same as for Set I. However, in this set MS did not degrade as completely as in Set I over the 12 week period, and FO degraded better than in Set I, but MS still decomposed more completely than FO, as shown in Table 4.3.^[5]

Table 4.2 – Recovered Oil after Biodegradation in Terrestrial Systems, Oil on Top

Methyl Soyate Added: 13.5g				Fog Oil Added: 13.5g		
2 weeks				2 weeks		
Section	Slice Wt (g)	Oil Wt (g)	Slice Thickness (mm)	Section	Slice Wt (g)	Oil Wt (g)
1	8.4	0.11	2	1	15.5	3.10
2	10.2	0.13	2	2	11.8	2.25
3	18.2	0.19	3	3	18.7	2.67
4	27.5	0.23	5	4	28	2.73
5	29.6	0.17	5	5	25.8	2.30
6	55.7	0.35	10	6	49.2	
7	63.6	0.82	10	7	55.4	
Total	213.2	2.00		Total	204.4	13.05
4 Weeks				4 Weeks		
Section	Slice Wt (g)	Oil Wt (g)	Slice Thickness (mm)	Section	Slice Wt (g)	Oil Wt (g)
1	12.8	0.15	2	1	5.4	0.64
2	9.2	0.13	2	2	9.0	1.40
3	16.5	0.21	3	3	17.8	1.52
4	30.2	0.28	5	4	24.9	2.24
5	26.7	0.19	5	5	28.2	1.34
6	50.9	0.40	10	6	48.0	2.33
7	54.5	0.49	10	7	47.7	2.17
Total	200.8	1.85		Total	181.0	11.64
12 Weeks				12 Weeks		
Section	Slice Wt (g)	Oil Wt (g)	Slice Thickness (mm)	Section	Slice Wt (g)	Oil Wt (g)
1	11.3	0.10	2	1	10.1	1.30
2	13.2	0.14	2	2	11.4	1.52
3	16.2	0.11	3	3	18.1	1.60
4	31.2	0.15	5	4	33.0	2.03
5	33.2	0.15	5	5	29.5	1.40
6	66.5	0.24	10	6	54.2	2.10
7	58.4	0.27	10	7	55.1	1.90
Total	230.0	1.16		Total	211.4	11.85

Table 4.3 - Recovered Oil after Biodegradation in Terrestrial Systems, Oil in Middle

Methyl Soyate Added: 13.5g				Fog Oil Added: 13.5g		
2 weeks				2 weeks		
Section	Slice Wt (g)	Oil Wt (g)	Slice Thickness (mm)	Section	Slice Wt (g)	Oil Wt (g)
1	19.1	0.31	2	1	18.7	0.16
2	28.5	0.16	2	2	27.8	0.16
3	24.8	0.32	3	3	23.9	0.65
4	21.6	0.21	2.5	4	22.1	2.85
5	15.1	0.42	2.5	5	18.9	3.61
6	20.5	0.24	2	6	15.8	2.52
7	17.9	0.24	2	7	18.8	1.45
8	21.8	0.25	3	8	20.6	1.07
Total	169.3	2.15		Total	166.6	12.47
4 Weeks				4 Weeks		
Section	Slice Wt (g)	Oil Wt (g)	Slice Thickness (mm)	Section	Slice Wt (g)	Oil Wt (g)
1	20.8	0.33	2	1	19.6	0.12
2	25.6	0.19	2	2	24.8	0.13
3	19.9	0.28	3	3	20.6	0.52
4	22.6	0.19	2.5	4	21.9	2.75
5	16.5	0.37	2.5	5	19.3	3.31
6	22.4	0.23	2	6	18.9	2.31
7	17.5	0.22	2	7	20.5	1.25
8	20.9	0.21	3	8	21.7	1.02
Total	166.2	2.02		Total	167.3	11.41
12 Weeks				12 Weeks		
Section	Slice Wt (g)	Oil Wt (g)	Slice Thickness (mm)	Section	Slice Wt (g)	Oil Wt (g)
1	19.8	0.19	2	1	20.6	0.11
2	26.8	0.17	2	2	25.9	0.14
3	17.3	0.26	3	3	19.6	0.46
4	21.9	0.20	2.5	4	22.1	2.82
5	13.9	0.21	2.5	5	19.6	3.20
6	21.6	0.17	2	6	17.9	2.25
7	22.6	0.15	2	7	22.9	1.10
8	23.2	0.23	3	8	24.6	0.85
Total	167.1	1.58		Total	173.2	10.93

With relative biodegradation established, another study was the evaluation of mutagenicity by exposing different strains of *Salmonella typhimurium* to the obscurant oils. This modified Ames test uses *Salmonella* strains that have a point mutation in their genes which requires the presence of histidine in minimal glucose medium for the strains to grow. The presence of any mutagenic substances can reverse the mutation, allowing strains to grow freely when no histidine is present. Therefore, the data analysis relied on the numbers of strains counted in a sample, and any remarkable increase in counts after exposure to test substances indicate a mutagenic substance. Samples were exposed to neat oils as well as condensates of aerosolized oils that had gone through the tubular furnace generator. Tables 4.4 and 4.5 illustrate that no significant differences were seen, which indicated that neither fog oil nor methyl soyate were mutagenic.^[5]

Similar testing previously conducted and reported investigated the toxicity of these oils and condensates of their aerosols. The results showed that aerosols of fog oil were particularly lethal to bacterial cultures and methyl soyate was mostly toxic to strains of *Salmonella typhimurium*, *Klebsiella pneumonia*, *Escherichia coli* 25922,

Table 4.4 – Mutagenicity Tests on Neat Obscurant Oils

Samples	TA97	TA98	TA100
Control	120 colonies	19 colonies	100 colonies
Fog oil	135 colonies	30 colonies	140 colonies
Methyl soyate	127 colonies	24 colonies	135 colonies

Table 4.5 – Mutagenicity Tests on Obscurant Oil Condensates

Strain	Control	350°C	450°C	550°C
TA97	130 colonies	105 colonies	120 colonies	115 colonies
TA98	25 colonies	30 colonies	20 colonies	20 colonies
TA100	125 colonies	140 colonies	145 colonies	140 colonies

Pseudomonas aeruginosa (fog oil only, methyl soyate still showed some colonies), *Enterobacter cloacae*, *Serratia marcescens*, TA97, TA98, and TA100 after 2 minutes of aerosol introduction and 48 hours of incubation time at a temperature of 37 °C. Exposure of Kim-wipes, paper and agar plates to the aerosols of these aerosols produced a lasting toxic effect which rendered them unfit for bacterial growth. However, these same aerosols have been found nontoxic to laboratory test mice and rats, suggesting a potential for use as a decontaminant.^[5]

With methyl soyate chosen as the lead candidate to replace fog oil, testing progressed to evaluate its performance as an obscurant aerosol fluid under various experimental conditions. Obscurant plumes generated in the laboratory scale tubular furnace-based generator were generated through a range of furnace temperatures to evaluate whether any significant differences were observed in particle size distributions and number densities as well as in the transmittance of visible light. Fog oil was tested at 450 °C and 500 °C on multiple trials, and the average results for each temperature were calculated. The results are shown in Figures 4.3, 4.4, 4.5 and 4.6.

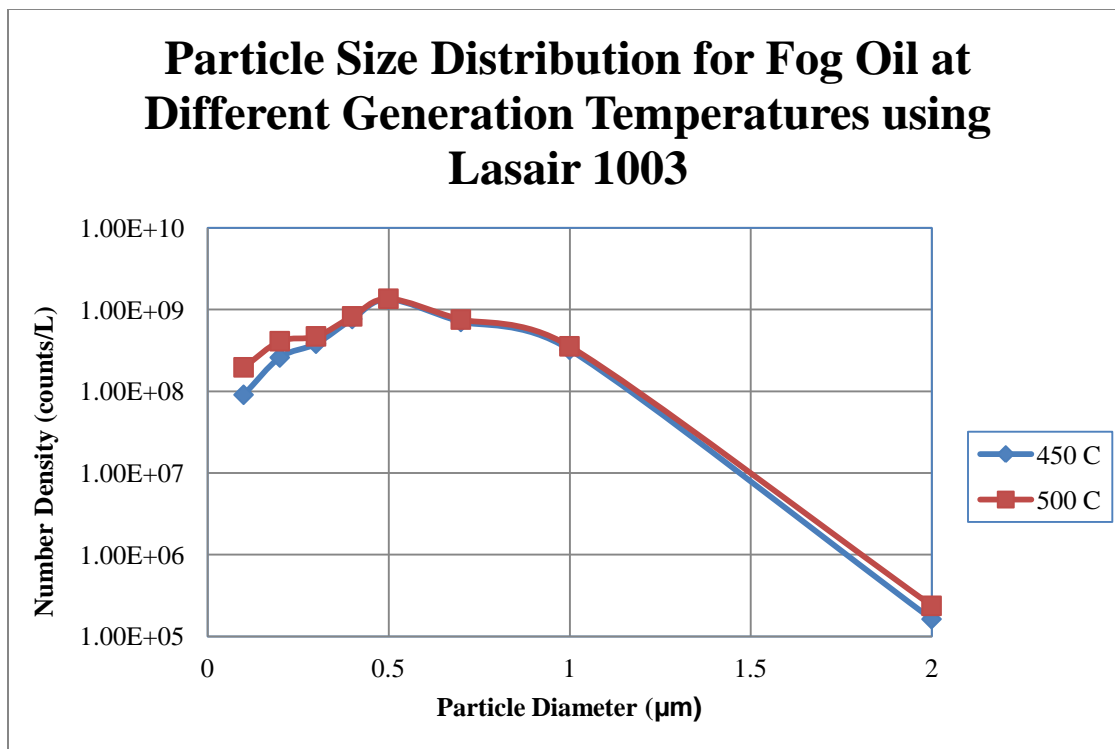


Figure 4.3 – Particle Size Distribution for Fog Oil at Different Generation Temperatures Obtained using Lasair OPC

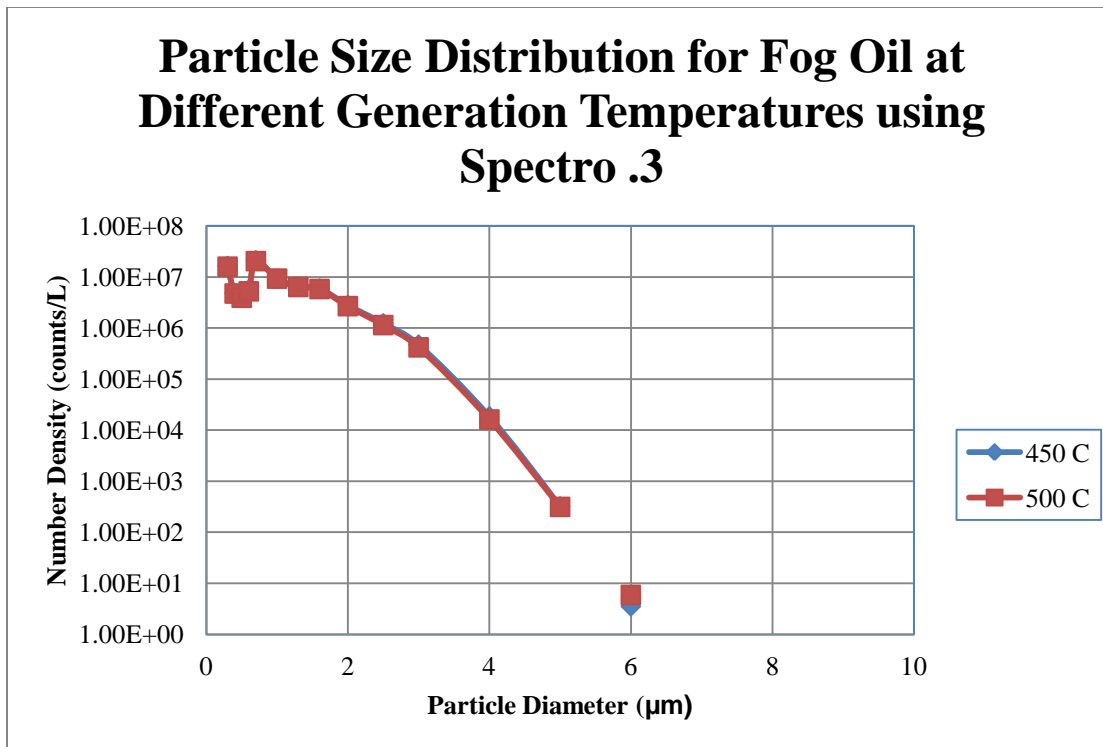


Figure 4.4 – Particle Size Distribution for Fog Oil at Different Generation Temperatures Obtained using Spectro OPC

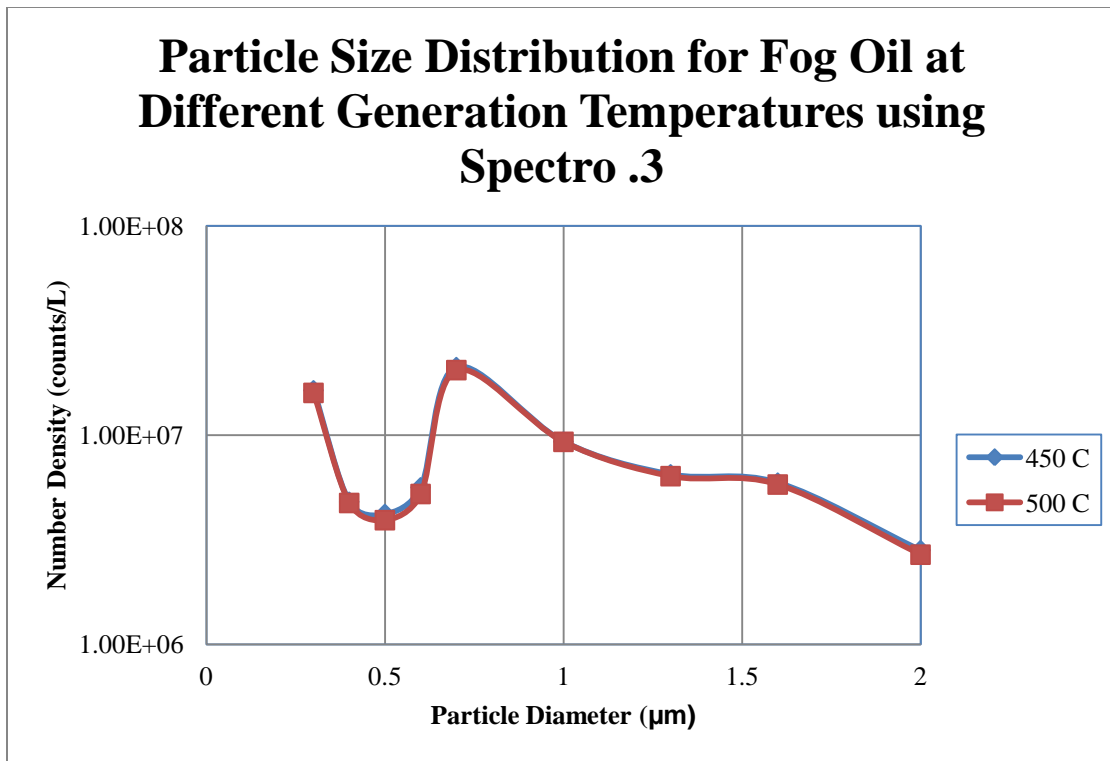


Figure 4.5 - Particle Size Distribution for Fog Oil at Different Generation Temperatures Obtained using Spectro OPC, Lower Size Ranges

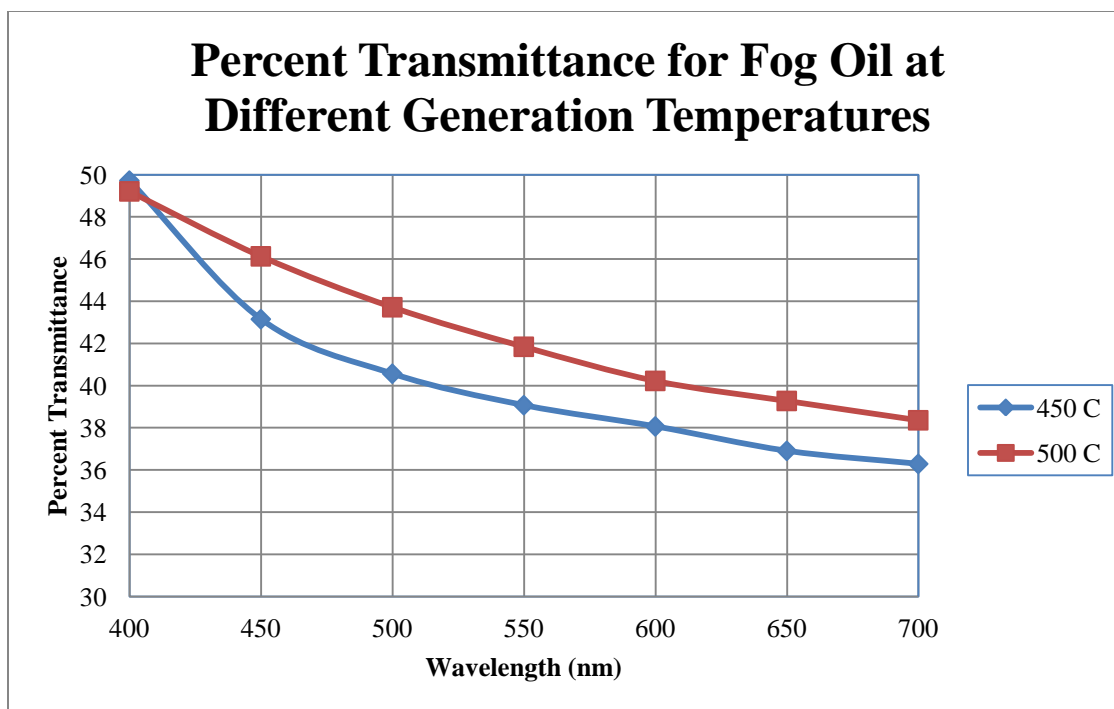


Figure 4.6 – Percent Transmittance of Visible Radiation through Fog Oil at Different Generation Temperatures

Slight differences were observed in the Lasair OPC particle size distribution data in that there appeared to be slightly fewer particles centered around $0.5\ \mu\text{m}$ than for the smaller and larger wavelengths in terms of relative numbers for the $500\ ^\circ\text{C}$ runs. However, in terms of particle counts this difference was not considered large. The particle size distribution data from the Spectro OPC had negligible differences between the data collected for the different generation temperatures, as seen in the overall counts as well as the enlarged portion of data for the lower diameter ranges. In regards to the percent transmittance of visible wavelengths, there was a slight increase of about 2 percent transmittance at higher generation temperatures for wavelengths of $0.45\ \mu\text{m}$ ($450\ \text{nm}$) through $0.7\ \mu\text{m}$ ($700\ \text{nm}$), which can correlate to the slight relative decrease in

number densities around the 0.5 μm particle diameters in the Lasair OPC data. A photograph showing the attenuation of visible light in the testing chamber is shown in Figure 4.7.

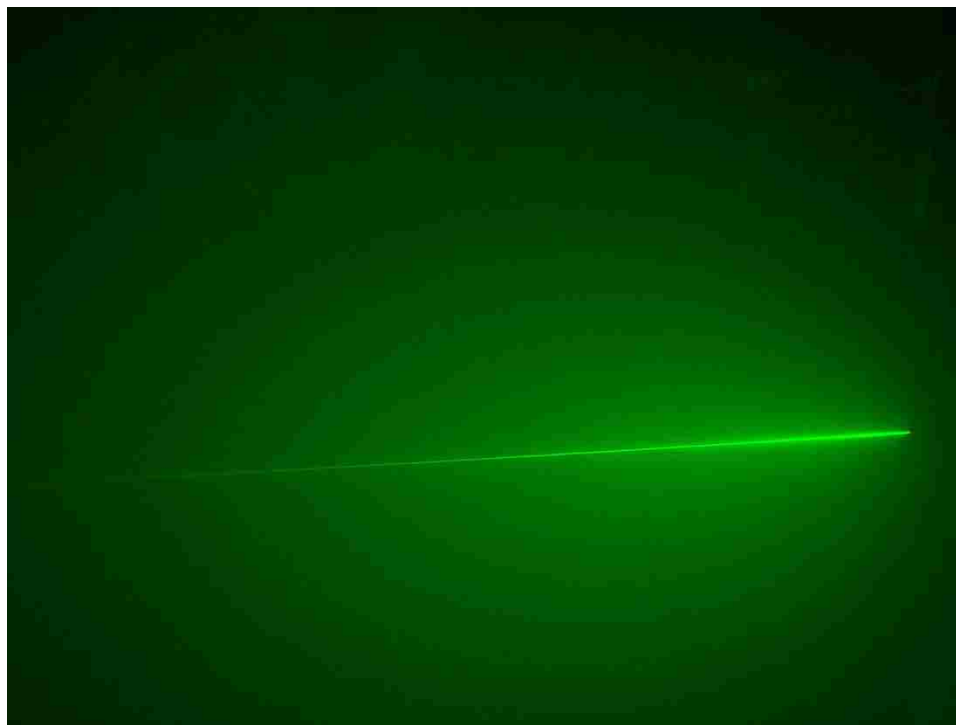


Figure 4.7 – Photograph of Visible Wavelength Laser Attenuation in Climate-Controlled Aerosol Testing Chamber

Identical testing was conducted on methyl soyate at 450 °C and 500 °C. Several trials were conducted at each temperature, shown in Figures 4.8, 4.9, 4.10 and 4.11, and the results averaged.

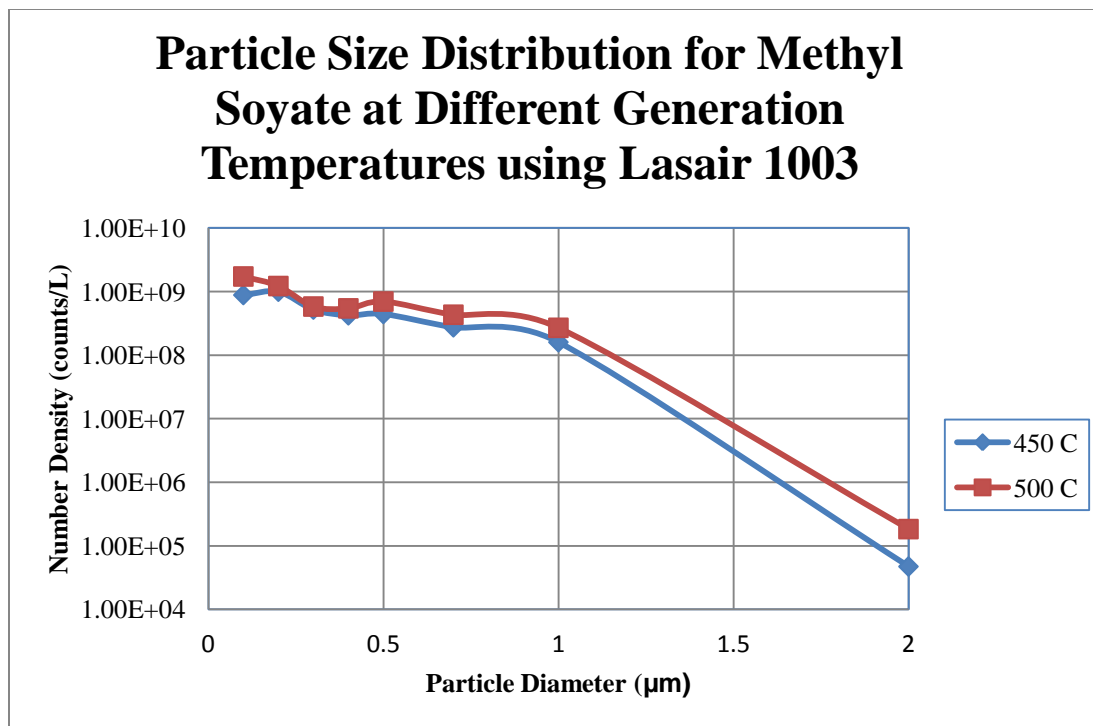


Figure 4.8 - Particle Size Distribution for Methyl Soyate at Different Generation Temperatures Obtained using Lasair OPC

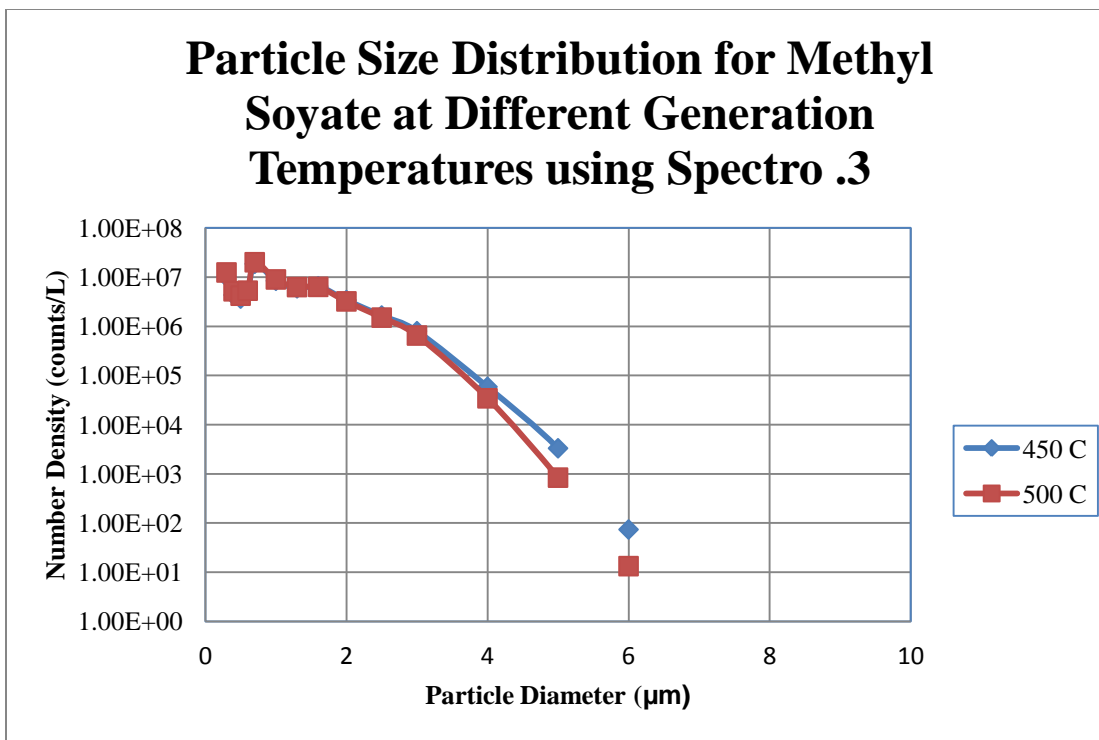


Figure 4.9 - Particle Size Distribution for Methyl Soyate at Different Generation Temperatures Obtained using Spectro OPC

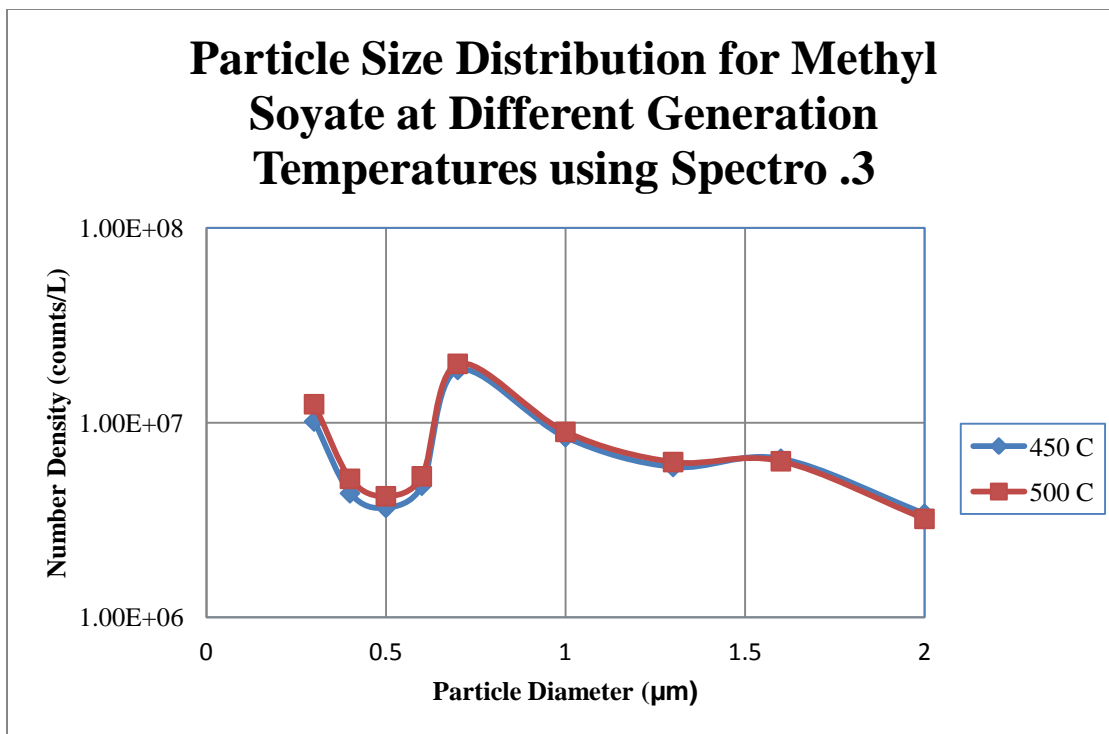


Figure 4.10 - Particle Size Distribution for Methyl Soyate at Different Generation Temperatures Obtained using Spectro OPC, Lower Size Ranges

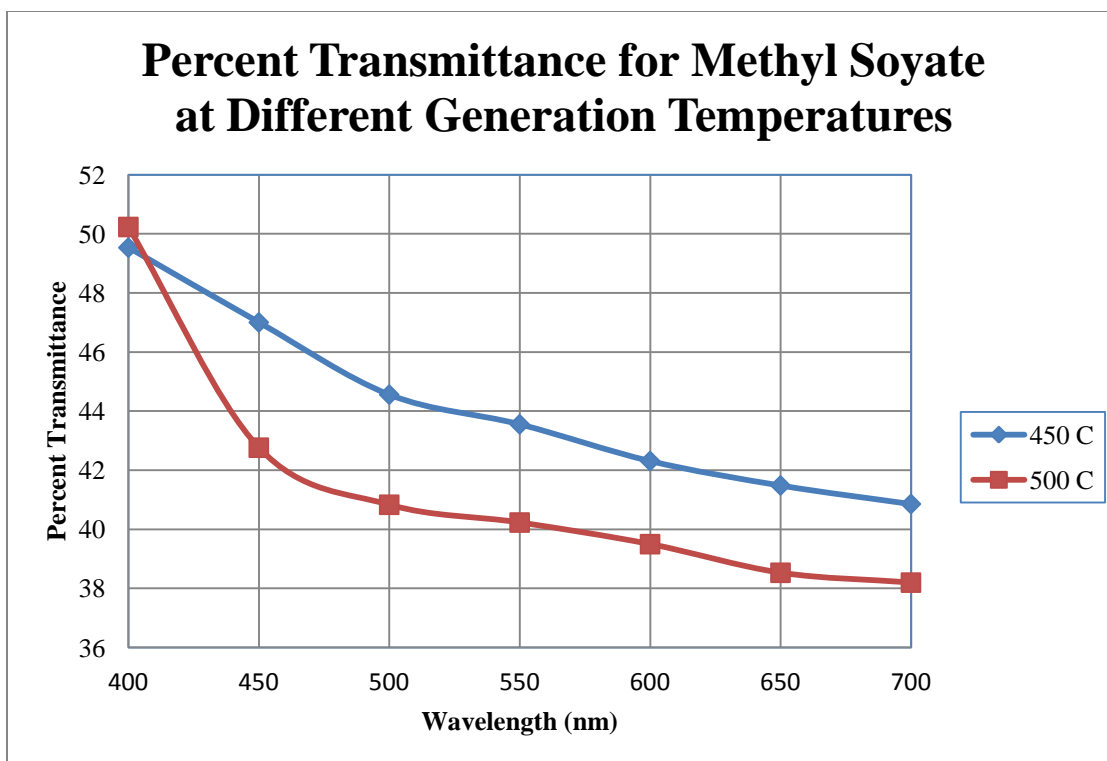


Figure 4.11 – Percent Transmittance of Visible Radiation through Methyl Soyate at Different Generation Temperatures

The Lasair data suggested that at elevated temperatures, there may be a slight relative decrease in the number of particles around 0.3 μm diameters as compared to slightly smaller and larger particles, whereas for Fog Oil the difference was observed around 0.5 μm diameters. The particle size distribution data from the Spectro OPC indicate very slight differences in particle size distributions between generation temperatures for lower particle diameters at the smaller particle diameters, as seen in the enlarged chart, and also indicated that there were fewer particles at higher diameters as the generation temperature was increased as seen in the full range chart. The light transmittance data reflected that methyl soyate performs oppositely from fog oil, with lower percent transmittance at higher generation temperatures for most visible

wavelengths and a slightly higher percent transmittance at 400 nm wavelengths of visible light.

The particle size distribution data was also be compiled into one chart for both generation temperature tests of both oils. From the Lasair data methyl soyate appeared to have more particles at the very small diameter ranges from 0.1 μm to 0.3 μm than fog oil, and fewer particles in the 0.4 μm to 1.0 μm range. However, the Spectro OPC data does not show any significant differences between the types of oils at the lower particle diameter ranges, and some increasing difference at sizes above 1.5 μm where methyl soyate appeared to have higher counts per liter of sampled air. Data for aerosols formed at different generation temperatures is found in Figures 4.12, 4.13 and 4.14.

One set of testing was used to investigate the particle size distributions and number densities for fog oil when generated under constant conditions and exposed to different ambient environmental temperatures. In this case, the fog oil was injected into the tube furnace generator at a rate of 0.5 mL/min. Once introduced it was exposed to 400°C heat and a 5 L/min air flow for volatilization and aerosolization. The obscurant was introduced into the chamber for 3 minutes continuously, then the chamber was sealed for another 7 minutes of analysis giving a total data collection period of ten minutes. The test was run with a chamber internal ambient air temperature of 10°C, 22°C and 45°C. The data is found below in Figure 4.15. There is no significant distinction between the aerosols exposed to this range of ambient air temperatures. The highest particle counts is observed at 0.5 μm particle diameters, with a successively decreasing relative number of particles when looking at lower and higher diameters. The least number of particles is observed when looking at the 2.0 μm particle diameter range.

In this testing, particle sizes around 0.5 μm are beneficial due to the Mie scattering theory of light, in which light is most scattered when its wavelength is approximately equal to the diameter of the scattering body (the airborne aerosol particles). The region around 0.5 μm corresponds to the visible region of the electromagnetic radiation spectrum.

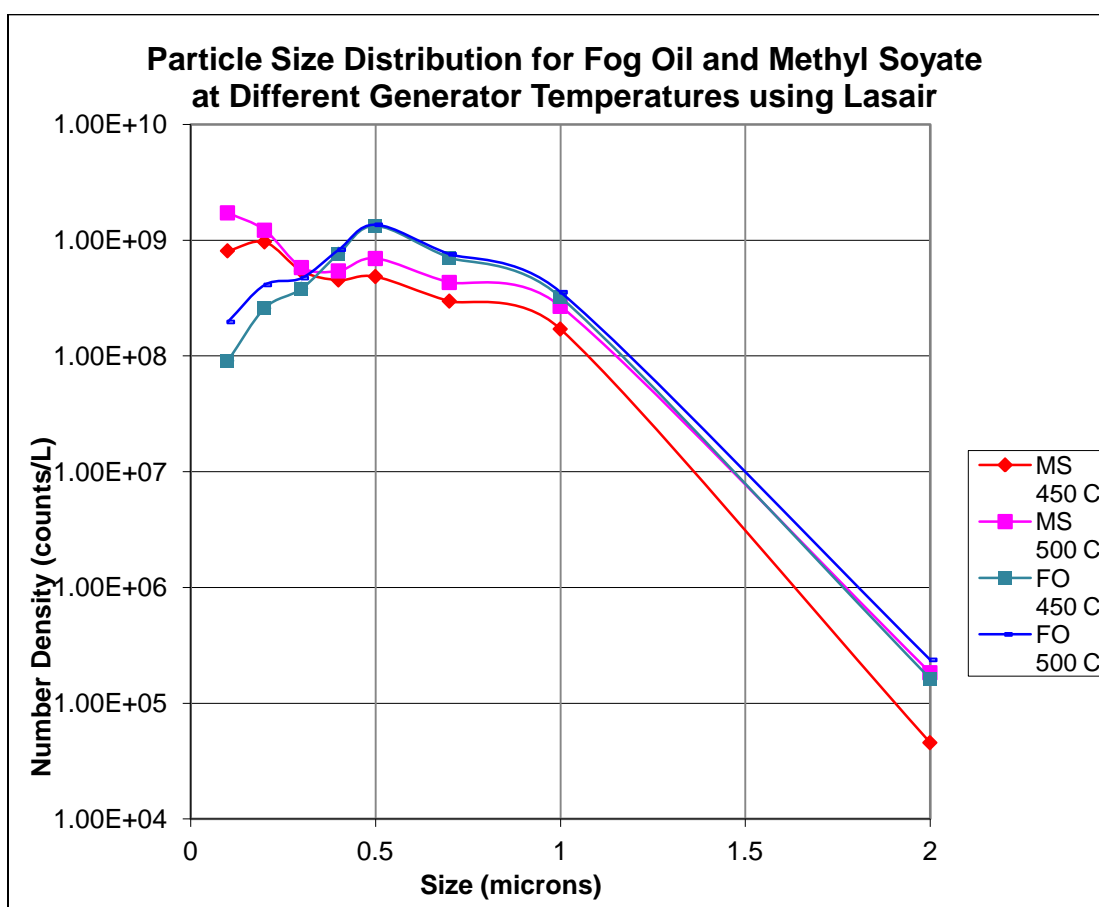


Figure 4.12 – Comparison of Particle Size Distribution Data for Methyl Soyate and Fog Oil at Different Generation Temperatures Obtained using Lasair OPC

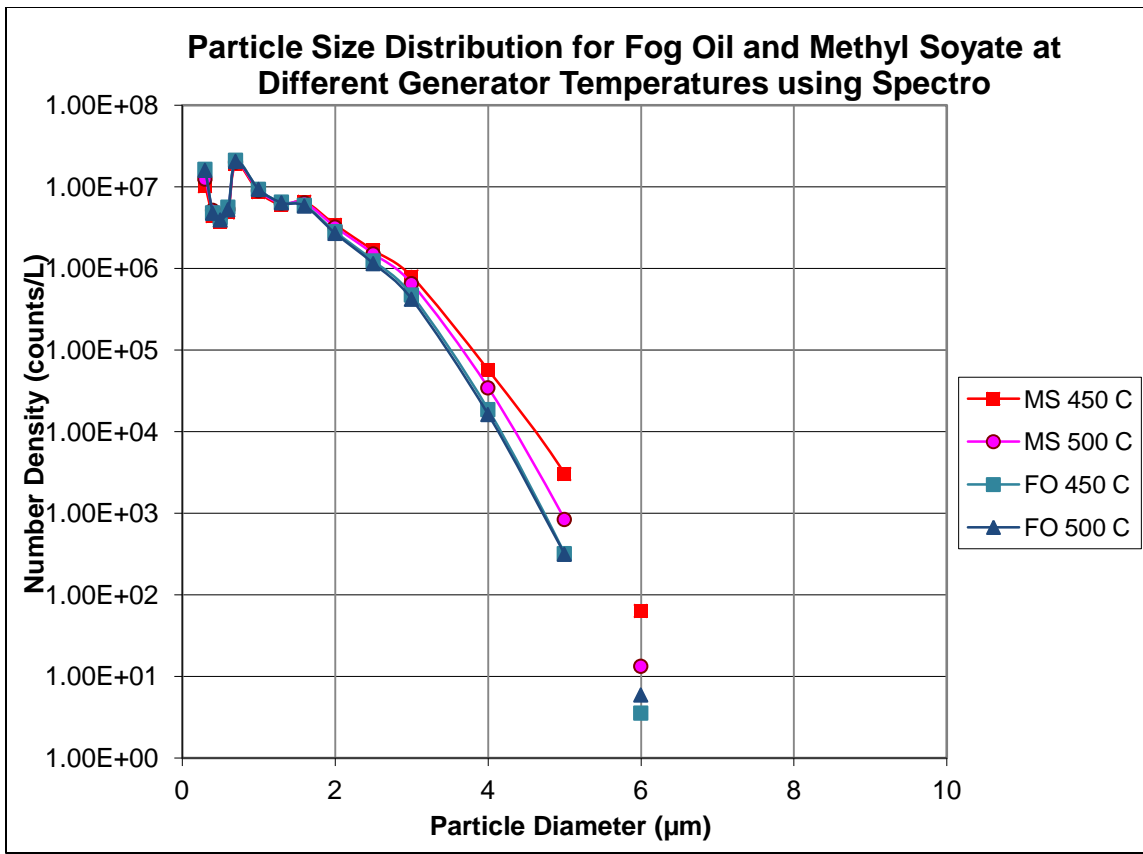


Figure 4.13 - Comparison of Particle Size Distribution Data for Methyl Soyate and Fog Oil at Different Generation Temperatures Obtained using Spectro OPC

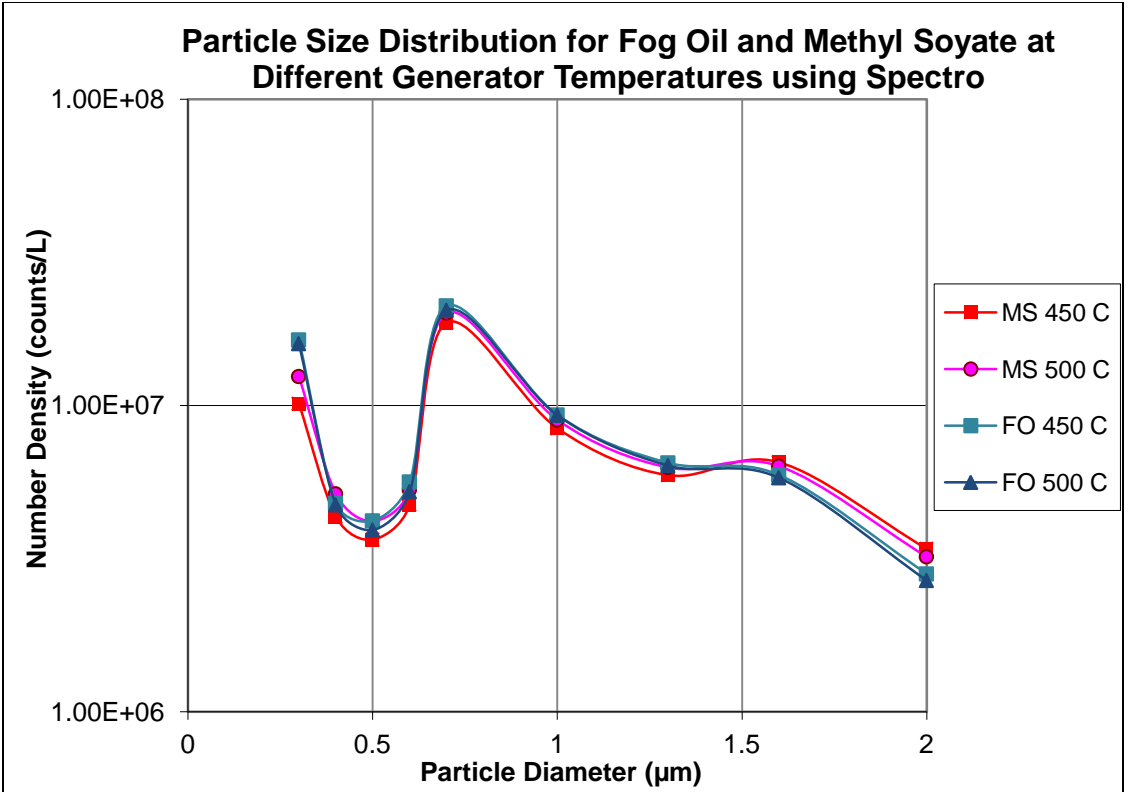


Figure 4.14 - Comparison of Particle Size Distribution Data for Methyl Soyate and Fog Oil at Different Generation Temperatures Obtained using Lasair OPC, Lower Size Ranges

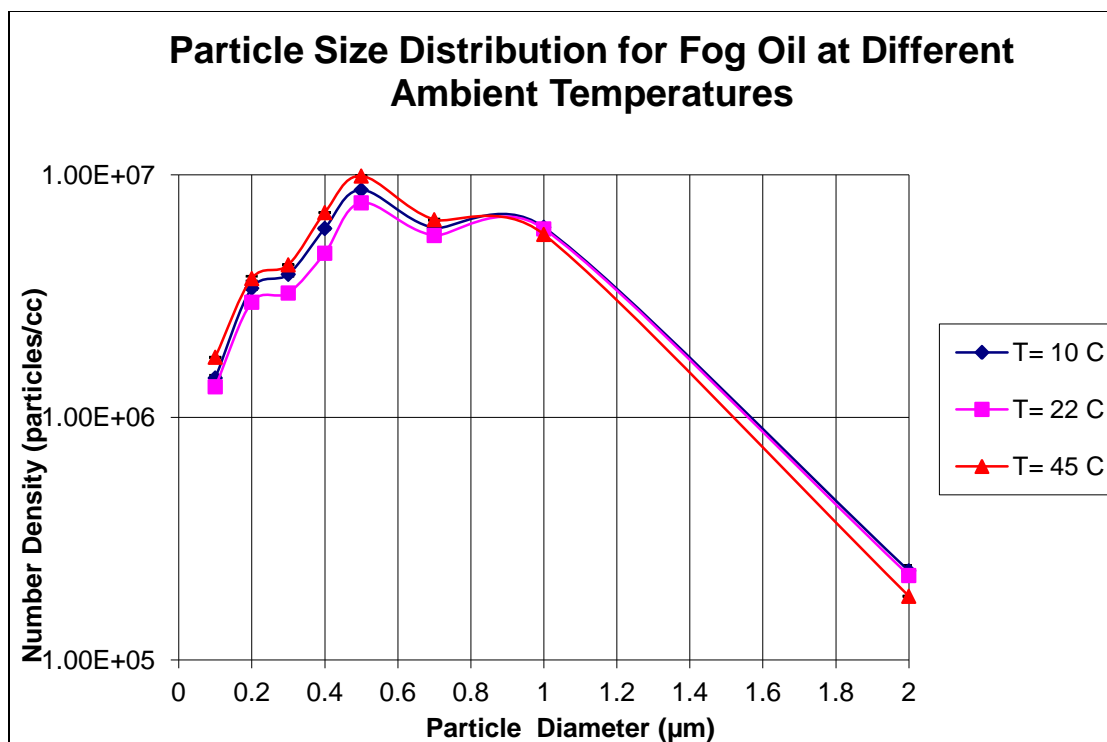


Figure 4.15 – Particle Size Distribution for Fog Oil at Different Ambient Temperatures

It may also be observed that methyl soyate gives similar particle counts at the different particle diameters for 10 °C and 22 °C, but the counts appeared to vary in distribution at 45 °C, shown in Figure 4.16. This observation of differences could have resulted from errors in obscurant generation or data collection procedures. Since the overall numbers of particles are lower with a higher number of smaller diameter particles for the 45 °C data, it is possible that the larger sized particles saw decreases from insufficient air mixing within the chamber.

Comparing between the fog oil and methyl soyate data sets, it was observed that the methyl soyate series has an overall higher number of counts. It is possible that the oil pumps moved methyl soyate more effectively than fog oil and resulted in more methyl

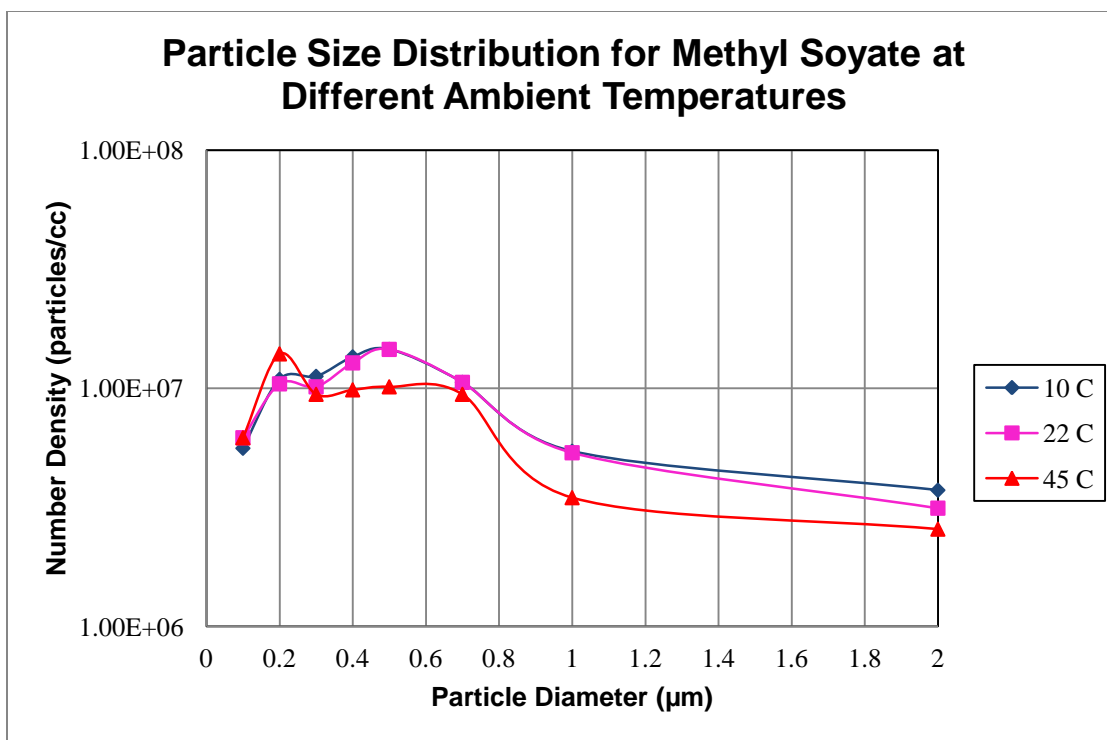


Figure 4.16 - Particle Size Distribution for Methyl Soyate at Different Ambient Temperatures

soyate oil entering the generator. It can also be noted that the general maximum numbers of particles is slightly shifted to a different particle diameter. Fog oil saw the highest particle counts between 0.4 µm and 1.0 µm. Methyl soyate saw the highest particle counts between 0.3 µm and 0.7 µm. Due to this slight shift in maximum counts in the particle size distribution, methyl soyate may attenuate visible wavelengths slightly more effectively than fog oil. Despite these differences, both fog oil and methyl soyate are generally stable and effective at scattering visible wavelengths when exposed to ambient temperatures ranging from 10 °C to 45 °C.

Another set of testing, Figure 4.17, investigated whether the addition of polymers such as polystyrene dissolved in methyl soyate could provide a nucleation site during the

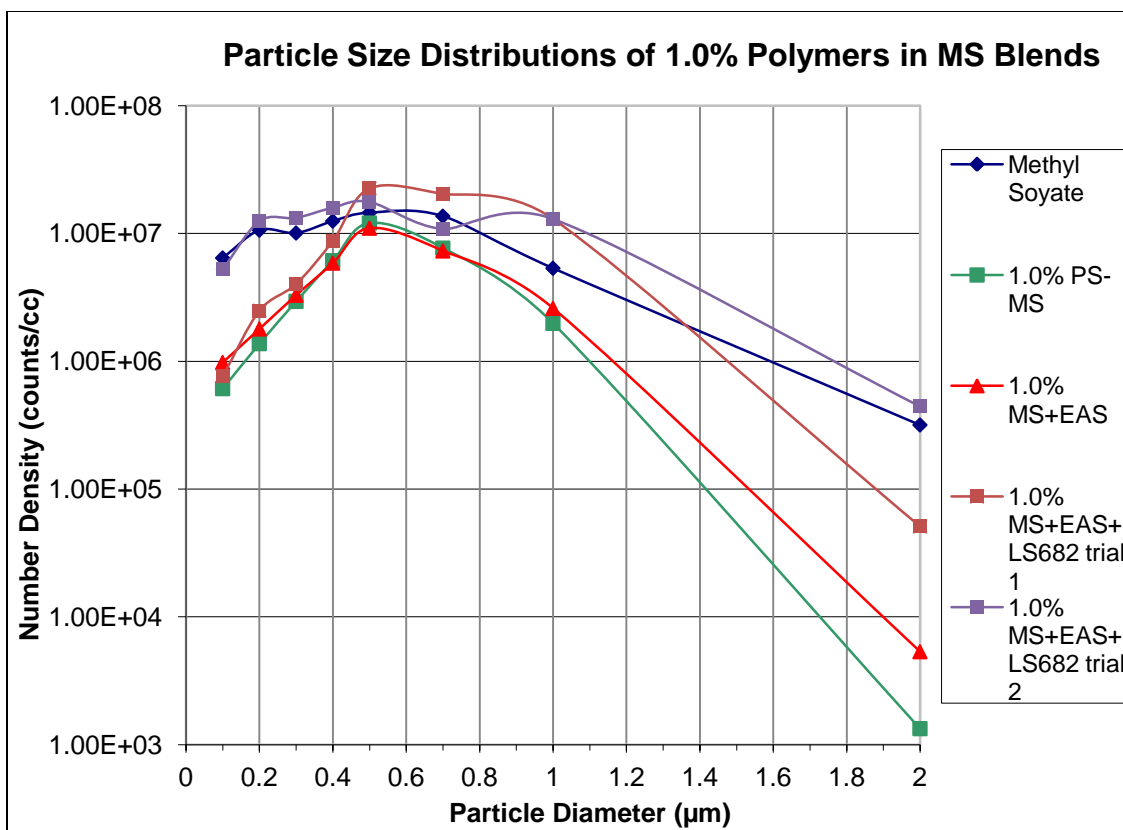


Figure 4.17 – Particle Size Distribution of Methyl Soyate Blended with Polymers

formation of aerosol droplets and thus form larger diameter particles capable of attenuating longer wavelengths such as infrared. Percentage compositions were calculated as weight percents of polymers to oil. These blended oil samples were tested the same way as normal pure oil samples: an oil flow rate of 0.5 mL/min, an air flow rate of 5 L/min and 3 minutes of plume introduction time into the chamber. The generator temperature was 450 °C. Polystyrene (PS) and EAS were added at 1.0% amounts for this testing, and in the case of EAS+LS682 hardener the hardener was added at a 70% amount relative to the amount of EAS. It may be noted that the testing was not highly reproducible when involving polymeric materials due to the problems of the polymers leaving solution in the heated generator tube and combusting within the tube. This led to

tube obstruction and highly variable particle number densities, with no observed beneficial shift in the predominant particle sizes.

Similarly, when comparing percent transmittance values of visible light exposure over time as shown in Figures 4.18 and 4.19, it can be seen between 0.5% PS-MS and 1.0% PS-MS that the percent transmittance is increasing, showing that less visible light is being scattered as the amount of polystyrene increases. The change is most clear at the end of the plume introduction time, where 0.5% PS-MS has approximately a 15% transmittance at these wavelengths while 1.0% PS-MS has approximately a 23% transmittance. This is also attributed to the fact that with higher concentrations of polymer in solution there was more obstruction formed within the generator tube and a lesser amount of obscurant aerosol plume could be formed.

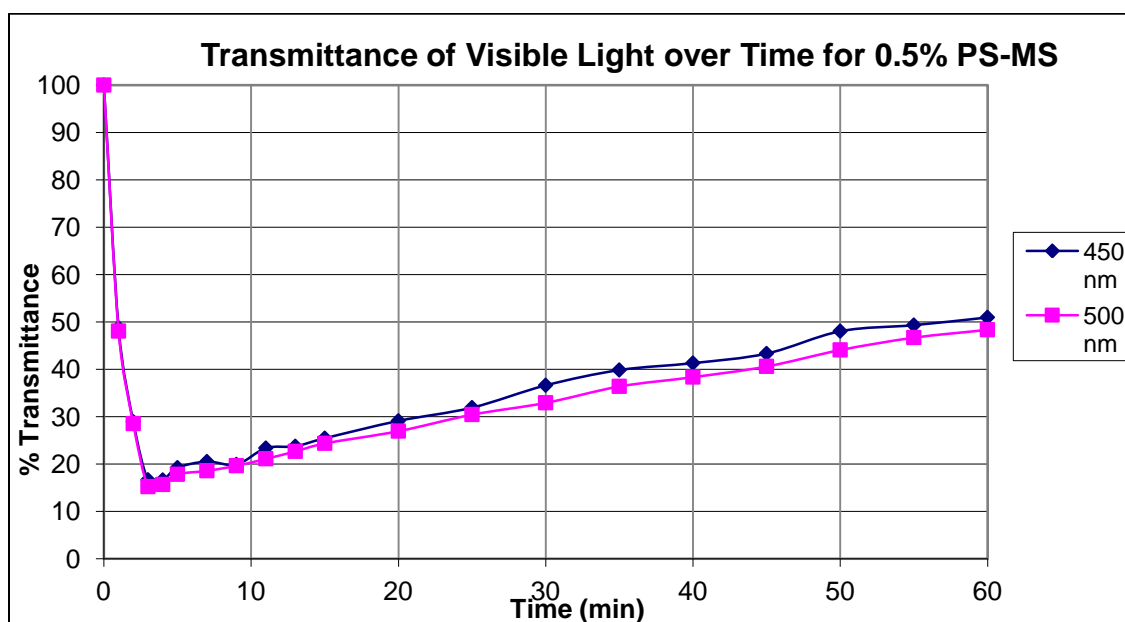


Figure 4.18 – Transmittance of Visible Radiation through 0.5% Polystyrene-Methyl Soyate Blend Over Time

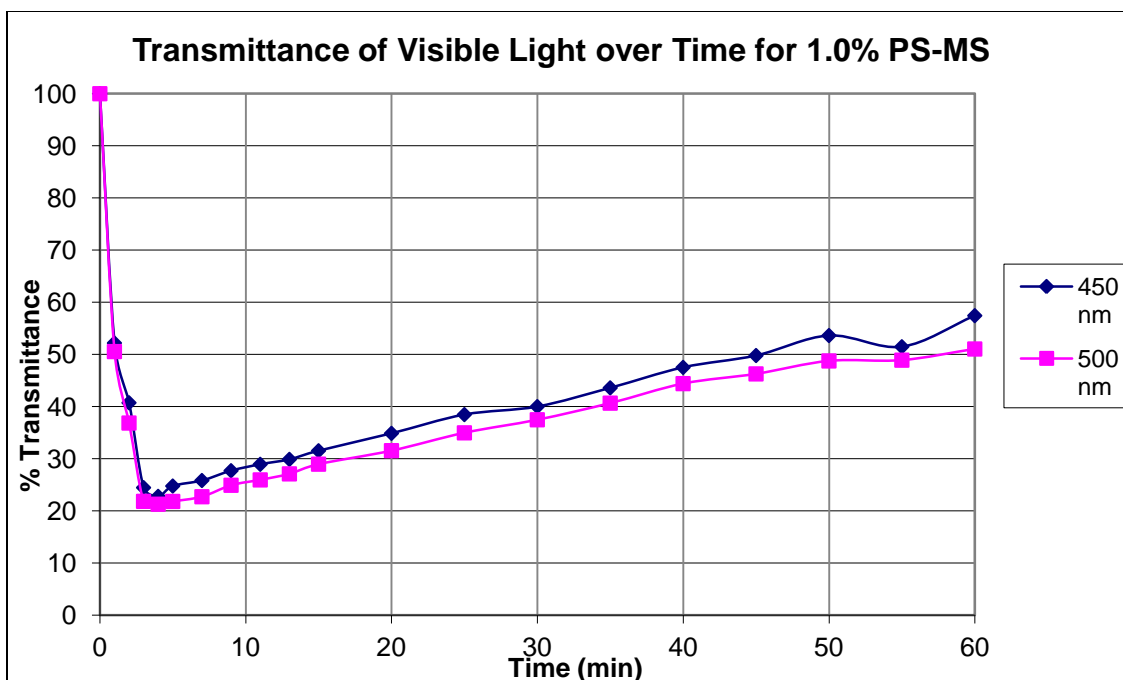


Figure 4.19 – Transmittance of Visible Radiation through 1.0% Polystyrene-Methyl Soyate Blend Over Time

This data is further supported by another comparison between MS and 1.0% MS+EAS, seen in Figure 4.20. As polymeric material is added, the percent transmittance of visible light increases which means there is less scattering of light. This problem with polymer decomposition and combustion could not be overcome due to the nature of this aerosol generation system and the relatively long aerosol flight path surrounded by heated walls onto which the polymers impacted and stuck.

A different test was done to investigate the effect of generation temperature upon the particle size distributions for a 1.0% PS-MS sample as compared to fog oil and stock methyl soyate data. This test showed how unpredictable the tests became when dealing with polymers dissolved into the oil. In these tests, the PS-MS behaves similarly to stock

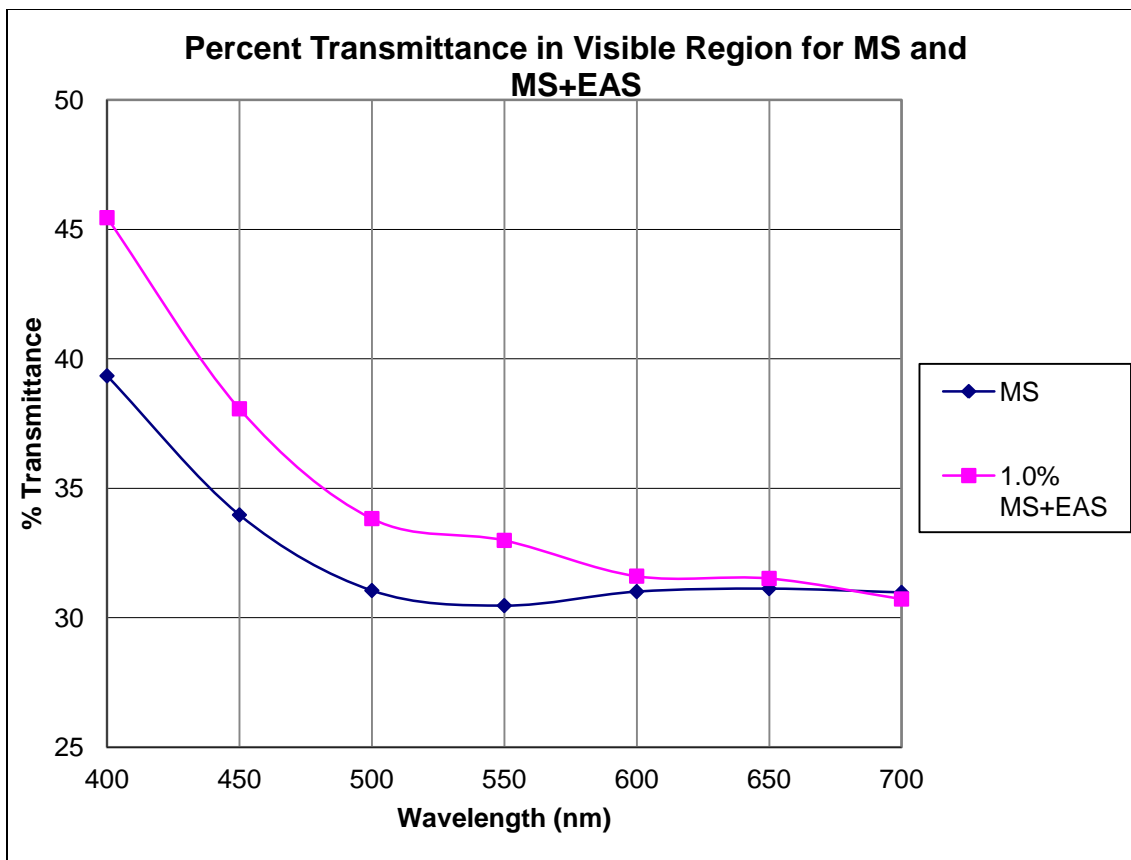


Figure 4.20 - Transmittance of Visible Radiation through 1.0% EAS-Methyl Soyate Blend Over Time

MS at particle diameters below $0.7 \mu\text{m}$, and at $0.7 \mu\text{m}$ and larger diameters the PS-MS appeared to have a detrimental impact on the particle counts. Rather than promoting the formation of larger particles the data indicated that perhaps it caused fewer larger particles than stock MS, possibly from decomposition upon exposure to the heated walls of the generator tube. This data is found in Figures 4.21, 4.22, 4.23 and 4.24.

The tubular furnace obscurant aerosol generator was used to identify whether air flows changed the particle size distributions, represented by Figure 4.25. Methyl soyate was used at $350 \text{ }^\circ\text{C}$, $375 \text{ }^\circ\text{C}$, and $400 \text{ }^\circ\text{C}$ with air flows of 5 LPM and 10 LPM. At 350

°C and 375 °C there were higher number densities at smaller particle diameters, while at 400 °C it was observed that the particle number densities decreased with increased air

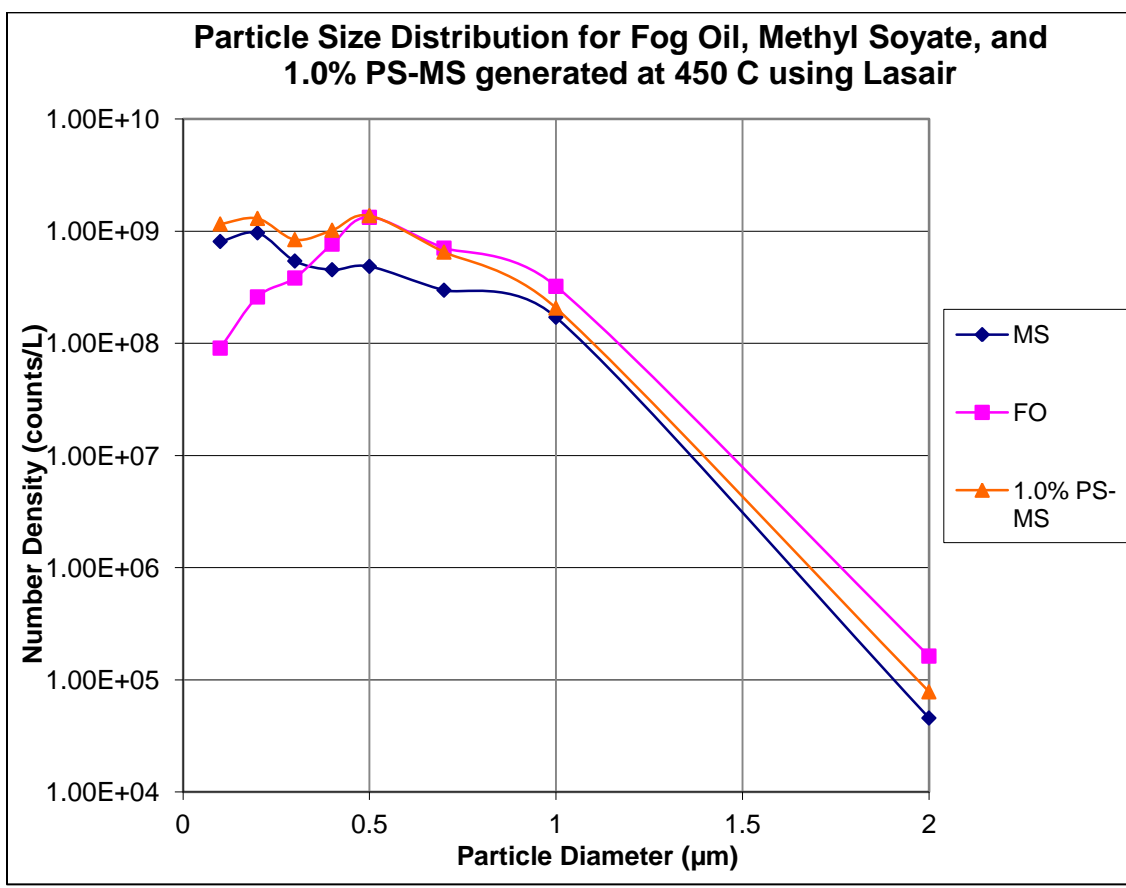


Figure 4.21 – Particle Size Distribution Obtained using Lasair Comparing Fog Oil, Methyl Soyate, and PS-MS When Generated at 450 C

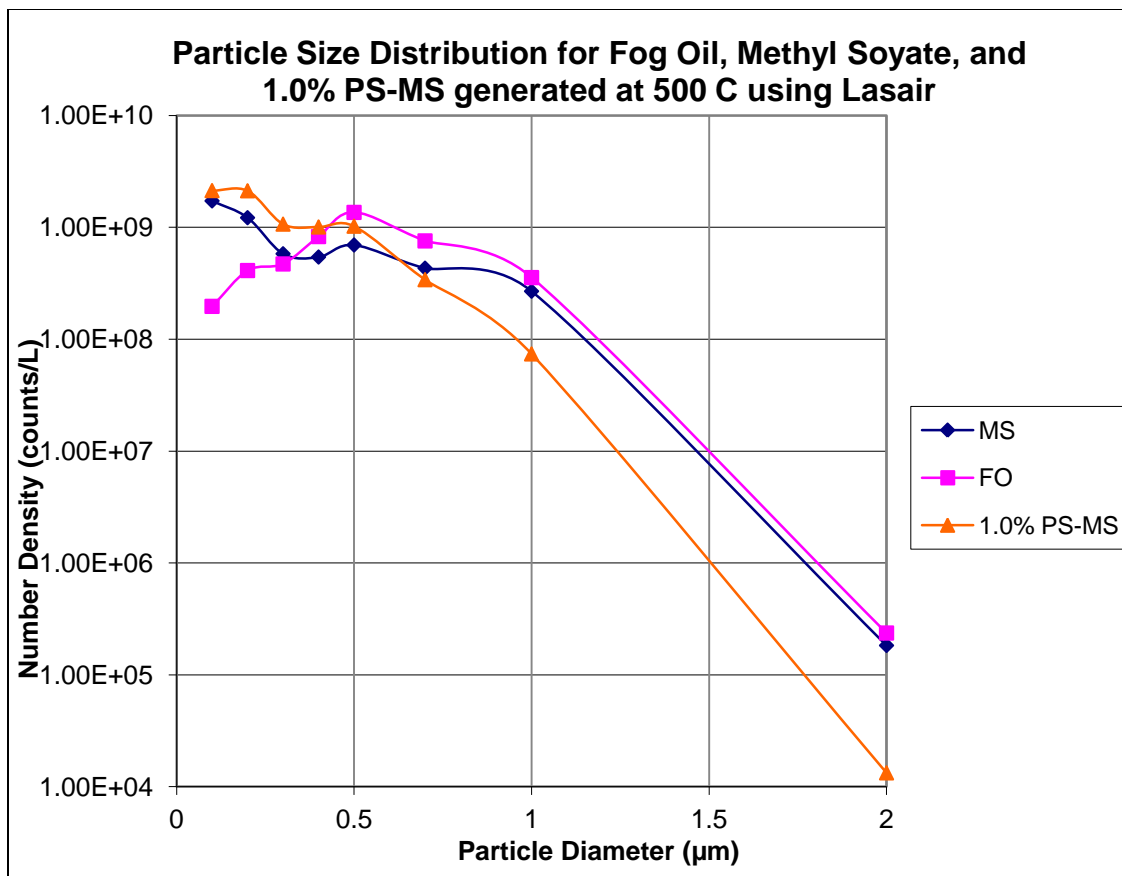


Figure 4.22 - Particle Size Distribution Obtained using Lasair Comparing Fog Oil, Methyl Soyate, and PS-MS When Generated at 500 C

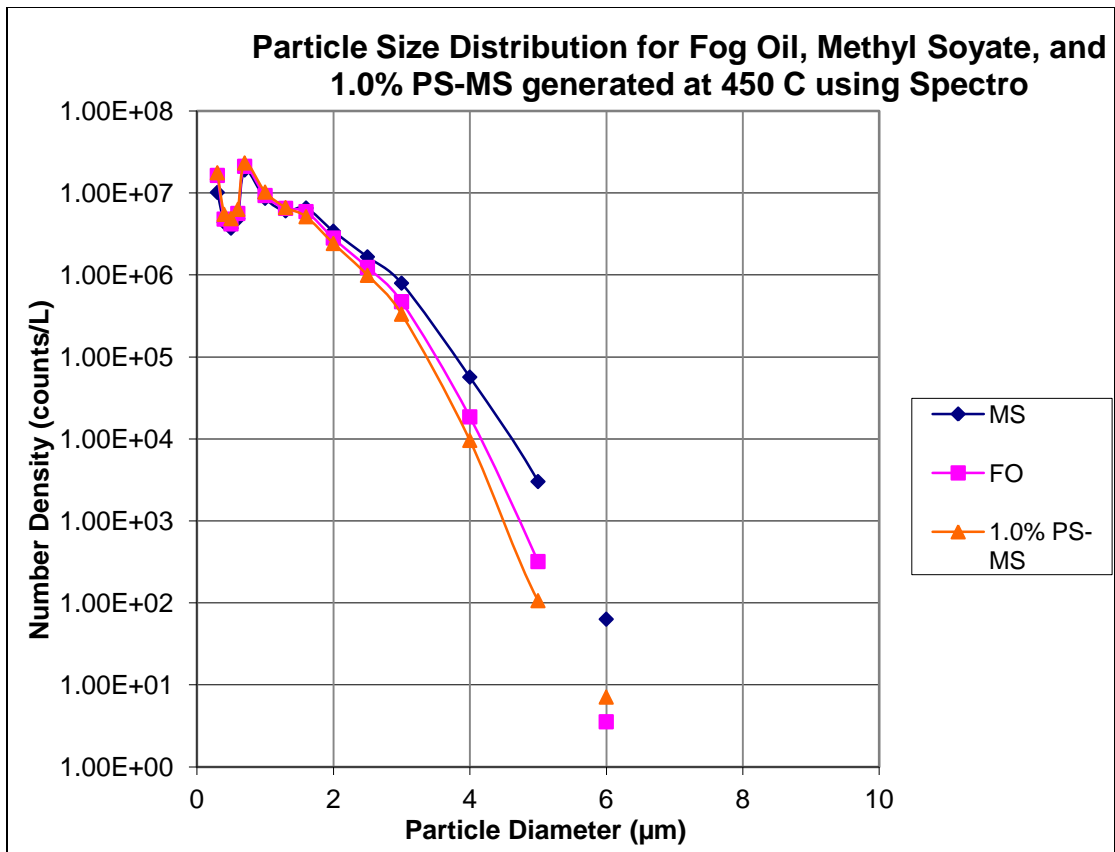


Figure 4.23 - Particle Size Distribution Obtained using Spectro Comparing Fog Oil, Methyl Soyate, and PS-MS When Generated at 450 C

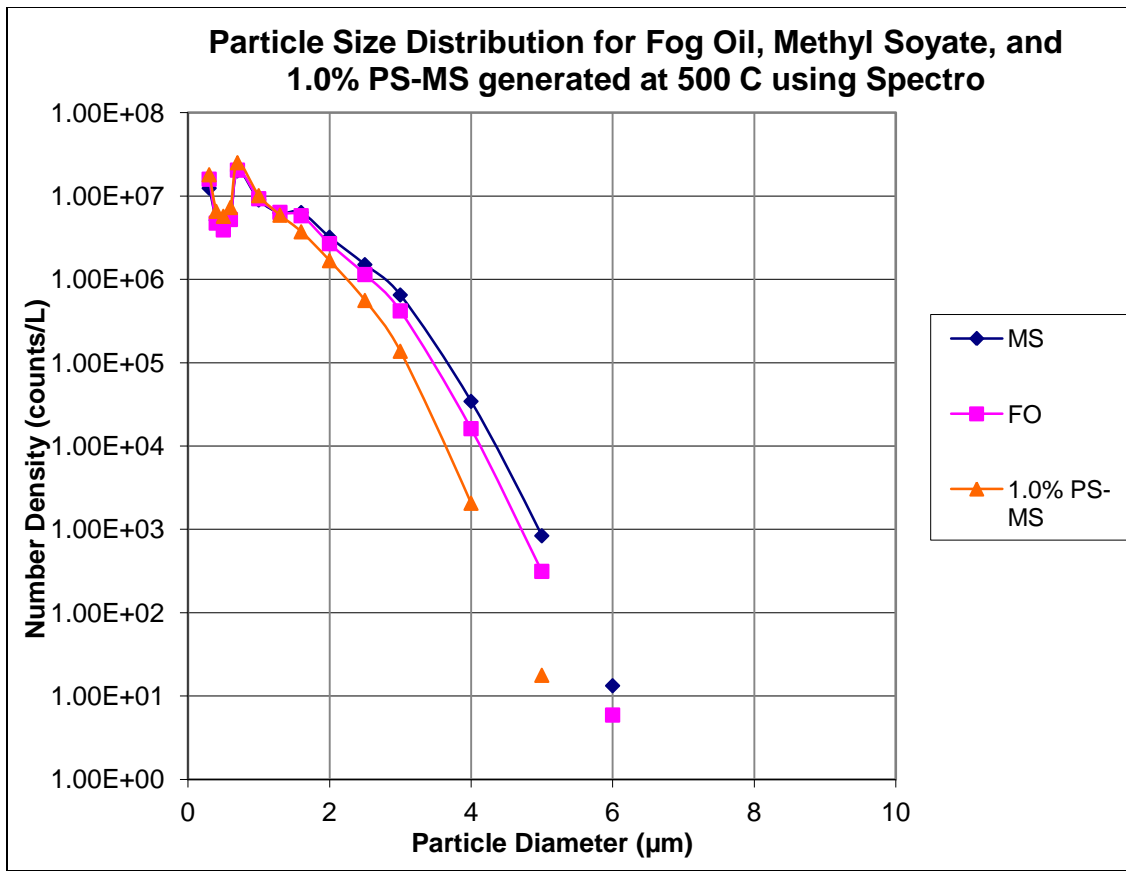


Figure 4.24 - Particle Size Distribution Obtained using Spectro Comparing Fog Oil, Methyl Soyate, and PS-MS When Generated at 500 C

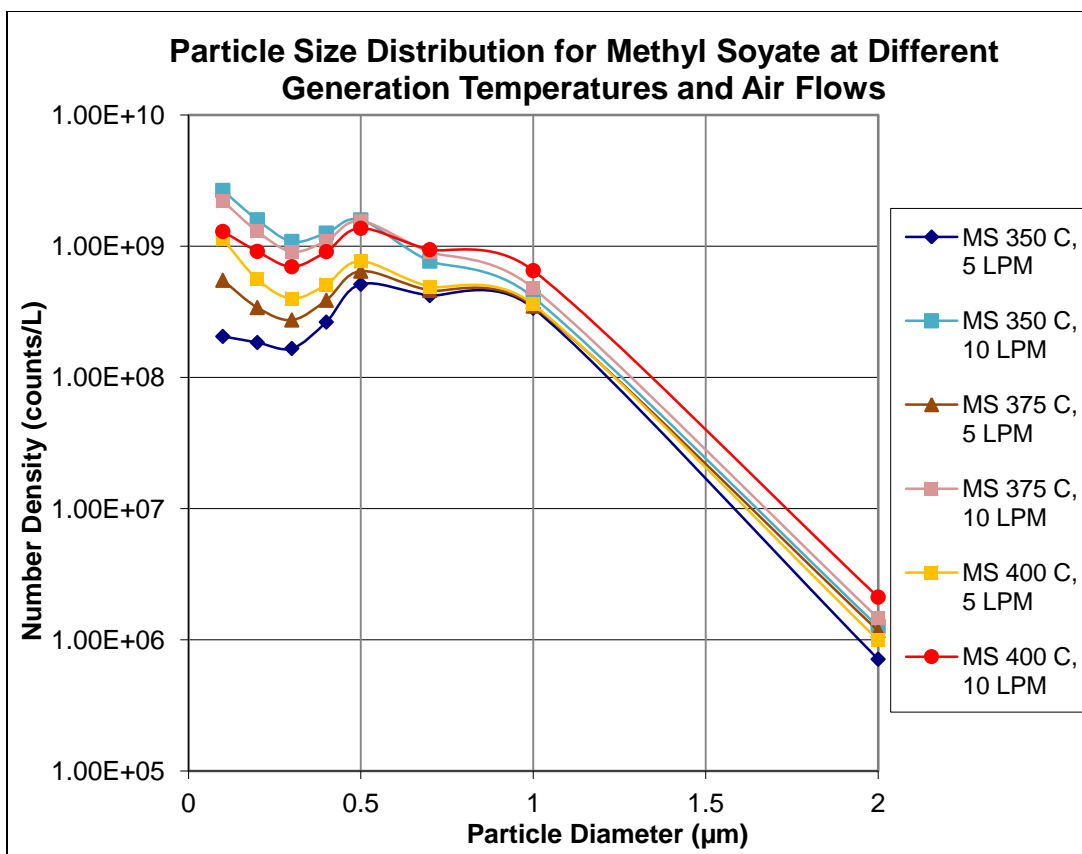


Figure 4.25 – Particle Size Distribution Obtained using Lasair for Methyl Soyate Aerosolized at Different Generation Conditions

flow. This could potentially be attributed to the beginnings of oil combustion with elevated temperatures and elevated oxygen supply causing the decreased counts.

Throughout all laboratory scale testing using the tubular furnace-based obscurant aerosol generator methyl soyate performed approximately equally to fog oil. It was capable of producing a thick white plume which was visually identical to the plume from fog oil, and gave particle size distributions and number densities very similar to that of fog oil. However, methyl soyate has a distinct environmental advantage in that it is a biogenic oil that has been previously tested and found to have a faster rate of decomposition in soil and aquatic environments. It has also been previously studied and

shown to have no carcinogenic compounds in its composition, while fog oil is known to naturally have some hazardous components.

4.1.2. Effects of Generation Parameters. Experimentation conducted by prior students showed the most favorable aerosolization properties for methyl soyate over other biogenic oils such as the methyl, ethyl and propyl esters of palm oil, sunflower oil, safflower oil, and rapeseed oil. Therefore this testing almost exclusively was performed comparing methyl soyate against the currently used fog oil for purposes of obscurant aerosol generation. Within the laboratory environment using the tube furnace generator there are relatively few variables. These variables include oil flow rates, air flow rates, generator temperature and duration of generation.

Oil flow rates were moderately changed in initial testing and showed that a reasonable rate fell around 0.5 mL/min. Oil rates above this amount saw too much unaerosolized oil entering the collection flask post-generator due to thermal energy limitations within the generation tube, and rates below this had “thinner” resultant plumes because it was less oil than could be reasonably expected to aerosolize. Therefore all recorded laboratory data was generated at an oil flow rate of 0.5 mL/min.

Air flow rates were also varied to check for proper oil aerosolization. If the air flow was too low then the oil samples would not move away from the heat source quickly enough and would begin to degrade and combust within the generation tube. However, if the air flow was too high the heat was drawn out of the generation tube too quickly and became insufficient for vaporization and aerosolization. Most laboratory testing used an air flow rate of 5 or 10 mL/min with good results.

The generator temperature was also varied between 400°C and 650°C. Overall, higher temperatures gave aerosol plumes with equal particle sizes and relative number densities, though higher temperatures were more prone to accumulating combusted and degraded oil material within the generation tube that would have to be cleared out after each sample run.

Another consideration for laboratory testing was the runtime of obscurant aerosol introduction into the testing chamber. Generally samples were introduced for three minutes. By introducing aerosols for much more than this duration the concentration of aerosolized particles within the confines of the chamber became unrealistically high and saw saturation conditions. In real world field conditions the obscurant plumes may expand and dilute in the air, so any values obtained under saturation conditions were irrelevant. As an example, after 11 min of aerosol introduction there was no light transmittance across the 1 m width chamber, and visual observance of a 532 nm green laser beam showed the beam was completely scattered before reaching 0.5 m into the chamber. Also the OPCs could not read measurements due to the sheer numbers of particles present within the chamber. Three minutes of runtime appeared to be sufficient to give satisfactory differences in results between oil types, while remaining below saturation conditions.

4.1.3. Environmental Temperature Fluctuation. In real world applications of obscurant aerosols there may be a wide range of ambient environmental temperatures encountered. Laboratory experimentation was conducted with the climate-controlled testing chamber to identify whether there were changes in relative number densities or

particle size distributions when the obscurant aerosol plumes were exposed to chamber temperatures ranging from 4°C to 50°C. No significant differences were observed over the range of temperatures tested.

4.1.4. Addition of Polymers. Some polymers were added to the sample oils in determining whether they could act as nucleation sites for the aerosolized particles to gather on and form larger particles with shifted wavelengths of attenuation. It was hypothesized that the addition of polymers could lead to particle sizes more conducive to the blockage of infrared wavelengths, a range frequently used in military weapon targeting systems. Polymers including polystyrene in the form of granular type Styrofoam packing shells (~25000 MW) and 1% (w/w) epoxidized allyl soyate (EAS, both with and without LS-682 hardener) were dissolved into oil samples with moderate heating. Polystyrene (25000 MW) was added in 0.1% (w/w), 1%, 2%, 5%, and 10% levels. Polystyrene was also added in a test at a 1% (w/w) level for polymer molecular weights of 4075, 45730, 95800, and 401340 to determine whether there was any noticeable difference in the resultant aerosol particle characteristics. Overall it was not found that the addition of polymeric material enhanced any properties of the resultant obscurant aerosol. It was either too heavy to remain airborne, or more likely did not survive past the aerosolization stages as indicated by significantly larger accumulations of decomposed and combusted materials within the generation tube near to the oil sample outlet at the start of the heated region when these polymer-containing oil samples were used.

4.1.5. Copper Nanoparticles in Solution. The military has used mechanically ground flakes of brass as well as graphite as an additive to some obscurant plumes. These substances act as conductive particles which can reportedly scatter infrared and microwave signals. The M76 grenade, launched from vehicles, contains stearic acid-coated brass particles that are approximately 8 μm wide by 0.3 μm thick put into a 66 mm shell as a slurry. Recent literature also suggests the use of milled nanoparticulate copper flakes or titanium dioxide particles to attenuate infrared signals.^[10] Additional testing has looked at the manufacture and application of silver and gold nanoparticles and nanoplates to serve as plasmonic obscurants which can scatter and absorb visible and near-infrared wavelengths more efficiently than ordinary particles.^[11] More recent laser targeting systems use infrared lasers to “paint” targets, and infrared blackbody radiation can be used by thermal targeting systems. Microwave systems are also being explored for use, so it is important to find ways of blocking these types of radiation.

The synthesis of copper nanoparticles in solution has been reported in literature, and these nanoparticles should remain airborne for longer durations than brass flakes due to the smaller size while still remaining conductive. The first tests to create copper nanoparticles for potential use as an obscurant plume additive used cupric chloride dissolved in water combined with aqueous sodium borohydride. Initial amounts used approximately 0.50 g CuCl_2 and 1.00 g NaBH_4 and was found to rapidly produce a black precipitate which was filtered and dried in an oven and had a mass of approximately 0.20 g.

This test was scaled up to use larger volumes of solution which were pumped using a pair of pulsing diaphragm chemical resistant pumps into sprayers which could be

mounted behind the turbojet engine, seen in Figures 4.26 and 4.27. The sprayers were aligned at a 45° angle relative to the axis of exhaust, pointing downwind from the exhaust, so the sprays would intersect and provide mixing and reaction. This system had some limited success, with the main drawbacks being the difficulty of coordinating the pulsing of the pumps and the more limited mixing due to having a spray intersecting a spray, in which some droplets do not see contact with droplets of the other solution. However, some interaction did take place, so the system was tested with the turbojet engine running. Air sampling pumps were placed approximately 1.5 m from the exhaust of the engine with filters to collect any particulate matter. There were also filters placed openly on metal screen mesh in the engine exhaust so particles could directly impact the filters rather than having to be drawn in by a pump. The cupric chloride solution was prepared at 4.004 g $\text{CuCl}_2 \cdot 2\text{H}_2\text{O}$ in 200 mL water and 1.810 g NaBH_4 in 200 mL water. The solutions were sprayed for six minutes, and the filters were analyzed under the Scanning Electron Microscope for particles, an image of which is shown in Figure 4.28. No significant numbers of copper particles were found. It is likely that the engine exhaust flow prevented the bulk of the sprays from reaching the intersection point, thus allowing extremely limited reaction to occur. There was also no observed difference in the functionality of a radio controlled device placed in the path of the exhaust when the copper reaction sprayers were engaged. This line of testing was considered unsuccessful for producing conductive nanoparticles suspended in air to scramble infrared signals.

Another test used 0.0661 g of copper acetate, $\text{Cu}_2(\text{CH}_3\text{CO}_2)_4 \cdot 2\text{H}_2\text{O}$, placed into a small ceramic crucible and placed within a tube running through a tubular furnace. The

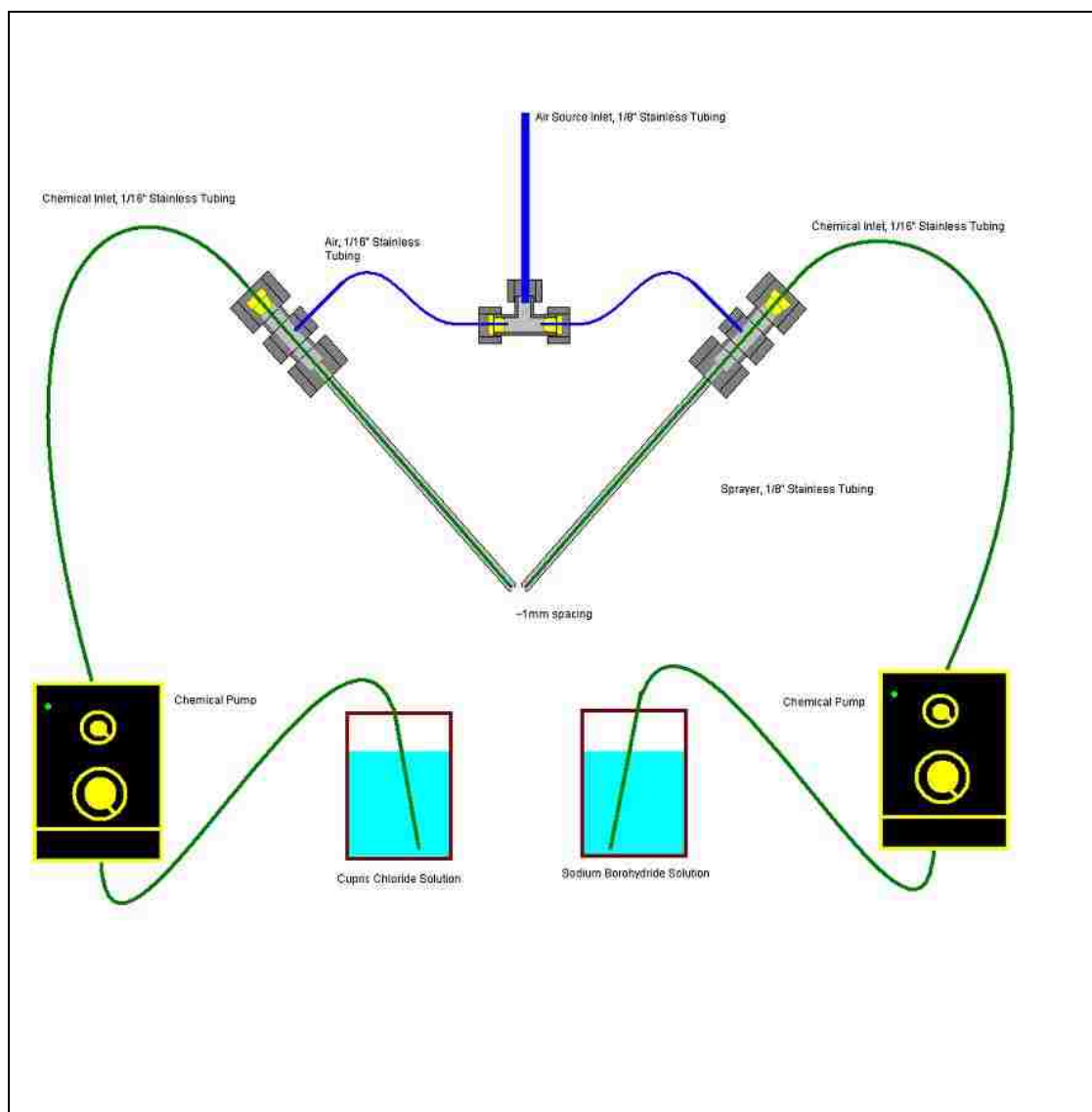


Figure 4.26 – Diagram of Aqueous Solutions Sprayer Assembly for Formation of Copper Nanoparticles

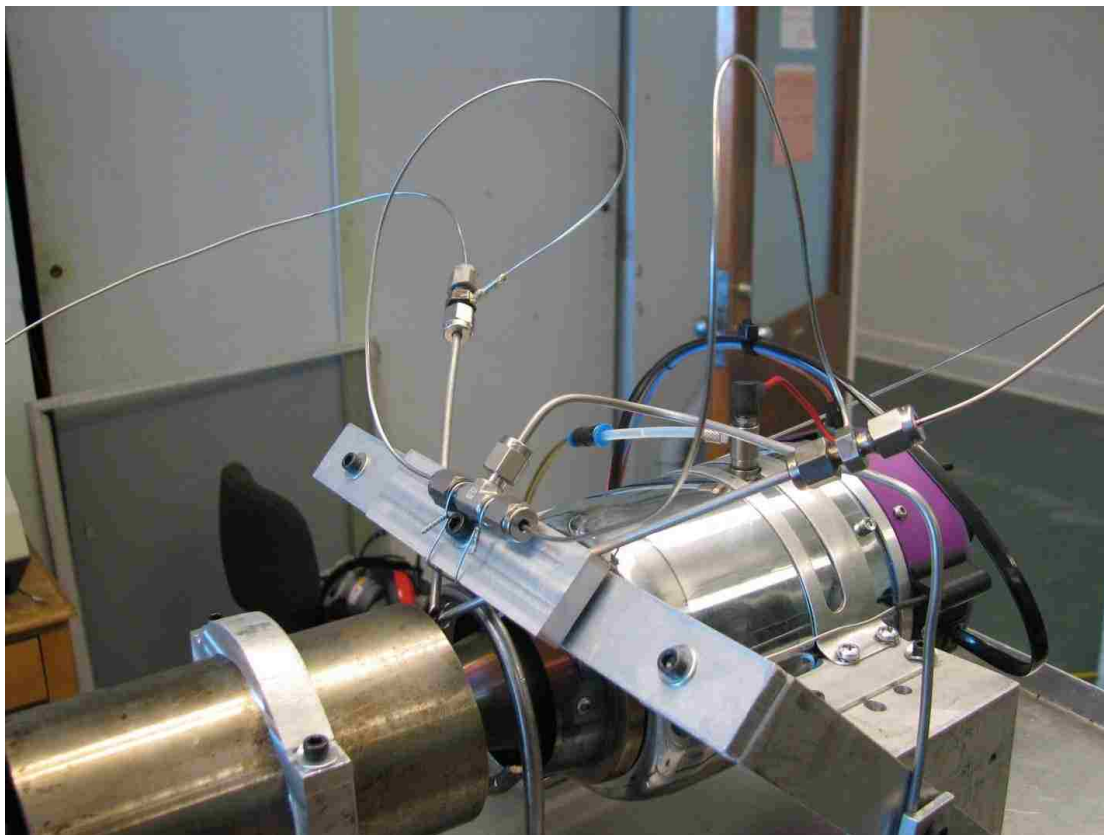


Figure 4.27 – Photograph of Aqueous Solutions Copper Nanoparticle Reaction Sprayer Mounted on JetCat P80 Generator System



Figure 4.28 – Scanning Electron Microscope Image of Copper Nanoparticles on Filter Fibers

tube was sealed to allow only nitrogen gas to pass over the sample, and the furnace was turned on at a set temperature of 400 °C for 7.5 hours. It was expected that the heat would decompose the acetate, leaving only elemental copper. After removal from the furnace, the mass of sample remaining was 0.01815 g, giving 86.43 % Yield. Although this test did produce some elemental copper, the rate of degradation was relatively slow so this was also not considered a viable option for producing copper particles suspended in obscurant plumes.

4.1.6. Addition of Copper Nanoparticles as Powder. Due to the unsuccessful attempts to create copper nanoparticles in the turbojet exhaust plume using aqueous

solutions, the attempt was made to produce dry powders of copper nanoparticles which could be put into the exhaust by mechanical means or by blending into the obscurant oils before being sprayed into the exhaust. A paper was found in literature which indicated that copper nanowires of nanoparticulate discs could be produced in solution, so this experiment was repeated for this testing. Initially approximately 0.0240 g $\text{Cu}(\text{NO}_3)_2 \cdot 3\text{H}_2\text{O}$ was dissolved into approximately 5 mL water, combined with 20 mL of 15M NaOH, amounts of Ethylene Diamine (EDA) ranging from 0.075 mL to 2.00 mL, and 25 μL 64% N_2H_4 (Hydrazine) all performed in a 60 °C water bath. Each solution liberated large amounts of gas and dark brown to black colored particles were seen forming. Solutions were allowed to react undisturbed for four hours, then centrifuged and the supernatant liquid was decanted. The particles were then rinsed with water, centrifuged and decanted several times to remove unreacted reagents, and finally repeated with acetone to help speed the rate of drying. All dried samples were taken to the SEM laboratory for analysis, a sample image of which is seen in Figure 4.29. There was no clear distinction as to the relative amounts of EDA used versus the size and shape of produced copper particles, but some samples saw rounded particulates of copper while others saw formations of clumped needle-like structures of copper.

This testing was continued in larger batches to make larger quantities of copper particles. The final batch sizes used approximately 78.00 g $\text{Cu}(\text{NO}_3)_2 \cdot 3\text{H}_2\text{O}$ in 10 mL water, combined with approximately 40 g NaOH dissolved in 63 mL water, 12 mL EDA, and 8 mL Hydrazine. This reaction sequence allowed production of approximately 20 g batches of copper product. However, the copper product would look metallic copper colored during the reaction but would quickly oxidize and turn black during the drying

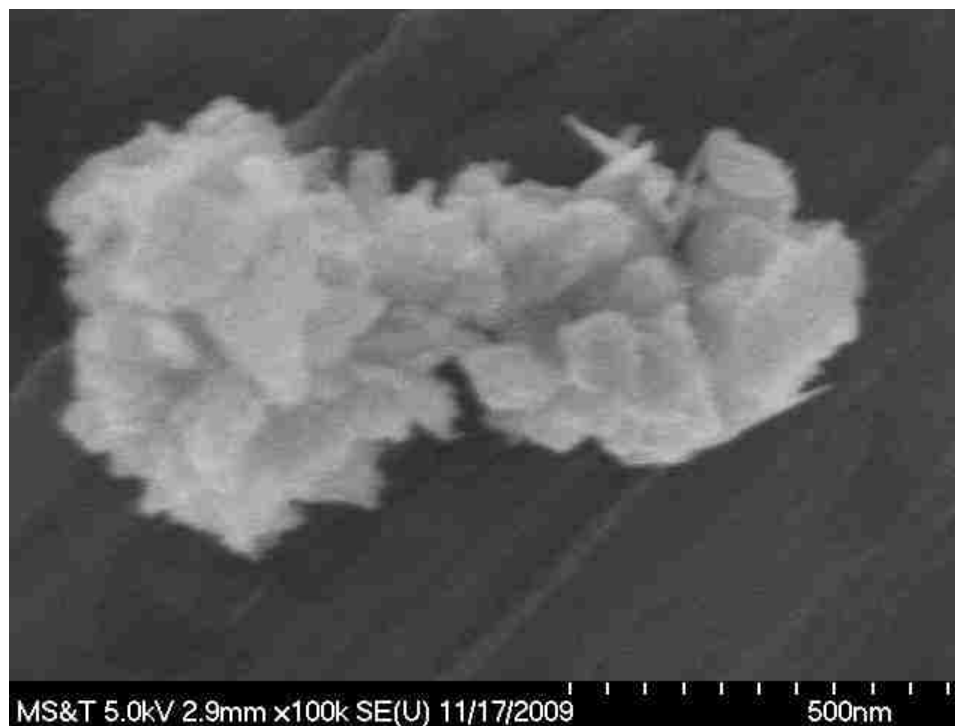


Figure 4.29 – Scanning Electron Microscope Image of Needle and Agglomerate Structures in Dry Copper Nanoparticle Powder

stages. A 20g sample of brass particles was sent to the Edgewood Chemical and Biological Center at Aberdeen, Maryland for testing, but the results did not appear promising for the application of these particles as a means of scattering infrared or microwave radiation, possibly due to the rapid oxidation of the particle surfaces. Transmittance measurements are found in Figure 4.30, and extinction coefficient measurements in Figure 4.31.

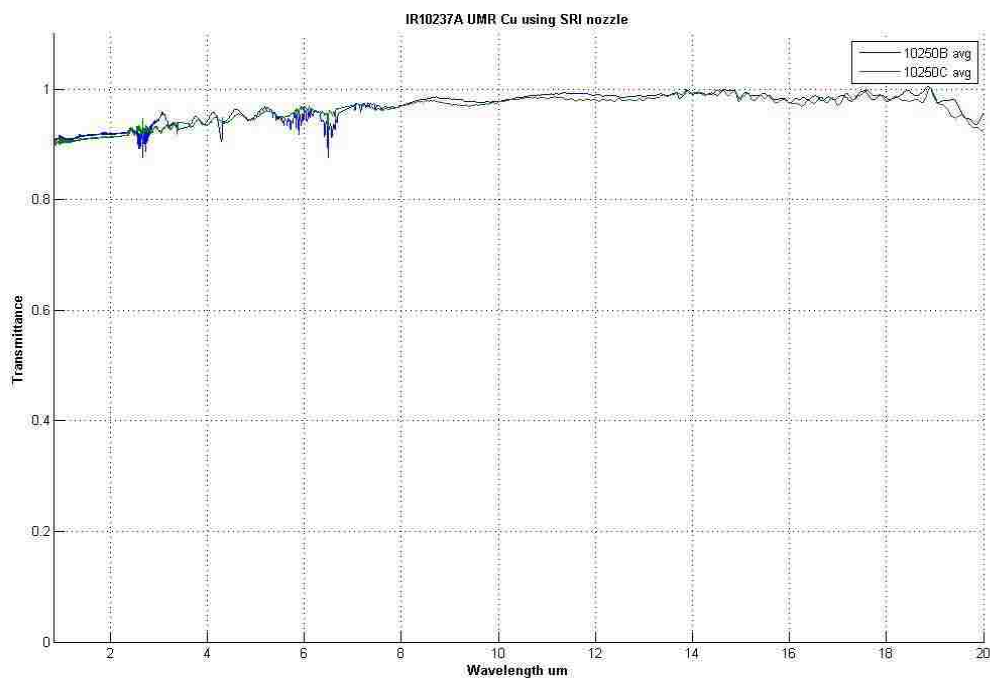


Figure 4.30 – Transmittance Measurements through Copper Nanoparticle Powder

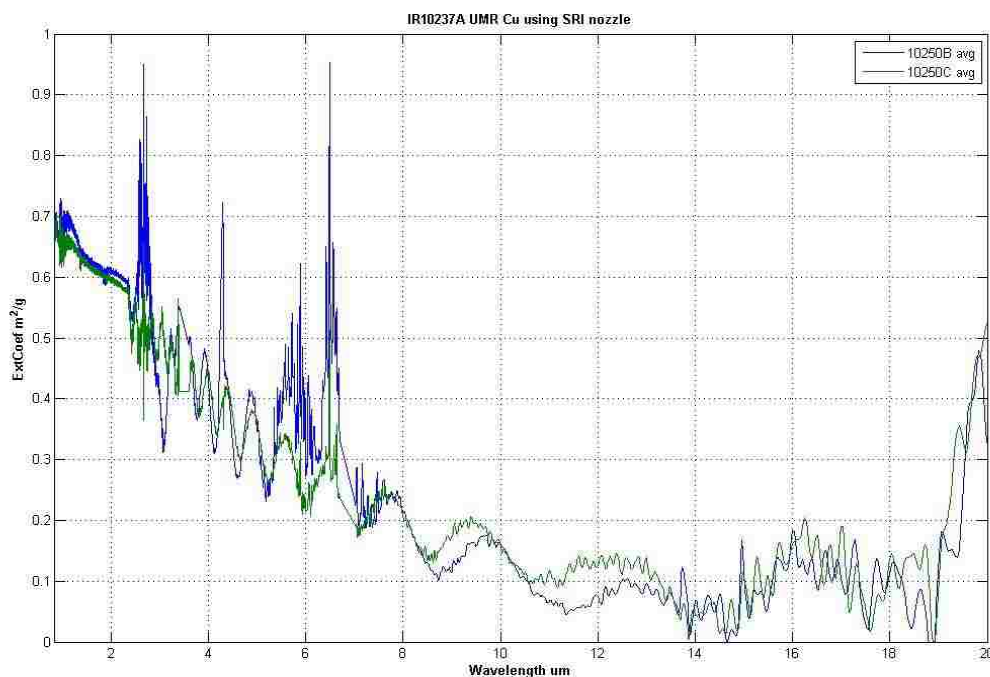


Figure 4.31 – Extinction Coefficient Measurements for Copper Nanoparticle Powder

A brass screen Faradic cage, Figure 4.32, was built with a small window opening on one side to test whether conventional commercial radio signals could be broken by a plume of copper particles passing in front of the window, but these tests were also unsuccessful. The Faradic cage also had varying results on its own for blocking radio signals, depending on the types of devices tested. An inexpensive 25 MHz radio controlled toy could have its signal blocked by the cage at a distance of 0.75 m, as well as a portable MP3 player tuned to a 105.3 MHz local radio station broadcasting from approximately 2 km away and a portable weather radio tuned to 162.500 MHz for a signal originating approximately 45 km away. A 2.4 GHz wireless video camera system was also blocked by the closed cage at a distance of 0.75 m between the source and receiver. However,



Figure 4.32 – Photograph of Brass Screen Faradic Cage

signals not affected by the brass screen cage included a 72.350 MHz radio controlled aircraft transmitter and receiver at a distance of 2 m, a 2-way radio set to the 162.500 MHz weather radio frequency originating from a distance approximately 45 km away, a 2-way radio set to a channel having a frequency of 467.6375 MHz originating from 200 m away, and a cellular telephone signal of 1.900 GHz originating from less than 5 km away. The telephone did see some reduction in the on-screen signal strength indicator,

but it was not completely blocked. This testing was also considered unsuccessful at this point.

4.2. FIELD TESTING

After determining that methyl soyate could perform similarly to fog oil in laboratory scale obscurant aerosol testing, both substances were tested on a larger scale in field environments using the turbojet-based obscurant generator prototypes. Information from these test was compared to data regarding the use of fog oil in the M56 Coyote generator.

4.2.1. Test Layout and Inherent Variables. Testing of obscurant plumes using full oil flows on a large scale obscurant generator required a different testing configuration than for laboratory scale tests. The multitude of particles produced in a very short run time was far in excess of what could be tested in a confined testing chamber, and any effort to contain the particles would have resulted in a saturated environment which would not accurately represent field conditions. In real world scenarios, aerosol plumes are generated and released into the environment where they are allowed to expand in coverage area while becoming increasingly diluted with ambient air.

As a result of testing plumes in outdoor environments there are several variables introduced. Sunlight and clouds mean the level of incident light is unstable, so a beam chopper had to be used on the laser systems to obtain a modulated signal for background subtraction. The photodiode detectors also required short segments of PVC tubing in

front of them, painted flat black to eliminate the possibility of sunlight directly striking the detectors and to reduce the glare of reflected sunlight. Another inherent variable was wind direction. The instrumentation had to be placed approximately 20 m downwind of the obscurant generator with the laser source and detector tripods stationed approximately 20 m perpendicular to this point in either direction from the axis of the plume, shown by Figure 4.33. With a 40 m span between source and detector the entire plume width was normally measured by the lasers. At times the wind could change speeds and direction which would result in some or all of the plume missing the detectors. As a result the particle size distribution values were sometimes skewed and the laser transmittance values would fluctuate during a run.

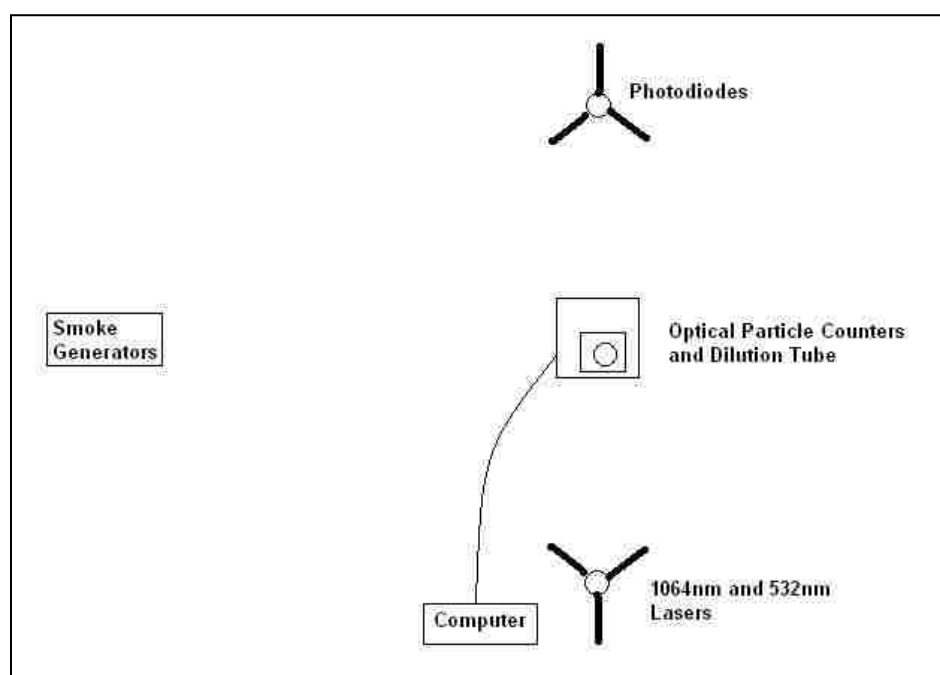


Figure 4.33 – Diagram of Field Testing Instrument Layout

4.2.2. Flow Rates. The M56 Coyote generator currently used by the U.S. Army aerosolizes between 3.8 L and 4.9 L (1.0 gal and 1.3 gal) of fog oil per minute of run time. Using the custom built oil sprayer nozzles used on the prototype turbojet-based generator units, each nozzle sprayed about 1.4 L (0.38 gal) of fog oil per minute or 1.8 L (0.48 gal) of methyl soyate per minute. By using dual nozzles the prototype generators were capable of spraying a total of 2.9 L/min (0.76 gal/min) of fog oil or 3.6 L/min (0.96 gal/min) of methyl soyate. The differences in flow rates between methyl soyate and fog oil were from the relative shear viscosities which came into play due to the nature of the oil pickup pumps. The flow rates of the prototype generators are comparable to the output of the much larger M56 Coyote generator, which satisfied one objective of the research.

4.2.3. Comparison Between Oils. Much field testing was done comparing fog oil and methyl soyate because of the variability in data as a result of uncontrolled parameters in natural environments. Wind speeds and directions affected the instrumentation because the plume could sway on and off target with the OPC sample ports. As a result, it was difficult to obtain consistent results between tests so a large number of tests had to be run to obtain an average understanding of each oil's performance. Tests were conducted at Wurdack Farm in Cook Station, Missouri. Generally, after performing these tests it could be said that methyl soyate is directly comparable to fog oil in the general nature of the particle size distributions and the visual quality of the plumes as evidenced by the percent transmittances in both the visual wavelengths and near infrared wavelengths.

The first set of tests were done using the SWB-11 turbojet generator, shown by data in Figures 4.34 and 4.35. This system used one obscurant oil sprayer nozzle, and the configurations were changed on future generator designs to take advantage of the added thrust and heat output.

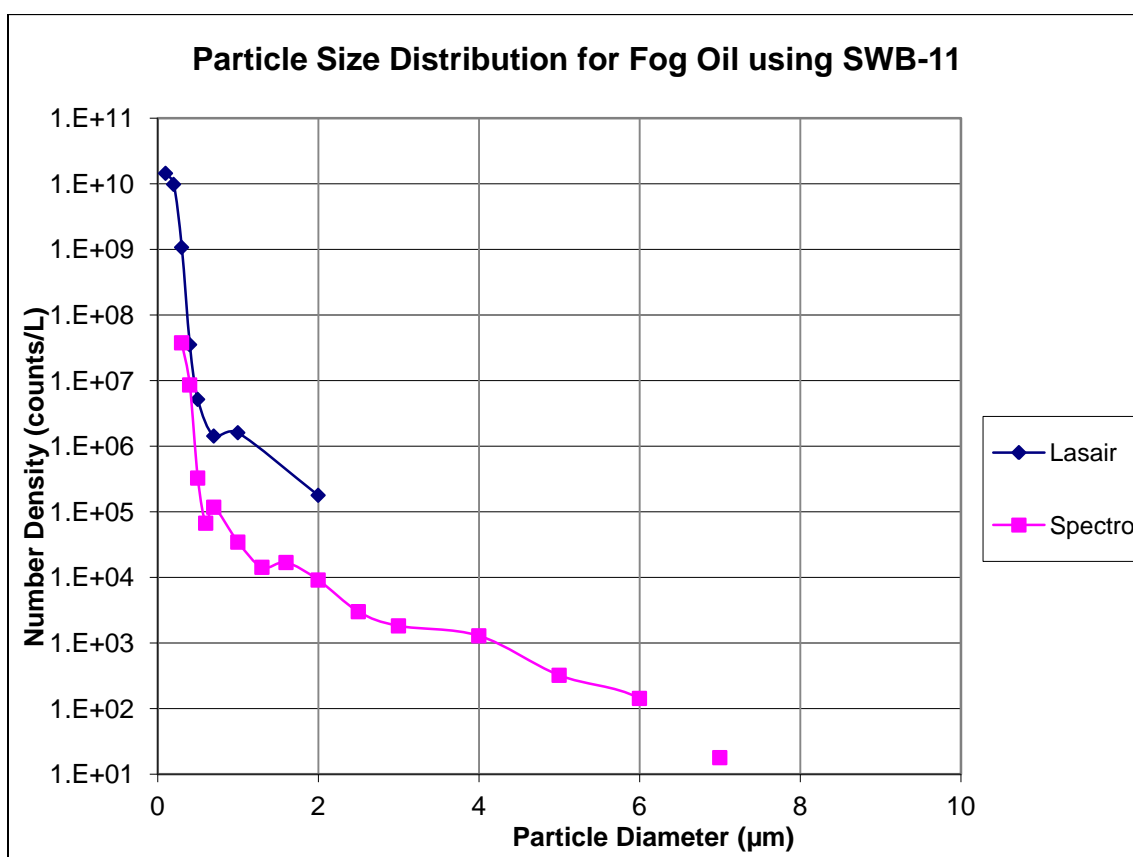


Figure 4.34 – Particle Size Distribution for Fog Oil from SWB-11 Based Obscurant Aerosol Generator

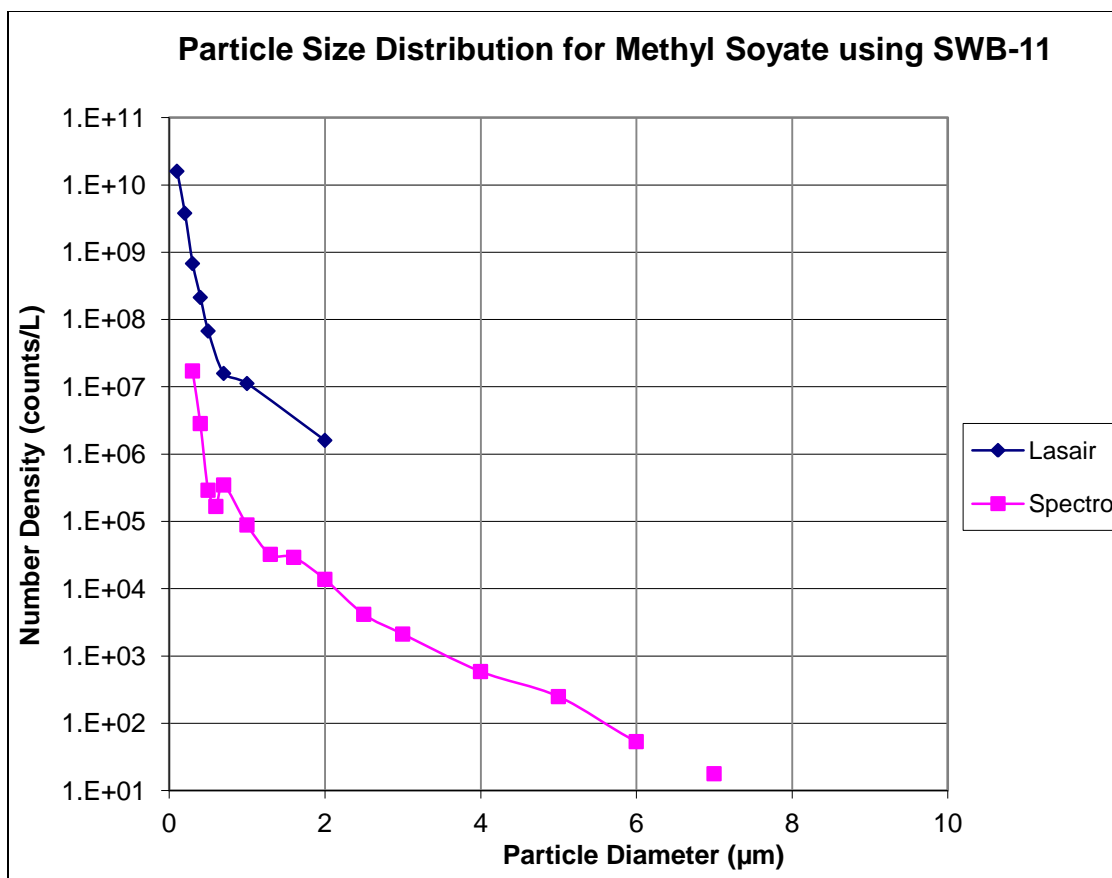


Figure 4.35 - Particle Size Distribution for Methyl Soyate from SWB-11 Based Obscurant Aerosol Generator

The same tests were repeated with the SWB-25 turbojet-based generator. The data, Figure 4.36, shows how similar the data can be between the petroleum-based fog oil and the biogenic methyl soyate. The shapes of the particle size distributions are nearly identical, but the methyl soyate gave higher number densities from 0.3 µm to 1 µm.

Another test was made to compare the particle size distribution data for methyl soyate generated using the JetCat P80 mounted on the angle iron stand versus the JetCat P80 mounted in the modular man-portable generator unit. There appeared to be some differences in the particle size distribution on this test, Figure 4.37, with higher particle

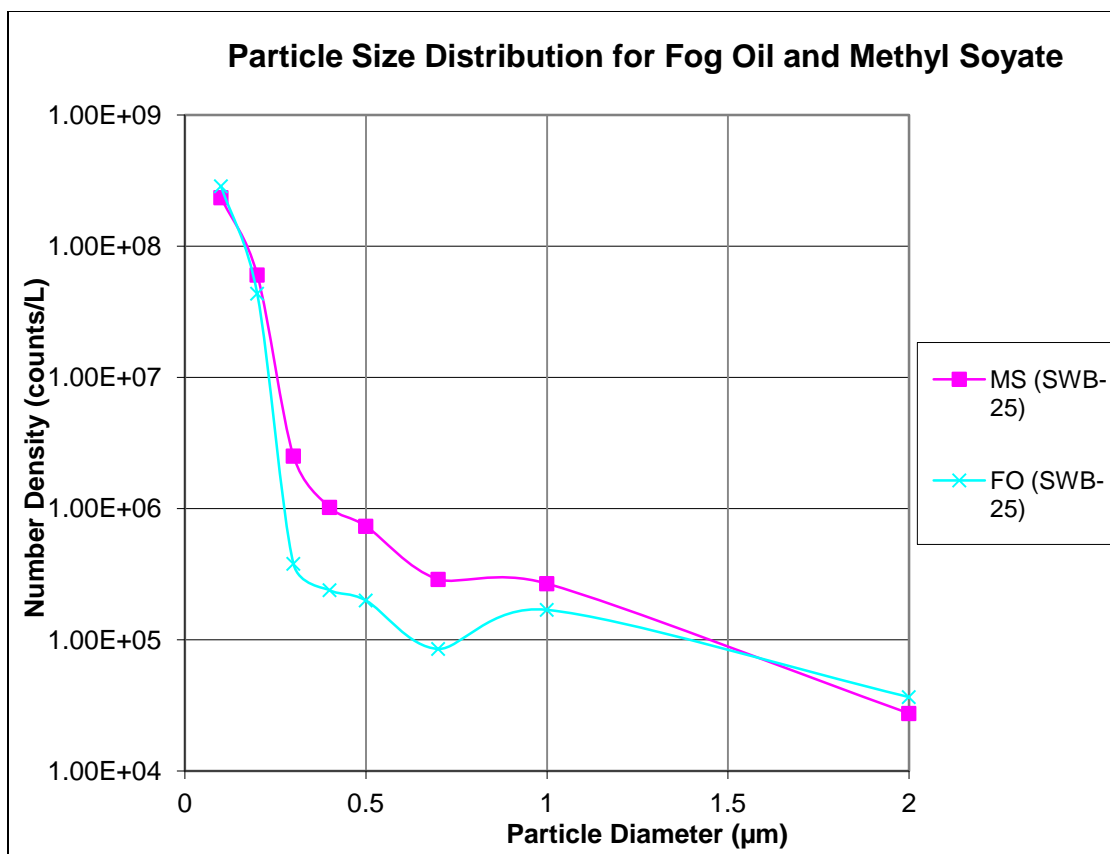


Figure 4.36 - Particle Size Distribution Obtained using Lasair OPC for Fog Oil and Methyl Soyate from SWB-25 Based Obscurant Aerosol Generator

counts at the smaller sizes below 5 µm and lower counts at the larger diameter size ranges. However, the visual quality was still excellent as well as the laser transmittance data from the modular generator on all future experiments. The differences could be attributed to the differences in configuration, where the modular generator is completely contained and may have a more restricted air flow that is possibly warmer from passing around the engine.

In order to help determine the maximum amount of methyl soyate that could be adequately aerosolized by the P80 turbojet-based generator some testing was conducted with different oil flow rates using the Laboratory High-Throughput Aerosol Testing

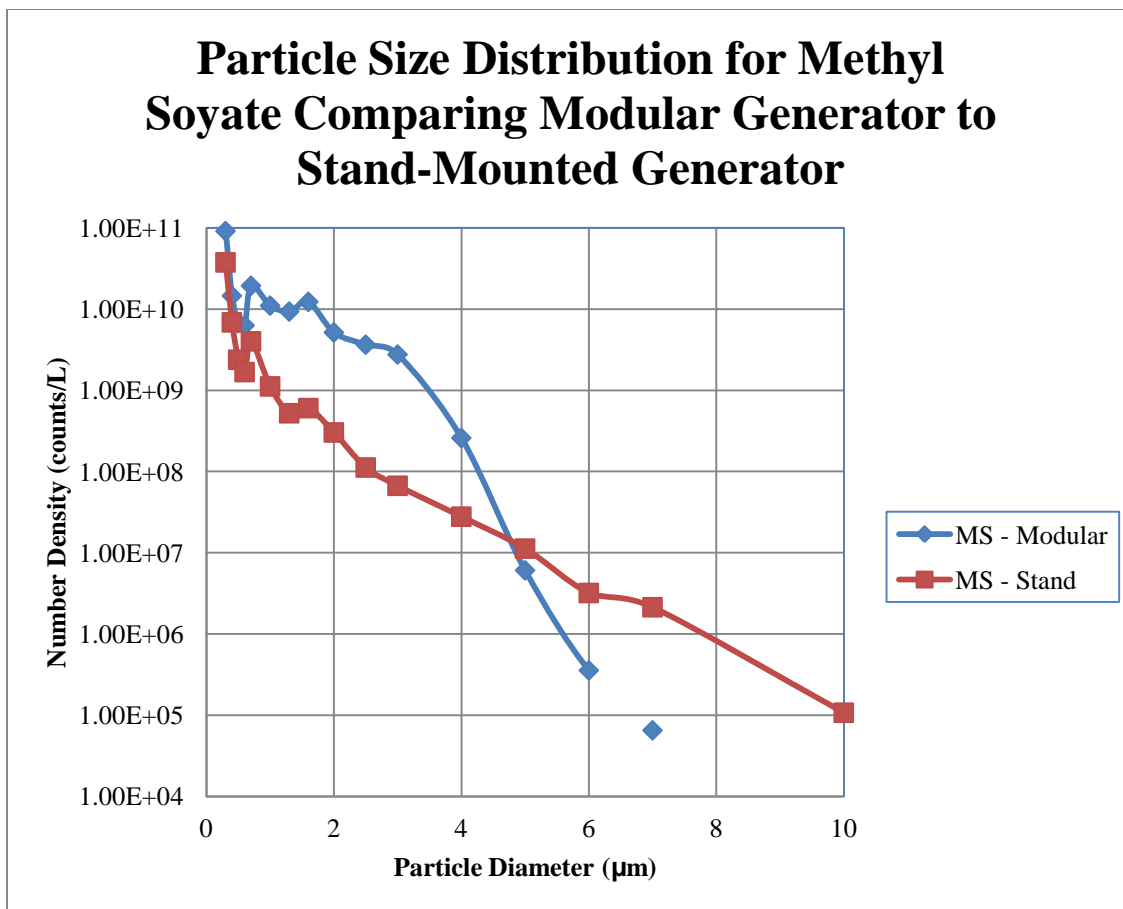


Figure 4.37 - Particle Size Distribution Obtained using Spectro OPC Comparing Methyl Soyate Aerosols from Modular versus Exposed SWB-11 Based Obscurant Aerosol Generator

Facility described in Section 4.2.5. On the Lasair OPC, Figure 4.38, it appeared that there were no significant advantages in the number densities with flow rates above 1 L/min, though the nature of the testing tube may skew the data. The aerosol is not given the opportunity to expand in volume normally as would occur during field tests. As a result, the volume of air within the testing tube becomes saturated, resulting in an abnormal number of interactions between oil droplets suspended in the air and causing a relatively large amount of oil to fall out of suspension. The Spectro OPC, Figure 4.39,

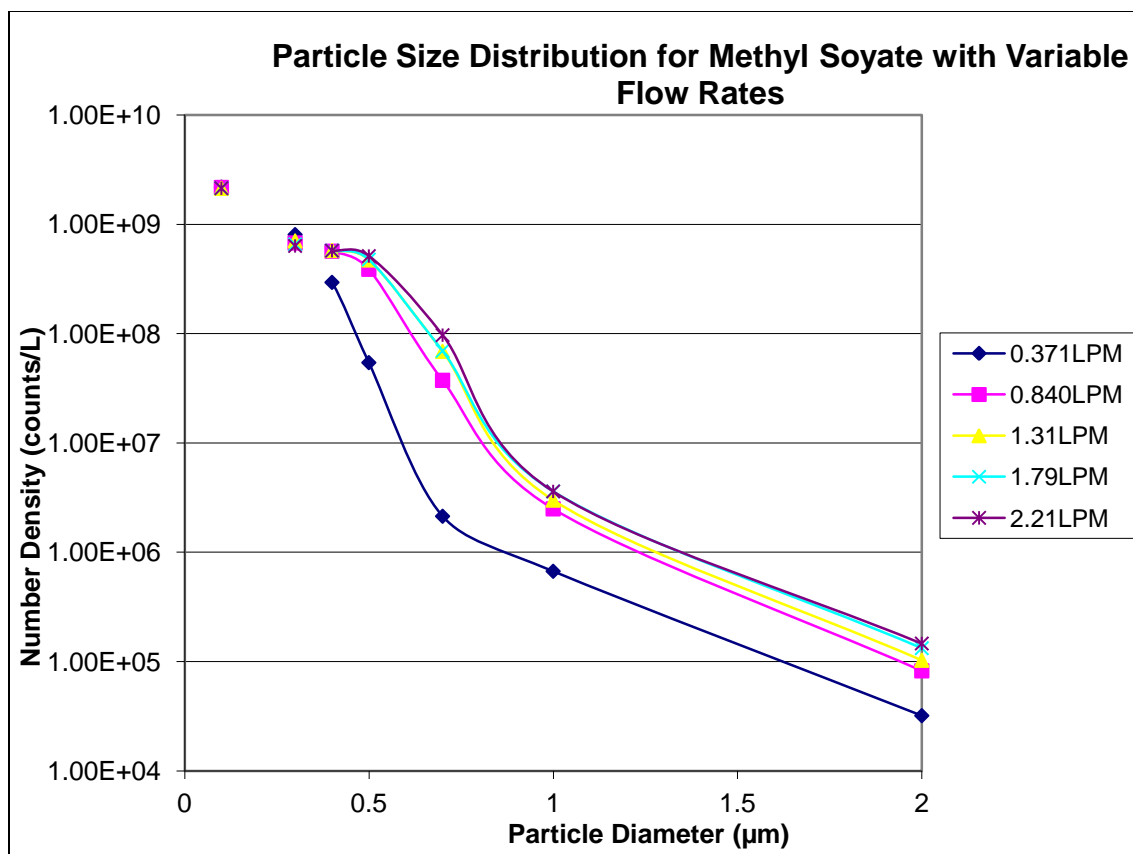


Figure 4.38 – Particle Size Distribution Obtained using Lasair OPC for Methyl Soyate using Different Oil Flow Rates

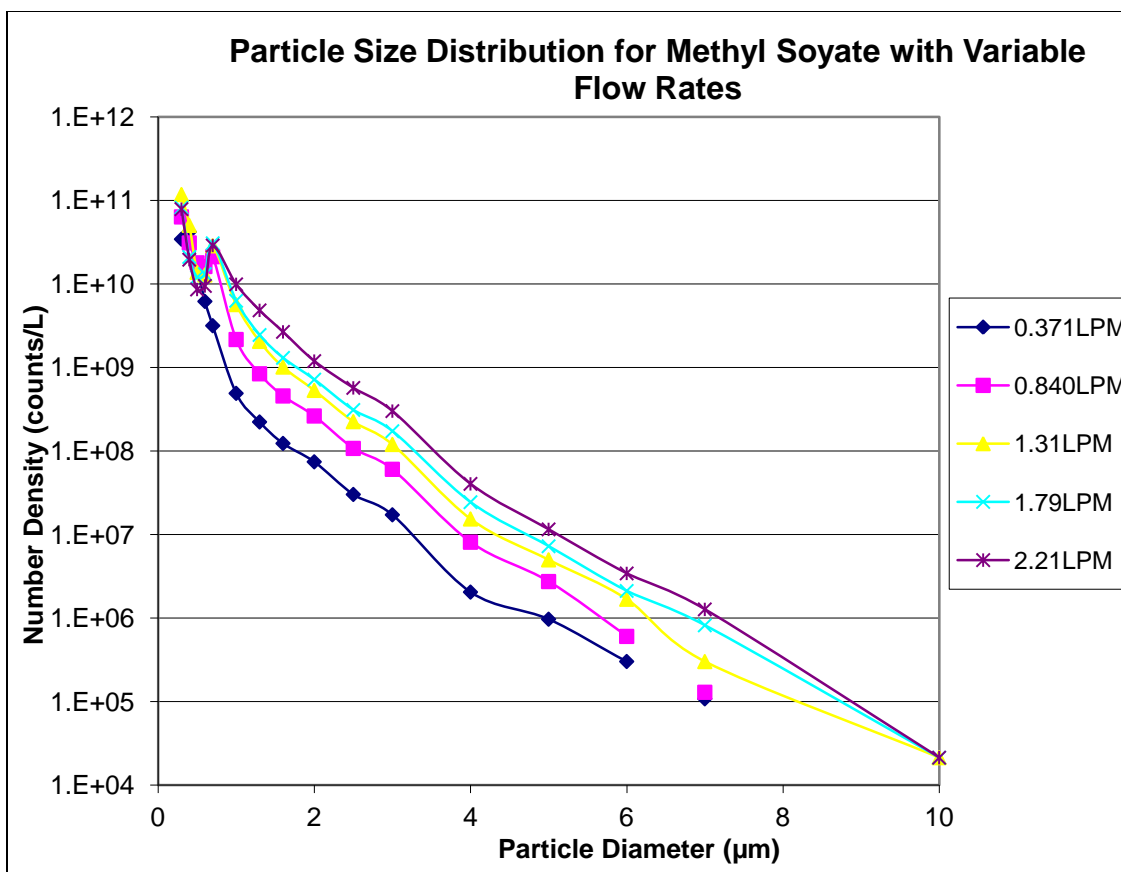


Figure 4.39 - Particle Size Distribution Obtained using Spectro OPC for Methyl Soyate using Different Oil Flow Rates

showed that the number of counts significantly increased with increasing oil flow rates at particle diameters of 0.6 µm and above. Laser transmittance values for different flow rates is shown in Figure 4.40, and similarly indicated that transmittance decreased at higher flow rates of oil being transformed into obscurant aerosols.

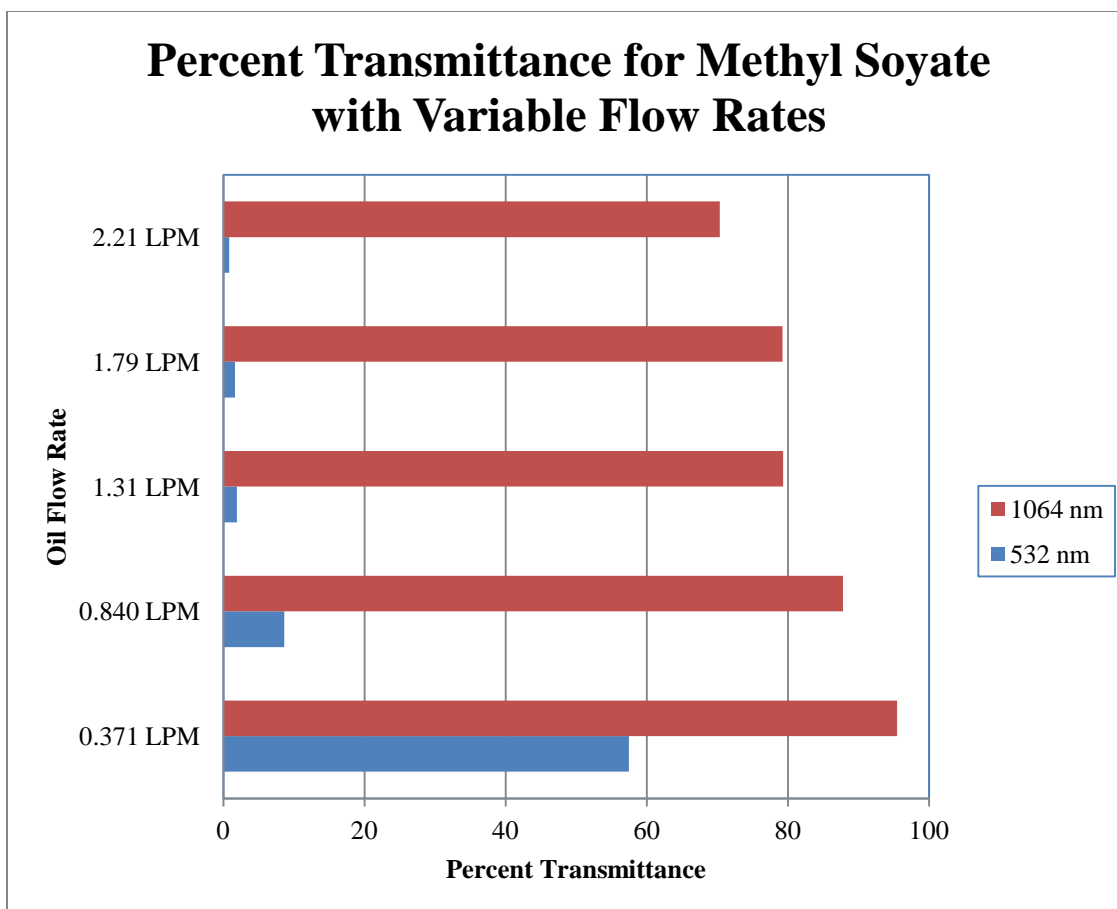


Figure 4.40 – Percent Transmittance of Visible and Near Infrared Radiation through Methyl Soyate at Different Oil Flow Rates

4.2.4. Comparison with M56. Testing was performed to directly compare the M56 Coyote generator with the SWB-11 turbojet-based generator. The SWB-11 had one sprayer nozzle connected for these tests, and the direct comparison was made for fog oil as given in Figures 4.41 and 4.42. As the tests were run it was visually distinct that the fog oil plume from the SWB-11 generator was thinner and less effective than the fog oil plume from the M56, found to be the result of a difference in shear viscosities between fog oil and methyl soyate in the oil pump mechanisms making methyl soyate be moved more efficiently. However, the methyl soyate plume from the SWB-11 was thicker and

more effective as an obscurant than the fog oil from the M56. Another difference noted between the two generators was the physical size. The SWB-11 generator was much smaller than the M56 unit as seen in Figure 4.43, and generally performed better on a size to output basis although the M56 can run for longer with its onboard fuel and obscurant oil capacities. It was also noted that although the SWB-11 was sometimes problematic to start due to its reliance on propane, it was still overall less problematic to start than the M56 used in our testing. The SWB-11 generator was also more portable and easier to reposition if the winds changed. Its stand only had to be rotated by hand, while the M56 required its Humvee be started and repositioned. It is also more difficult to place the M56 generator into a good position since it is limited to wherever its vehicle base can drive. The SWB-11 could be carried by hand through a forested area or through small alleyways in urban environments.

Another topic that had to be addressed was the difference in particle size distribution data comparing the use of one sprayer nozzle to the use of two sprayer nozzles on the JetCat P80 turbojet-based system. Fog oil saw an unexpected difference at 0.2 μm particle diameter, but otherwise both oils followed the expected trend of having a higher number density for all particle sizes as the number of sprayer nozzles was doubled and thus the amount of oil was doubled, shown in Figures 4.44 and 4.45.

4.2.5. Addition of Polystyrene. Large scale testing of methyl soyate with dissolved polystyrene originating from granular-type Styrofoam packagings was performed in laboratory and field environments. Testing in the laboratory used a special large diameter tube mounted atop a cart and rolled through an opened exterior window,

shown in Figure 4.46. The turbojet-based generator was placed at the end of this tube with the exhaust directed through the tube so everything could vent out the window.

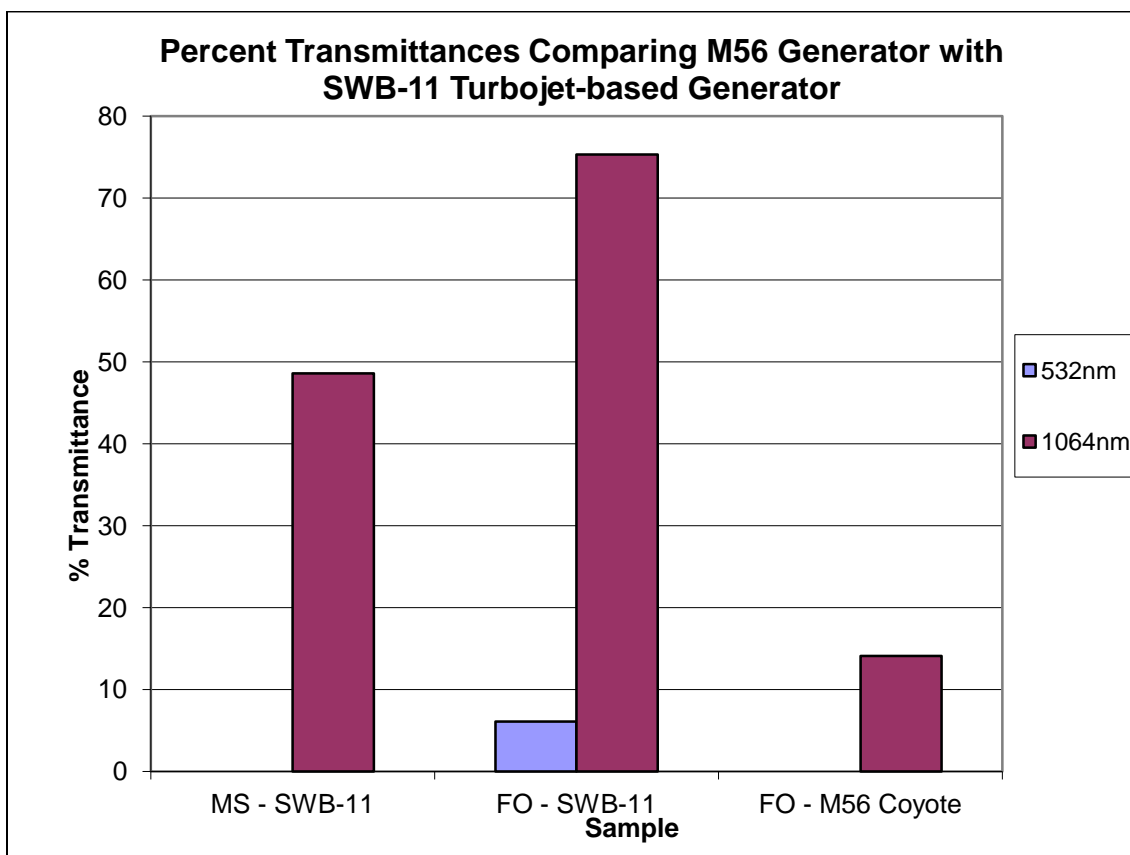


Figure 4.41 – Percent Transmittance Comparison of Visible and Near Infrared Radiation of SWB-11 Based Obscurant Aerosol Generator versus M56 Generator

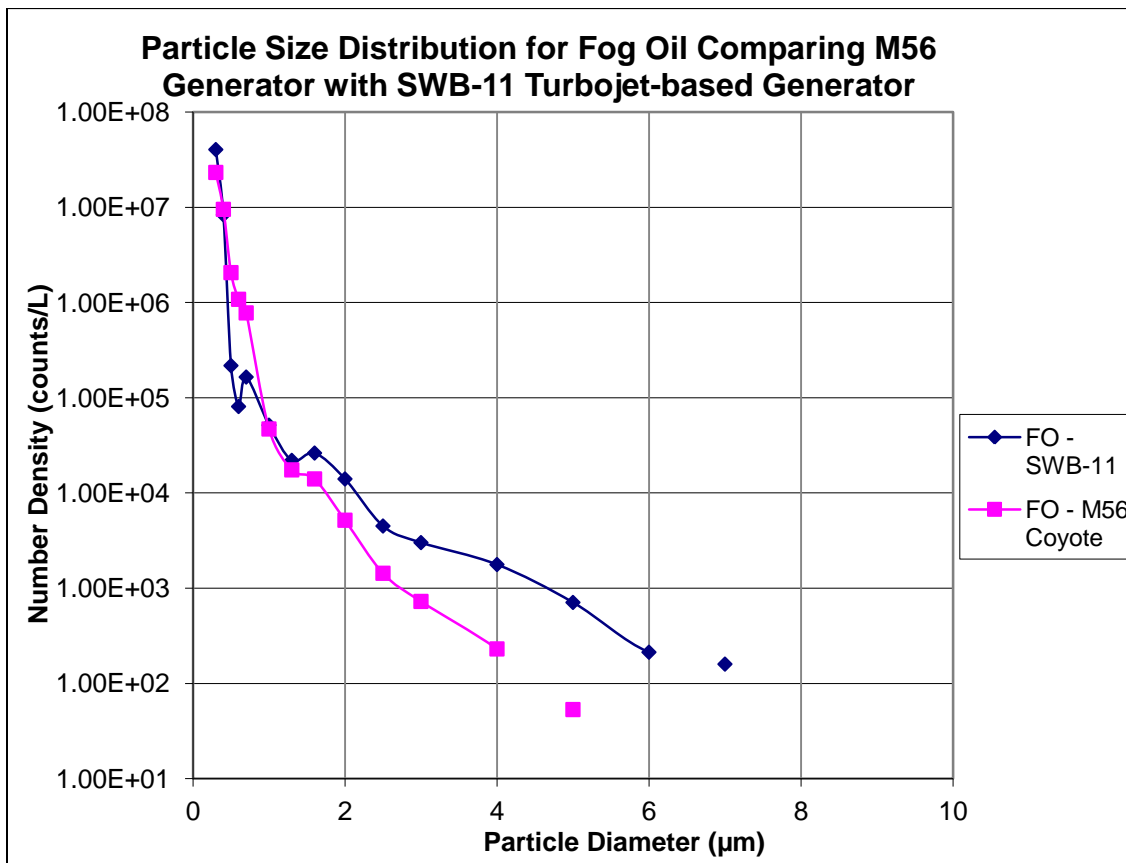


Figure 4.42 – Particle Size Distribution Comparison for Fog Oil from SWB-11 Based Obscurant Aerosol Generator versus M56 Generator



Figure 4.43 – Photograph of Relative Size Comparison of SWB-11 Based Obscurant Aerosol Generator versus M56 Generator

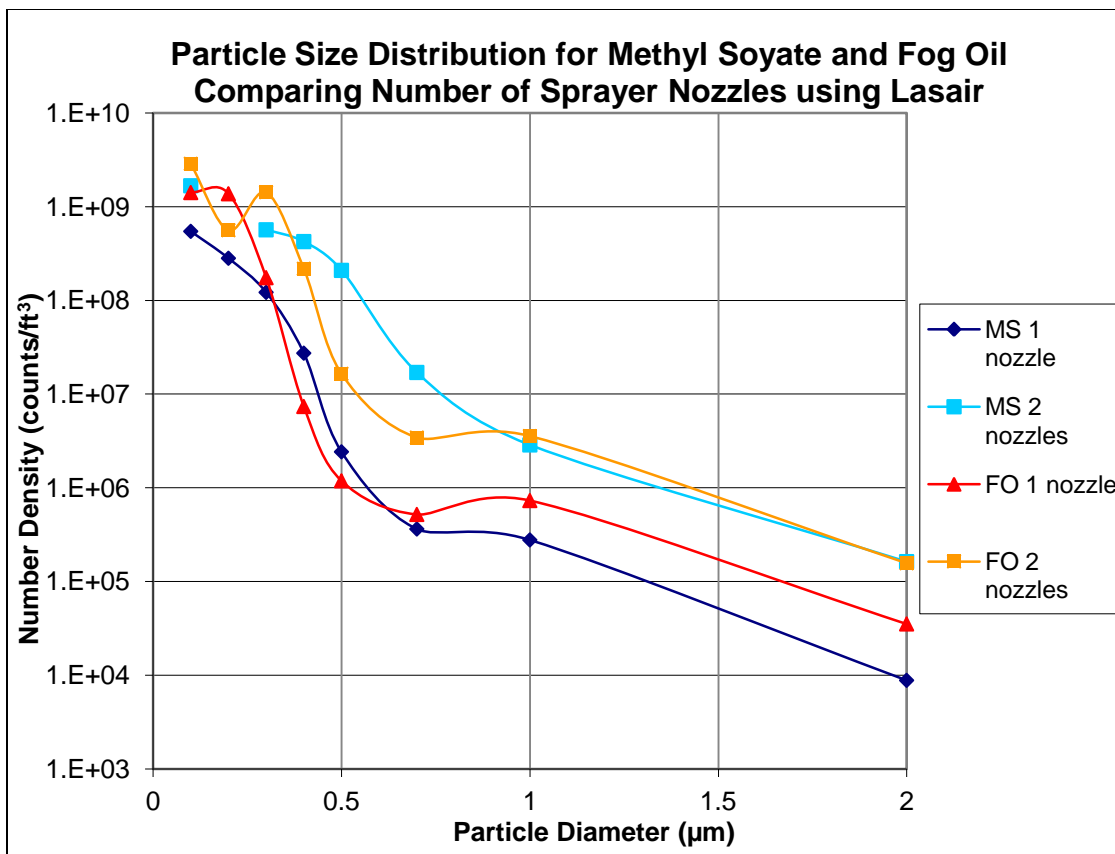


Figure 4.44 – Particle Size Distribution Data Obtained using Lasair OPC for Methyl Soyate and Fog Oil Comparing Different Numbers of Sprayer Nozzles

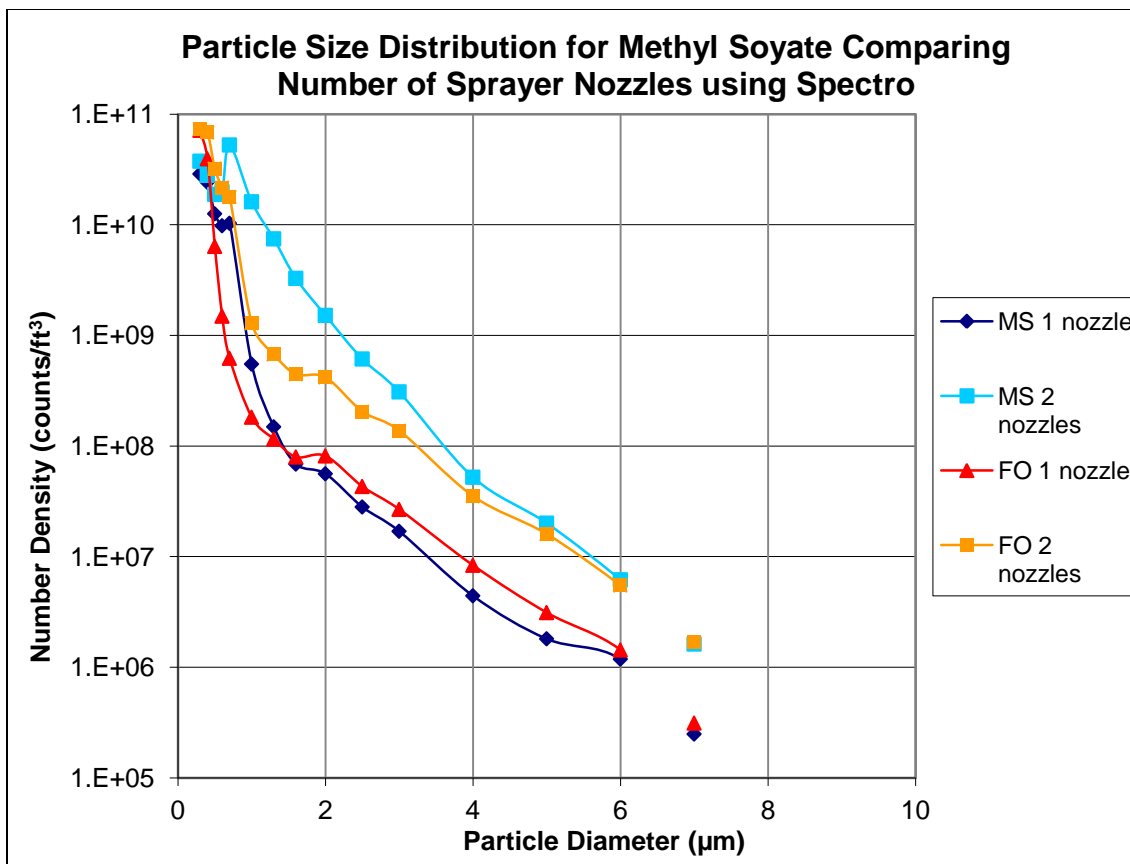


Figure 4.45 - Particle Size Distribution Data Obtained using Spectro OPC for Methyl Soyate and Fog Oil Comparing Different Numbers of Sprayer Nozzles



Figure 4.46 – Photograph of Laboratory High-Throughput Obscurant Aerosol Characterization Facility

The current laboratory testing setup was based around a galvanized steel tube having 3 meters length and 0.66 m (26 in) diameter. The steel tube was strapped with metal banding onto the top of a metal laboratory cart, with wooden blocks bringing the tube to a height suitable for venting the exhaust out the window. The wooden block spacers were three 10.16 cm (4 in) by 10.16 cm (4 in) pieces glued side by side, with a curve on the top to help maintain the steel tube's curvature. The interface between the wood blocks and the steel tube was lined with glass wool.

There were three temperature probes installed onto the sides of the steel tube at distances of 0.5 meter, 1.0 meter, and 2.0 meters from the inlet end. These temperature

probes were designed to allow measurements at user-defined distances perpendicular to the flow, ranging from the center of the steel tube and thus the center of the exhaust, out to the walls of the steel tube itself. This configuration allowed study of the temperature profile within the steel tube.

Two isokinetic sample ports were installed in the steel tube. They were made of quarter-inch copper tubing that had a gradual curvature so the inlet was close to the center of the steel tube. One was at a distance of 1.5 meters, and the other was closer to 2.5 meters. These sample ports allowed filter collection of aerosol samples for chemical analysis, and collection of aerosols for dilution and particle size distribution analysis. Cut into the side of the steel tube were two holes, one on either side at a distance of approximately 2.25 meters from the inlet end of the steel tube, with dimensions of 5.08 cm (2 in) by 10.16 cm (4 in). These rectangular holes allowed two lasers with wavelengths of 532nm and 1064nm to be directed through the plume of obscurant aerosol for light transmission measurements to be made for visible and infrared regions of the spectrum. The lasers were originally selected for long distance monitoring of light transmission in a field environment, but provided useful data in the laboratory as well. The lasers were mounted side by side behind a chopper, which sent a reference signal to a pair of lock-in amplifiers for modulating the detectors' voltage signals. These modulated signals were then sent into a data acquisition board and sent to a PC for processing by the LabView program. This program is set up to show the signal from both lasers on one voltage versus time plot, and record data at a rate of one hertz.

Another pair of windows was also installed onto the steel tube. These had round quartz lenses mounted within a round housing. One side had a tungsten filament light

bulb, and the other had a lens with fiber optics connecting it to the actual detector system. This spectrophotometer system was meant to allow continuous monitoring of a wide range of wavelengths spread over the visible and into the ultraviolet wavelengths of light. More data could be obtained about light transmittance due to the broader range of wavelengths recorded with this system as compared to the lasers' two defined wavelengths, but due to the difference in source intensity this apparatus was better suited for laboratory testing over small distances. To help prevent deposition of obscurant aerosol oils onto the quartz windows there was an air line attached which can pass a flow of sheath air over the lenses. However, this system was not used with the large amounts of obscurant aerosols produced because the light intensity was not strong enough to pass through the plumes.

Inside the steel tube was a rolling plate attached to a loop of steel wire tethered to pulleys at opposite ends of the tube. This plate could be positioned at any distance on the floor of the tube for the collection of deposited oil samples.

One set of testing investigated whether the amount of polystyrene dissolved in methyl soyate could significantly shift the particle size distribution, with polystyrene acting as a nucleation site for the formation of larger diameter aerosol particles capable of scattering longer wavelengths of electromagnetic radiation through Mie scattering of light. The first field test for polystyrene effectiveness used the SWB-11 generator. Its results indicated that the addition of polystyrene was disadvantageous in the production of obscurant plumes. Particle counts were generally lower for polystyrene-containing samples than for stock methyl soyate, and in general as the amount of polystyrene

increased the number densities of all but the smallest measured particle diameter were decreased. Data is shown in Figures 4.47, 4.48 and 4.49.

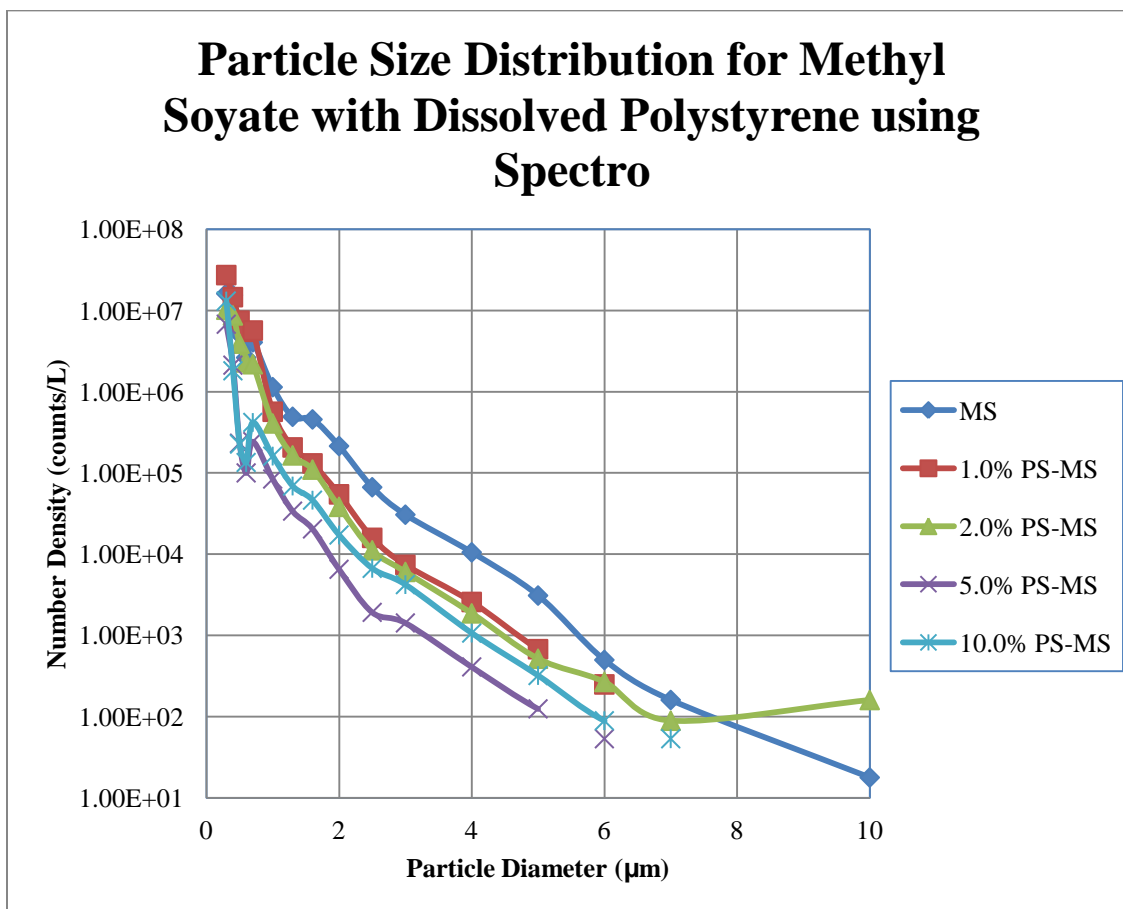


Figure 4.47 – Particle Size Distribution Data Obtained using Spectro OPC for Methyl Soyate with 0.0-10.0% Dissolved Polystyrene

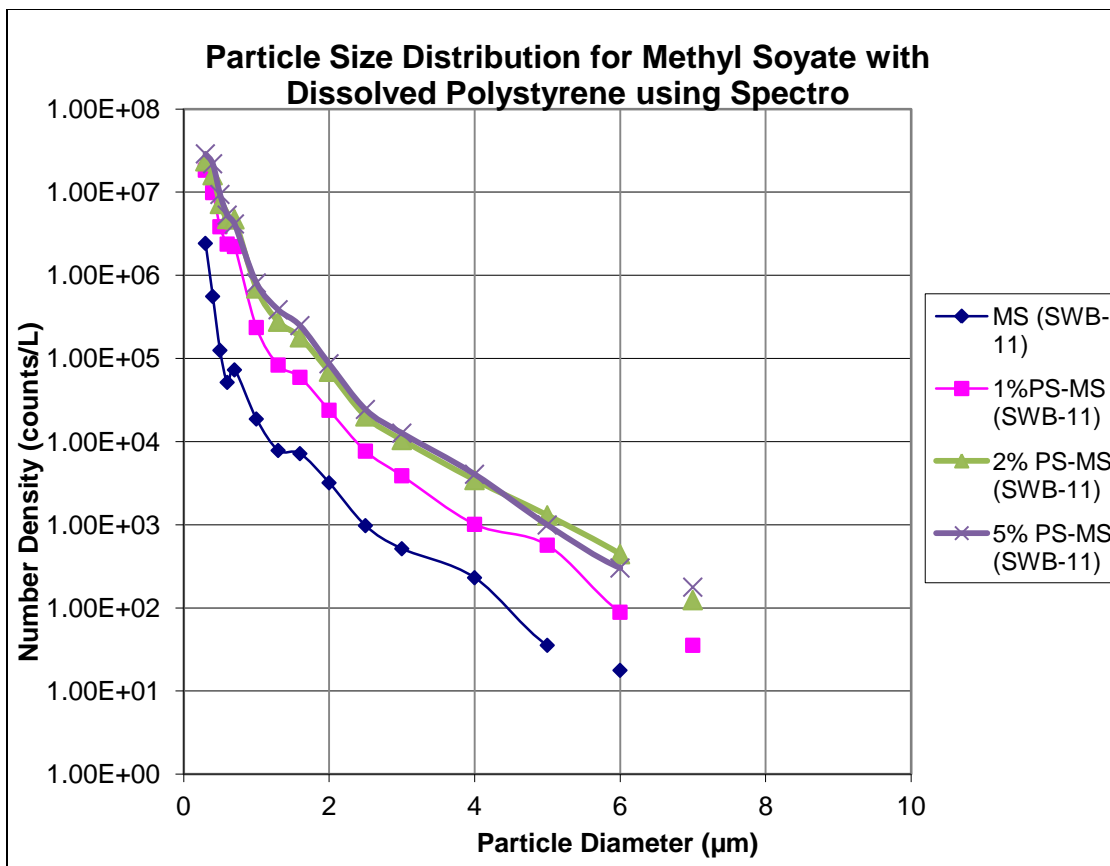


Figure 4.48 - Particle Size Distribution Data Obtained using Spectro OPC for Methyl Soyate with 0.0-5.0% Dissolved Polystyrene from SWB-11 Based Obscurant Aerosol Generator

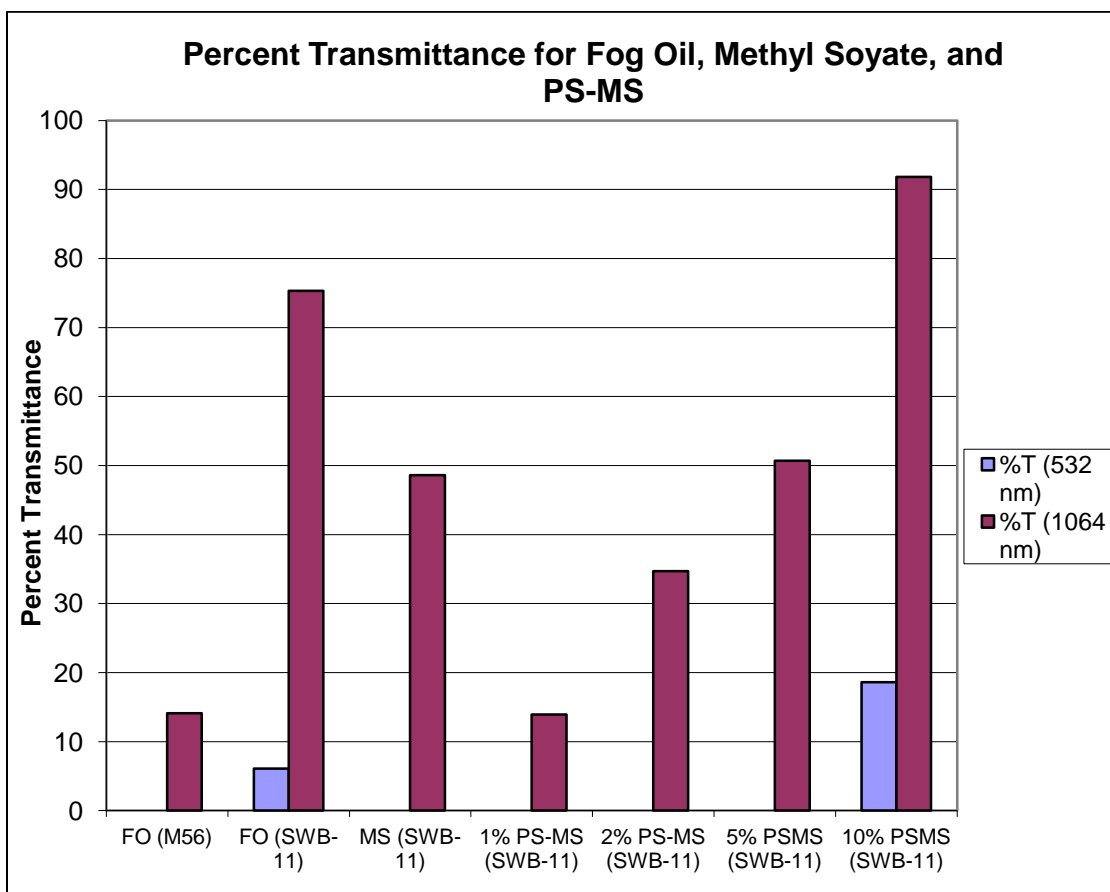


Figure 4.49 – Percent Transmittance Comparisons of Visible and Near Infrared Radiation through Fog Oil, Methyl Soyate, and 0.0-10.0% Polystyrene-MS Blends

Methyl soyate containing 0.5%, 1.0%, 2.0%, 3.0% and 4.0% polystyrene by mass was run through the JetCat P80-based obscurant generator and compared against standard methyl soyate. This data, Figures 4.50 and 4.51, suggested that as the amount of polystyrene increased, there was a larger number of particles produced at higher particle diameters, contrary to what laboratory scale generation techniques showed. This could be attributed to the aerosol generation technique. With the laboratory scale tubular furnace-based generator the oils were confined in a long heated tube which provided a

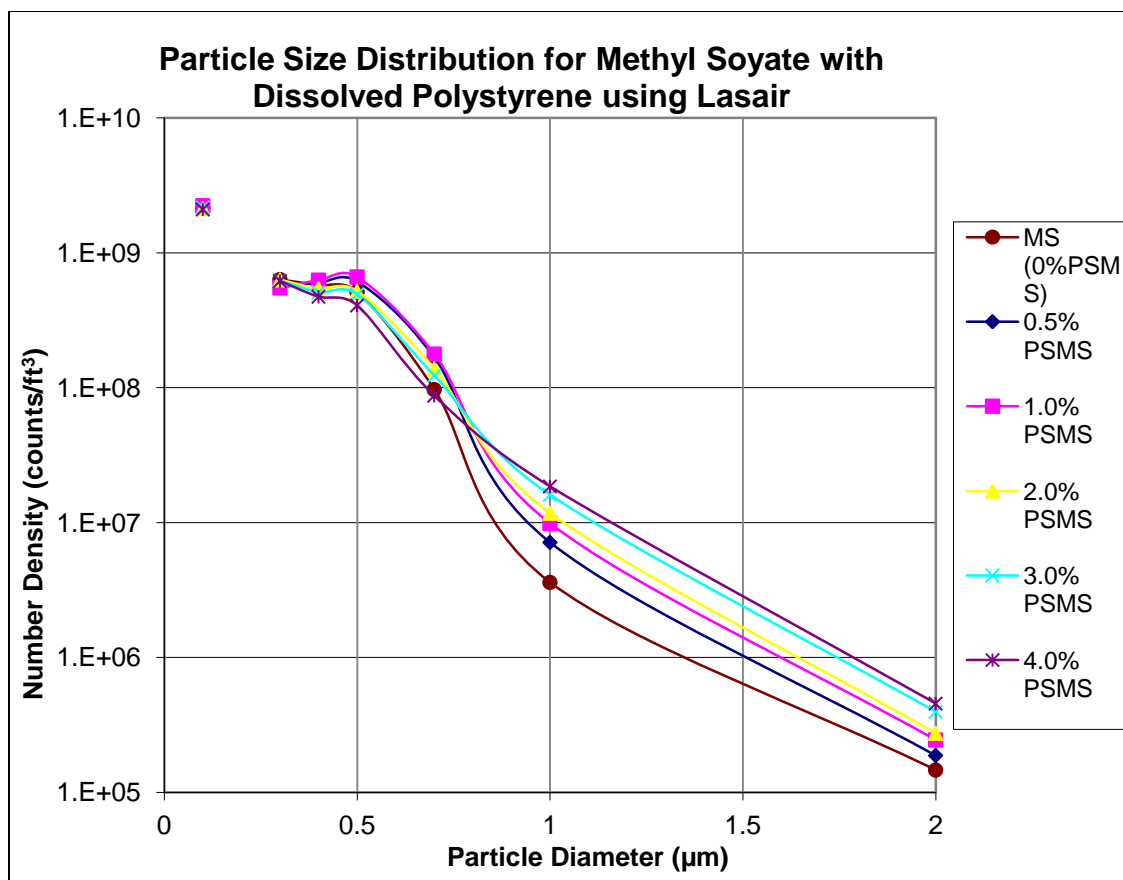


Figure 4.50 – Particle Size Distribution Data Obtained using Lasair OPC for Methyl Soyate with 0.0-4.0% Dissolved Polystyrene

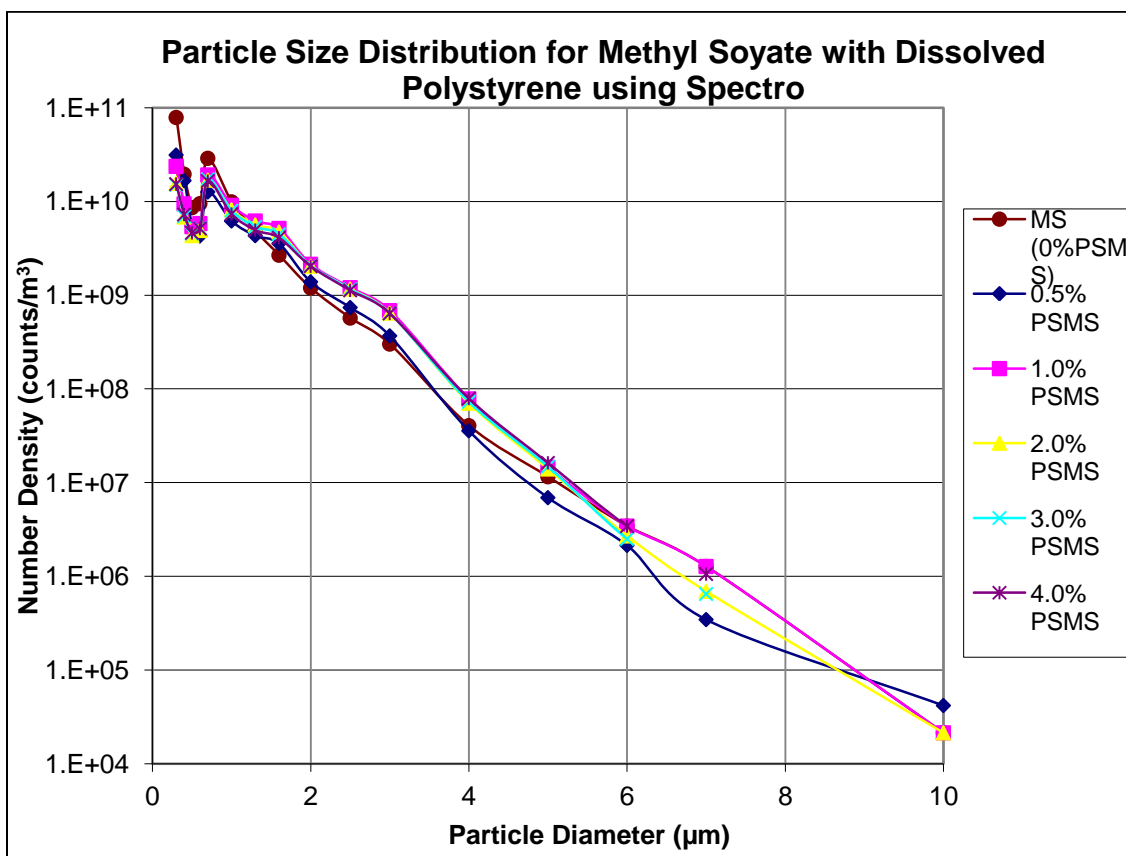


Figure 4.51 - Particle Size Distribution Data Obtained using Spectro OPC for Methyl Soyate with 0.0-4.0% Dissolved Polystyrene

large surface area onto which the oil and polymer could interact and be lost. With the turbojet-based generator the oils were kept outside of the heat until after being sprayed, and then were dispersed into ambient air with no contact surfaces. However, the laser transmittance data, Figure 4.52, did not reflect this difference in particle size distribution, and indicated that perhaps a very low concentration of 0.5% polystyrene may enhance particle size distribution shifts as well as lesser percent transmittances of visible and near infrared light. It was possible that the increased percentages of polystyrene concentration may have increased the viscosity of the oil to an extent that it could not be pumped as

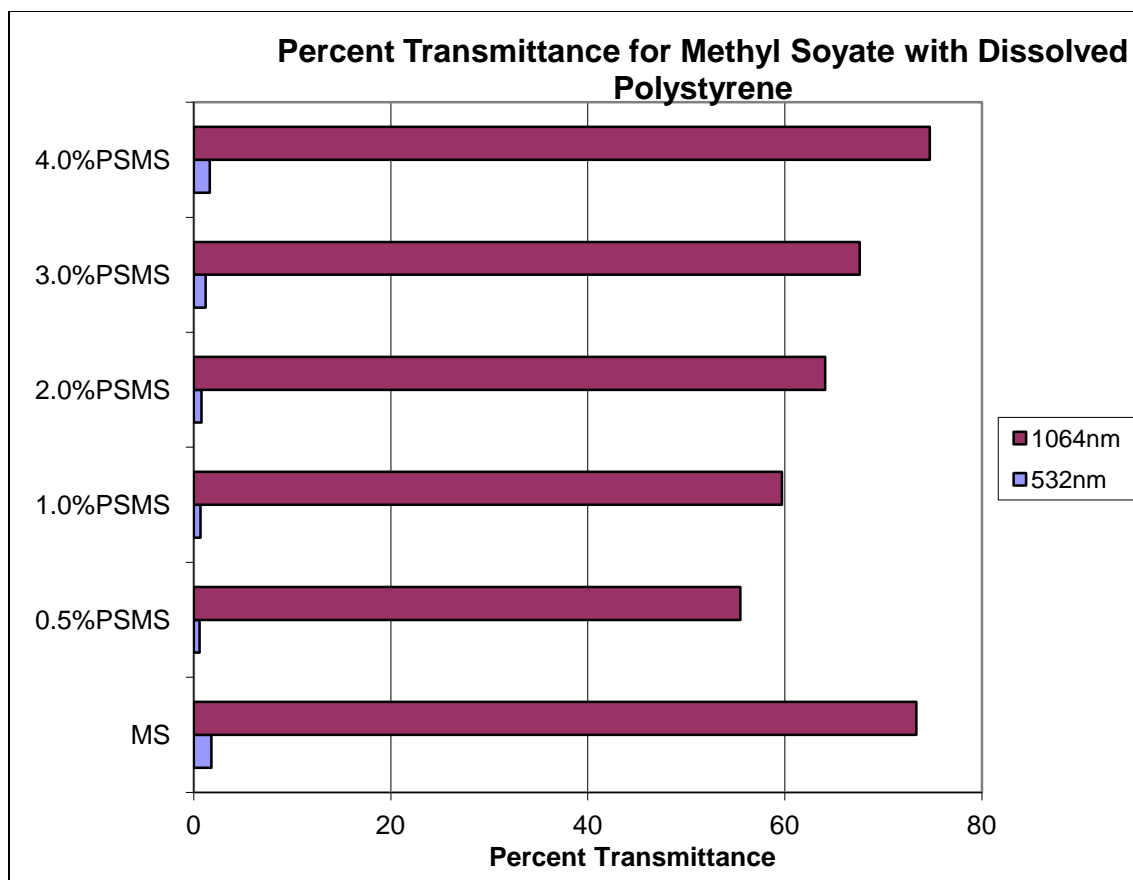


Figure 4.52 – Percent Transmittance of Visible and Near Infrared Radiation through Methyl Soyate with 0.0-4.0% Dissolved Polystyrene

well, resulting in a decreased amount of aerosolized oil which was counterproductive to the benefits of adding the polymer. Additional data may be found in Figures 4.53 and 4.54. Figure 4.55 shows testing being conducted in the aerosol characterization facility.

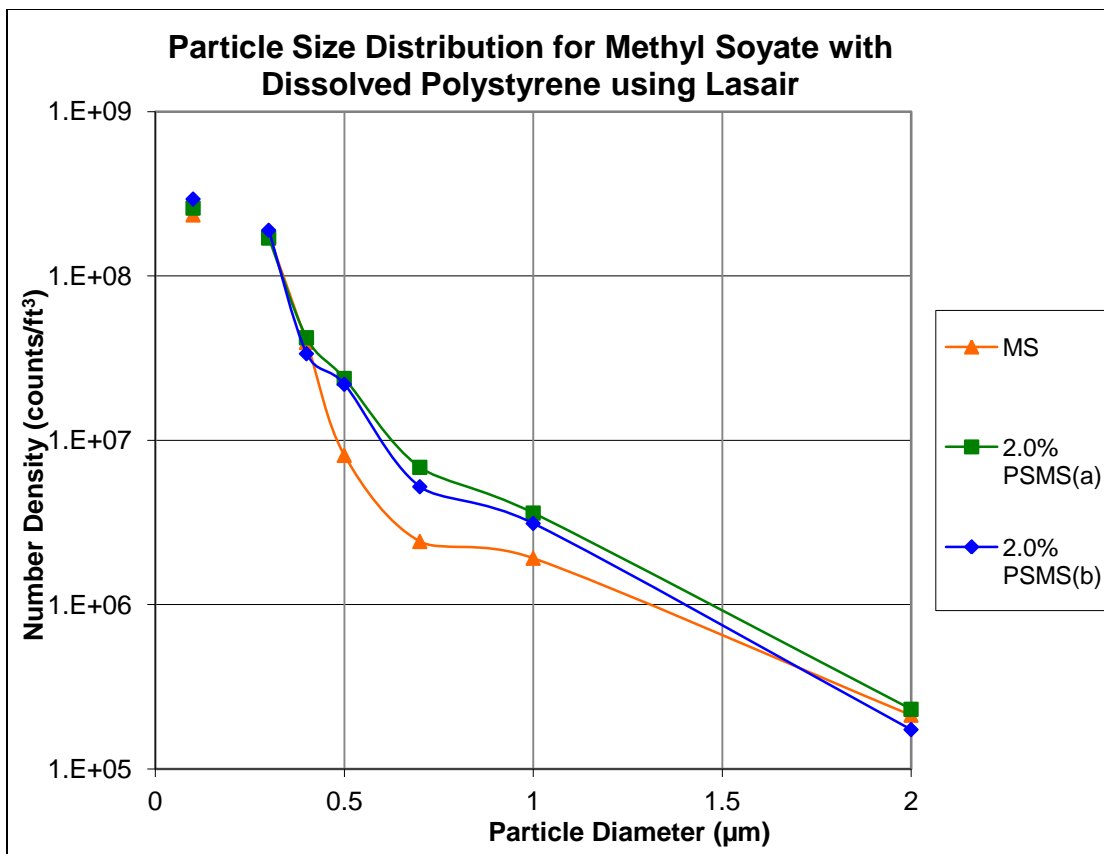


Figure 4.53 – Particle Size Distribution Obtained using Lasair OPC for Methyl Soyate with 0.0-2.0% Dissolved Polystyrene

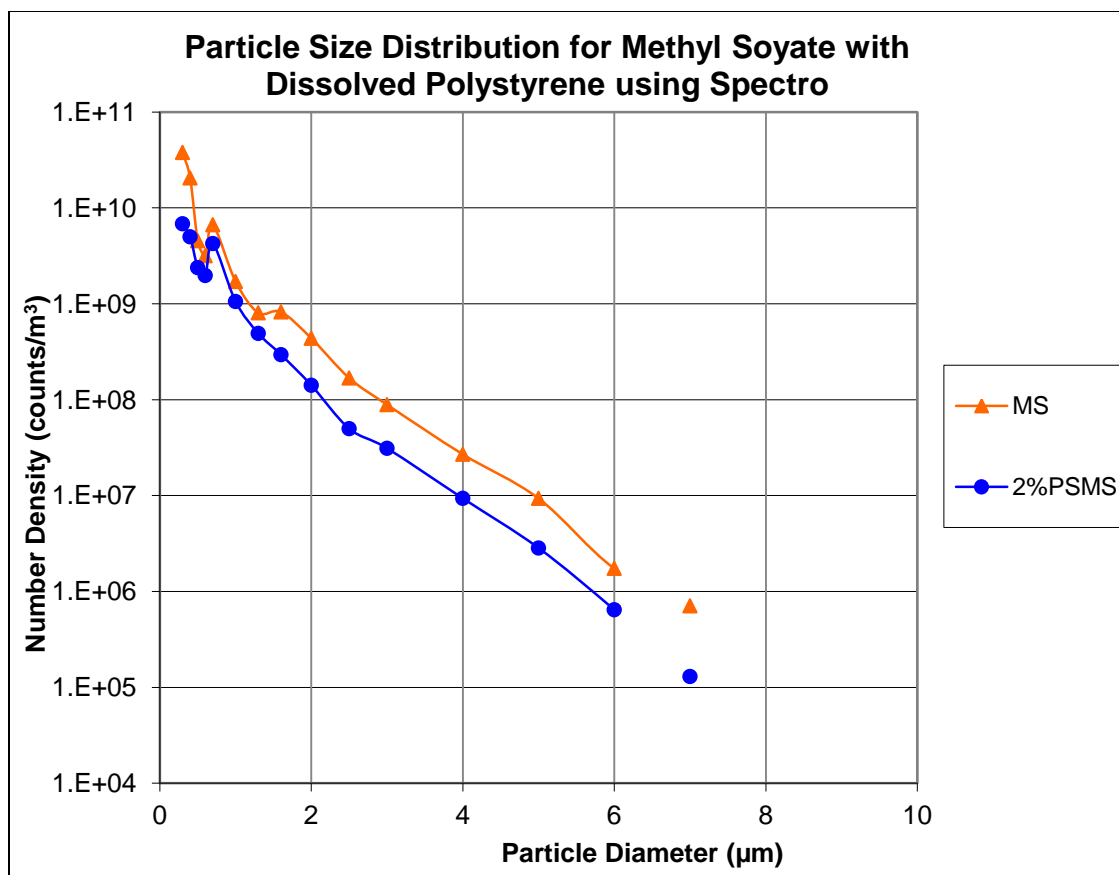


Figure 4.54 - Particle Size Distribution Obtained using Spectro OPC for Methyl Soyate with 0.0-2.0% Dissolved Polystyrene



Figure 4.55 – Photograph of Obscurant Aerosol Passing Through the Laboratory High-Throughput Aerosol Characterization Facility

Another set of tests were run in a field environment to compare results, but the set appeared much more random and had less of a trend, calling into doubt whether polystyrene-containing methyl soyate samples did in fact see any benefits from the addition of polymer to the oil. This data, reflected in Figures 4.56, 4.57 and 4.58, suggested that perhaps there were more particles created below $0.4\ \mu\text{m}$ diameters and more around $1.0\ \mu\text{m}$ diameters, with fewer particles created in the upper end of the visible wavelength regions and fewer at sizes of $2.0\ \mu\text{m}$ diameters. It is possible that the variability of field conditions such as unstable wind speed and directions led to the

inconsistent data, but no consistent trend was established for polystyrene-containing methyl soyate samples during field tests. Figure 4.59 shows a typical scene during field testing.

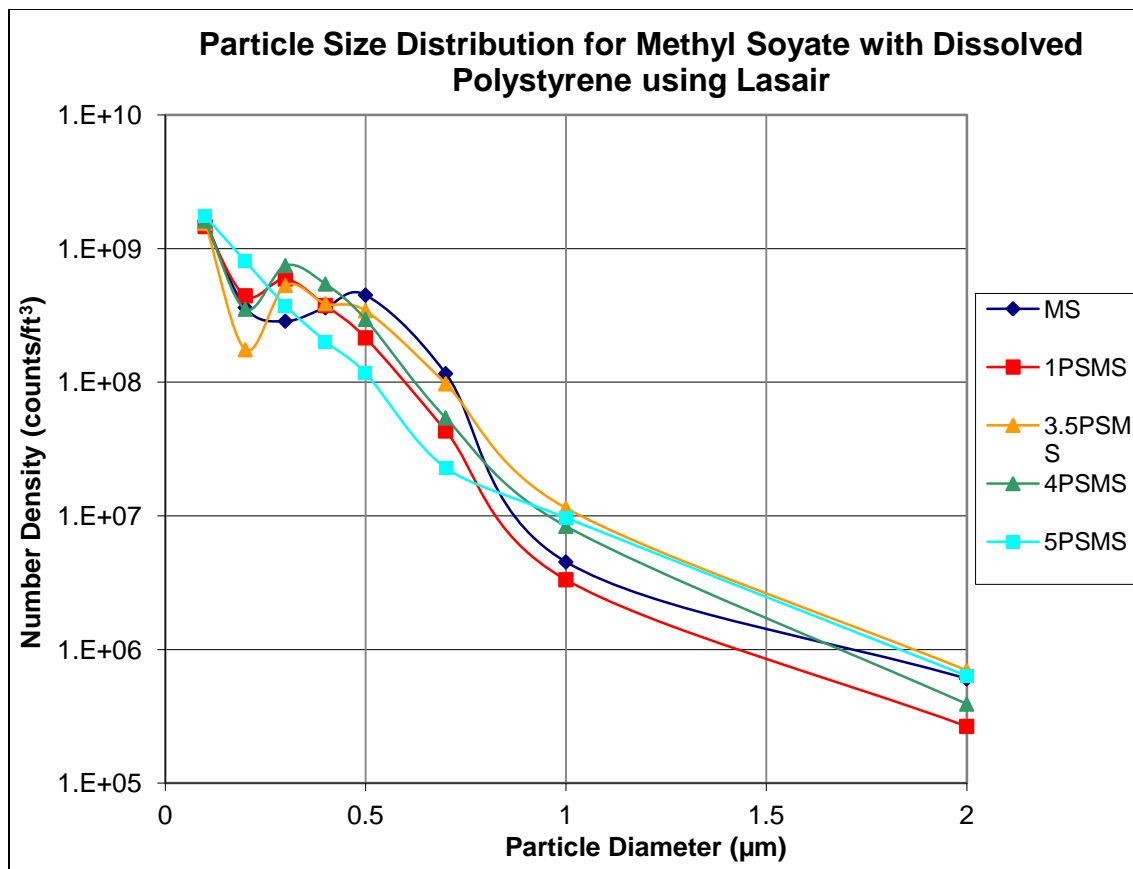


Figure 4.56 - Particle Size Distribution Obtained using Lasair OPC for Methyl Soyate with 0.0-5.0% Dissolved Polystyrene

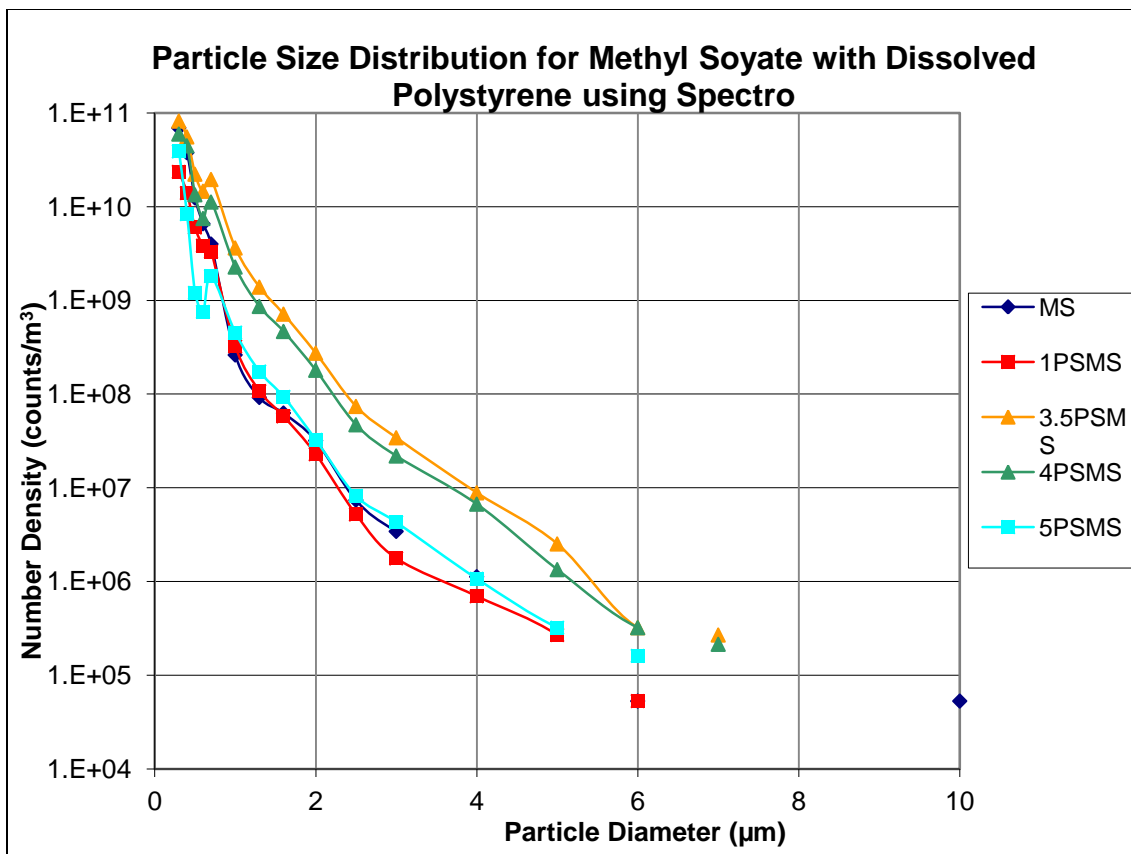


Figure 4.57 - Particle Size Distribution Obtained using Spectro OPC for Methyl Soyate with 0.0-5.0% Dissolved Polystyrene

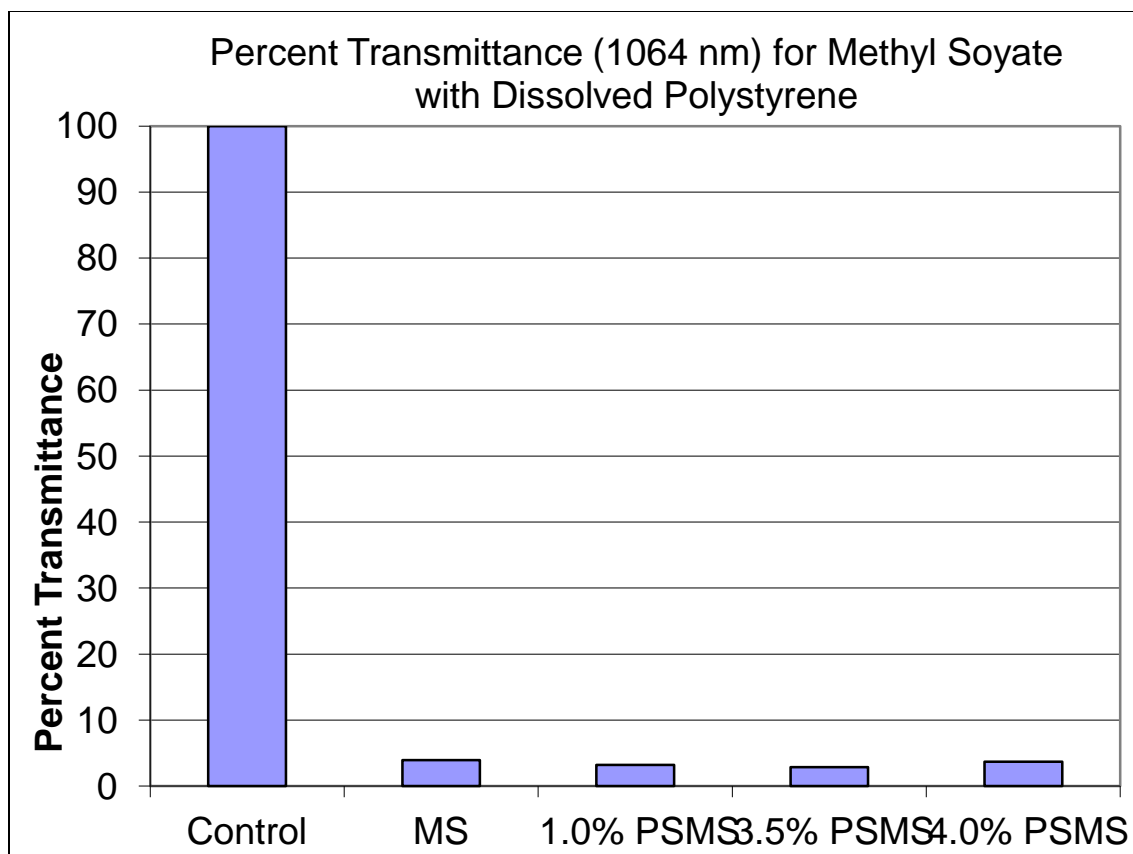


Figure 4.58 – Percent Transmittance of Near Infrared Radiation through Methyl Soyate with 0.0-4.0% Dissolved Polystyrene



Figure 4.59 – Photograph of Field Testing in Progress

4.2.6. Aerosol Deposition & Chemical Transformation Data. The length of the engine exhaust pipe was studied to determine whether it had any effect on the amount of unaerosolized oil or rate of oil deposition shortly after exiting the generator. An array of seven aluminum foil panels was staked out on a field, described by Figure 4.60, with the first plate approximately 4.6 meters (15 ft) downwind followed by two more plates at 9.1 m (30 ft) and 13.7 m (45 ft). Another two line of plates extending 13.7 m (45 ft) long were set up so their ends were 5.8 m (19 ft) away from the centerline, with plates at 9.1 m (30 ft) and 13.7 m (45 ft) as shown in the illustration. Each foil plate was 0.45 m (18 in) wide and 0.91 m (36 in) long. After exposure, the plates were picked up and folded to contain the deposited oils and returned to the laboratory where they were rinsed with aliquots of hexane three times and collected in a rotovap flask for removing most solvent, followed by transfer to preweighed glass vials for complete drying under nitrogen gas. It was found that the total amount of oil collected for each tube length increased as the length of the tube increased. The total amount of oil collected on all seven plates weighed 0.2114 g for the 8.89 cm (3.5 in) long tube, 0.5873 g for the 17.78 cm (7.0 in) long tube, and 0.9935 g for the 35.56 cm (14 in) long tube. The highest amount of deposited oil on any one foil plate was consistently the plate located 9.1 m (30 ft) directly behind the engine.

These collected oil samples were also dissolved in isooctane and analyzed by both GC-FID and GC-MS to check whether there were any chemical transformations as a result of heating and aerosolization. The stock methyl soyate used in this testing averaged a composition of 11.4% C16:0, 4.7% C18:0, 24.2% C18:1, 53.6% C18:2, and

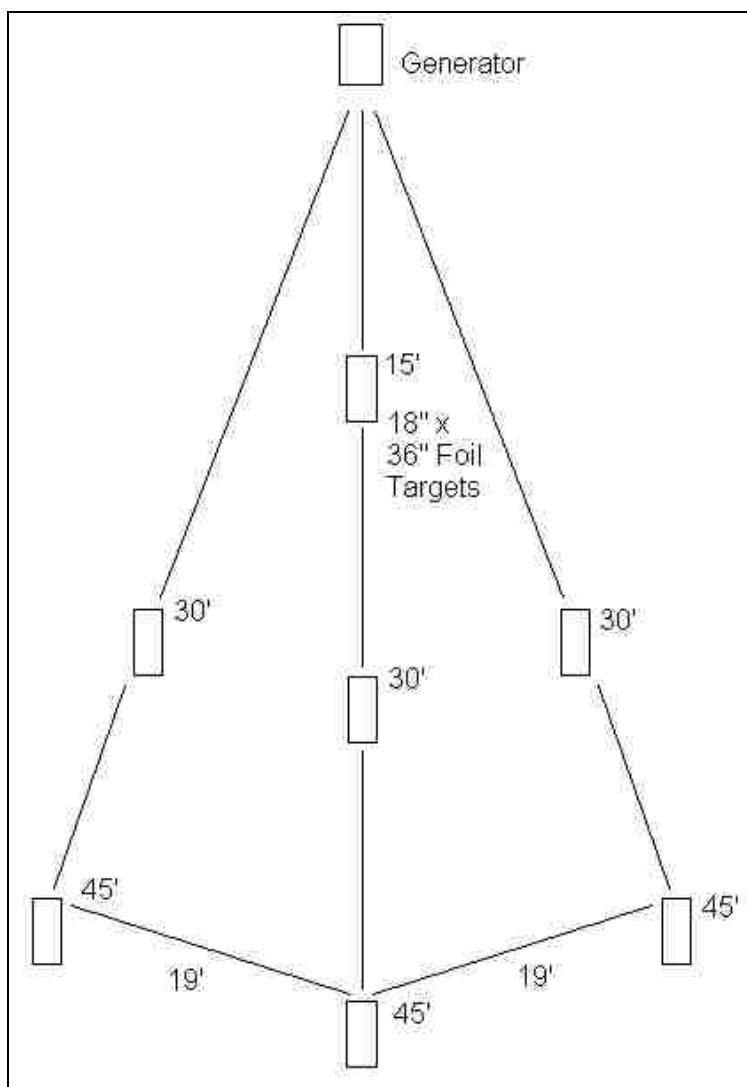


Figure 4.60 – Diagram of Aerosol Deposition Field Test Layout

6.2% C18:3. After being exposed to aerosol generation conditions, the ratios changed to approximately 20% C16:0, 10% C18:0, 44% C18:1, 25% C18:2, and 1% C18:3. Some of the long chain polyunsaturated compounds degraded and resulted in more shorter chain saturated and lesser unsaturated compounds, as expected by exposure to the high generator temperatures. Air samples were also taken and analyzed in the laboratory, but no hazardous byproducts were detected as a result of the aerosolization process.

4.2.7. Performance at Simulated Urban Warfare Area. The SWB-11 and JetCat P80-based prototype generators were taken for demonstration at a simulated urban warfare area at Fort Leonard Wood, Missouri. Multi-story buildings lined both sides of several two-lane streets, and the JetCat P80-based generator was used in the demonstration with a single nozzle. Military representatives were on hand for the demonstration. The engine was easily started and the system was run with methyl soyate. A thick white plume swept down the street toward a target structure and easily obscured the building within the few minutes it was running. The plume lingered for a short time before finally being carried away by a breeze. This demonstration is depicted in Figures 4.61, 4.62 and 4.63.

4.2.8. Remote Operation on ROV. One of the two prototype man-portable modular turbojet-based obscurant generators produced in this research was fastened onto the rear deck of an eight-wheeled amphibious LandTamer all terrain vehicle. This vehicle had previously been fitted with radio controlled operation, and provided an ideal platform for the demonstration of a remotely operated smokescreen generator application. The vehicle was taken to Wurdack Farm in Cook Station, Missouri for the demonstration. After starting the LandTamer, the generator was remotely started and the vehicle was remotely driven about 20 m across the field. Once in position the generator engine was ramped to full RPM and the obscurant was engaged with dual obscurant sprayer nozzles. While the obscurant was on, the vehicle was again remotely driven, shown in Figures 4.64, 4.65 and 4.66.



Figure 4.61 – Photograph of Fort Leonard Wood Simulated Urban Combat Site Before Obscuration with JetCat P80 Based Obscurant Aerosol Generator



Figure 4.62 - Photograph of Fort Leonard Wood Simulated Urban Combat Site During Obscuration with JetCat P80 Based Obscurant Aerosol Generator



Figure 4.63 - Photograph of Fort Leonard Wood Simulated Urban Combat Site After Obscuration with P80 Based Obscurant Aerosol Generator



Figure 4.64 – Photograph of Radio Controlled Prototype Modular Obscurant Aerosol Generator Mounted to Radio Controlled Amphibious Vehicle



Figure 4.65 – Photograph of Obscuration of a Farm in a Valley Using Prototype Modular Obscurant Aerosol Generator



Figure 4.66 - Photograph of Obscuration of a Farm in a Valley Using Prototype Modular Obscurant Aerosol Generator, After Plume Dissipation

After the test on the LandTamer was completed, it was brought to the staging area and placed next to another JetCat P80-based generator mounted on the stand. Another demonstration was performed to demonstrate the simultaneous operation of two systems side by side, shown by Figures 4.67 and 4.68. A massive plume of obscurant formed downwind where the two individual plumes combined and showed the capabilities of the system if multiple generator units would be run along a row. One intention of this research was to create a small, portable, modular unit that could potentially be attached to any vehicle in the military's arsenal. If every other vehicle had a generator engaged, or



Figure 4.67 – Photograph of Simultaneous Obscuration by Prototype Modular Obscurant Aerosol Generator on Amphibious Vehicle and Exposed Obscurant Generator



Figure 4.68 – Photograph of Obscuration of a Farm in a Valley with Simultaneous Application of Two JetCat P80 Based Generators

every third vehicle in a convoy, an entire valley could easily be covered by obscurant plumes.

Another demonstration was held in which the Edgewood Chemical and Biological Center at Aberdeen, Maryland loaned the second prototype modular generator to a company to attach to the roof of their prototype tracked vehicle. This demonstration aired on cable television and demonstrated how the system could be tethered to a fast moving vehicle passing over hilly fields and muddy roads while still performing

flawlessly. However, one clip showed a flame exiting the generator which is a result of improperly engaging the obscurant sprayer nozzles while the turbojet is at an idle RPM. If the engine was not running at full speed the sprayed obscurant oil could not move away from the engine's high temperature exhaust before oil ignition, resulting in a long flame. These demonstrations showed the applicability of a remotely controlled obscurant aerosol generator on various types of moving vehicles. It was important that obscurant not only be generated by a stationary source, but by a mobile source as well. It also illustrated that although the prototypes were not built with military specification electrical connectors, they could still withstand a fair amount of stress.

4.2.9. Single-Fluid Test. One goal was to create a generator that used the least number of fluids while maintaining an environmentally friendlier alternative to fog oil. The methyl soyate used as an obscurant oil is commercially available as biodiesel, which the diesel engines of Humvees and other military vehicles should be able to run on as a fuel source. It was unknown whether the JetCat P80 could run on methyl soyate as its fuel source, so one of the engines was tested using methyl soyate as the fuel combined with the standard 5% turbine lubricating oil. It was found that the P80 could not start normally on methyl soyate, though it could be switched over to methyl soyate from Jet-A after it was already running. This was further investigated by creating a bypass valve between the engine fuel routing solenoid valve and the engine itself, so the amount of fuel being sent to the engine's startup line could be varied manually despite the fuel pump programming being optimized for Jet-A. It was found that by beginning the startup sequence using a much reduced flow of methyl soyate to the startup line, the engine could

begin to ignite. The valve was slowly opened until a full normal oil flow reached the engine. Once the engine was fully started and had reached its idle RPM it could function normally running fully on methyl soyate. The bypass valve had to be used because too much methyl soyate was reaching the engine too quickly for the amount of heat provided by the starter ignition glow stick and could not properly ignite. By reducing the flow, there was a more appropriate heat to fuel ratio to allow for ignition but the oil flow still had to be gradually increased to prevent extinguishing the flame. It was believed that if the engine control module was reprogrammed the system could readily start on methyl soyate without the aid of any nonstandard equipment.

4.2.10. Discussion of Performance Evaluations. Throughout all testing it was clear that methyl soyate could make an obscurant as effective as fog oil. It consistently provided thick, white plumes that tended to follow the ground which had considerable longevity, properties which were necessary to have in a defensive obscurant aerosol. During laboratory testing using the tubular furnace-based generator it was demonstrated that heat and air flow were key factors in creating a good quality obscurant plume. Laboratory testing also showed that exposure to different temperatures of ambient air did not affect the particle size distributions or percent transmittances of the plumes throughout the range of temperatures tested.

The prototype modular generator units based on turbojet engines made plumes with methyl soyate that performed slightly better than with fog oil due to the minor difference in oil pickup at the pumps, but this difference was not detrimental to the effectiveness of obscuration of either oil tested. Within the plume an individual could not see anything more than 0.31 m (1 ft) away from the face. Everything nearby was visually

lost to the disorienting thick white fog, and if caught in the plume the safest choice was to remain stationary until the test was completed to avoid the risk of tripping on objects.

The modular generator prototypes performed reliably throughout testing. The extent of difficulties came in user errors arising from having the generator pointed into the wind, empty fluid tanks before the gauges were installed, and electrical connections coming loose during modifications. With some minor modifications these designs could be produced with more rugged electrical and fluid connections and with additional connectivity options for both power supply and fluid supply as well as controllability. The generators have fulfilled the goals of providing a reliable man-portable, radio controllable continuous obscurant aerosol generator that could be placed onto any vehicle for a range of applications. Additional photos of testing are provided in Figures 4.69 and 4.70.



Figure 4.69 – Photograph of Demonstration of Methyl Soyate Plume from Prototype Modular Obscurant Aerosol Generator Remaining Dense and Near the Ground



Figure 4.70 – Photograph of Methyl Soyate Plume Density Obscuring a Fence

5. CONCLUSIONS

Laboratory tests were carried out to assess the suitability of biogenic oils and their esters as potential replacement for FO in military obscurant applications under controlled conditions. MS was found to be the most suitable oil; it yielded aerosols with similar particle size distributions as those obtained with FO and as a result Mie scattering caused attenuation of visible radiation intensity (obscuration) similar to that of the FO. Because of the lower viscosity of MS relative to FO, higher volumes of MS were pumped into the hot generator exhaust and yielded denser obscurant plumes. As a result better obscuration was obtained in the NIR region. MS was found to be superior to FO from potential human health and environmental points of views. MS and aerosols were free of PAHs, had simple chemical compositions and a narrower boiling range. In addition it was found to be non-mutagenic and more biodegradable. Furthermore, MS was found to be a suitable fuel for the small turbines used as a component of the compact obscurant generators.

Performance of MS as a superior obscurant oil was validated through field trials. Field trials showed that MS leads to a thick, white plume which can easily obscure the visualization of equipment and large structures. The obscurant plumes generated with M56 or the compact generators were persistent for several minutes and cover nearly two kilometer long fields.

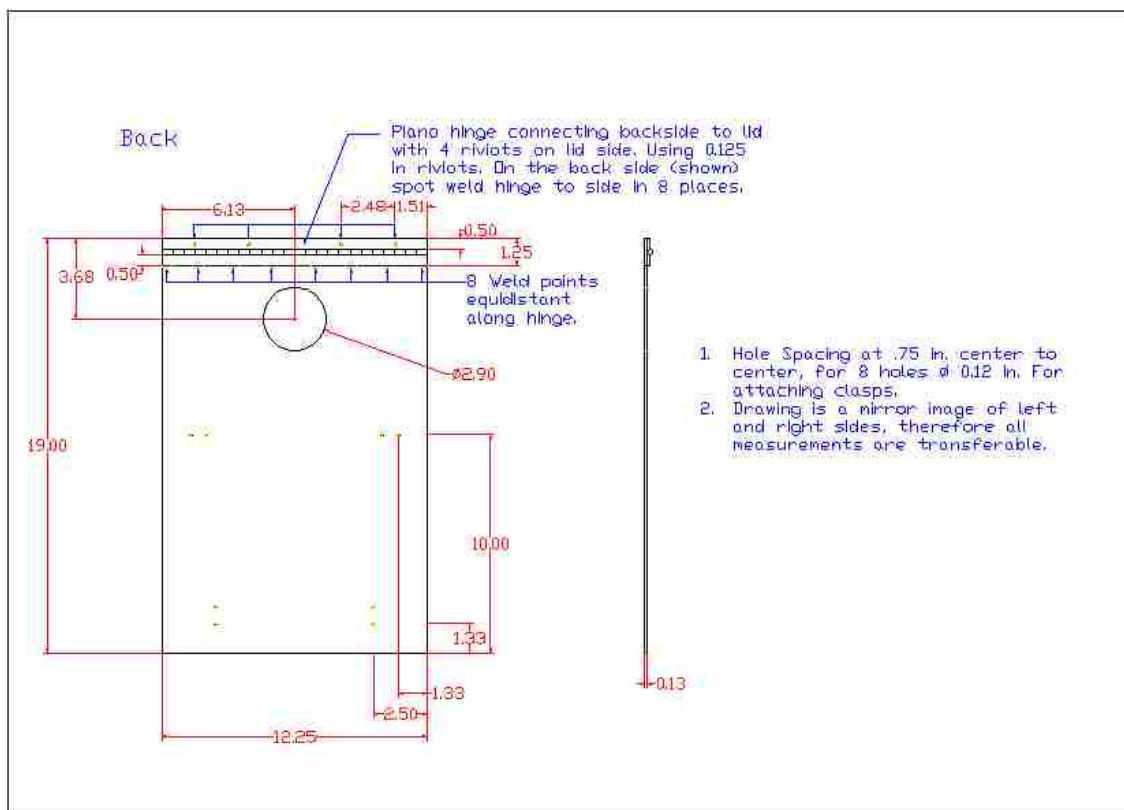
The compact modular man-portable obscurant generators developed as part of this research project were only one tenth in weight and volume of the M56. These generators could be readily carried by one person. With its small foot print, compact generators can

be mounted on a variety of vehicles rather than requiring dedicated vehicles as is the case with M56. The compact generators can provide obscurant plumes of same density and duration as the M56. Generators required only one 24V DC power source for all control and operational components. The generators were made remotely operable with off-the-shelf compact radio controlled robotics modules. Thus, the design and performance of the generator satisfactorily met all requirements set for the research program.

APPENDIX A

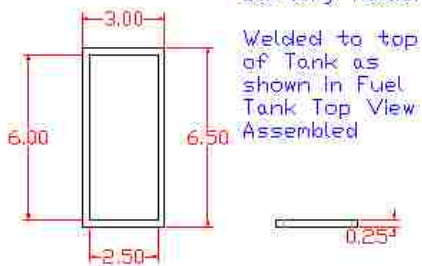
PORTABLE GENERATOR TECHNICAL DRAWINGS

A number of technical drawings were followed for the construction of the prototype modular obscurant aerosol generators. These were created by a third party at Missouri S&T for the use of both our laboratory and the company contracted to build the metal boxes that held the generators. There were some alterations to these designs over time.



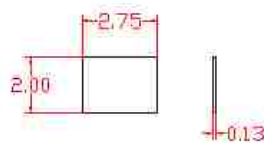
Battery Holder and Electronics Holder

Battery Holder

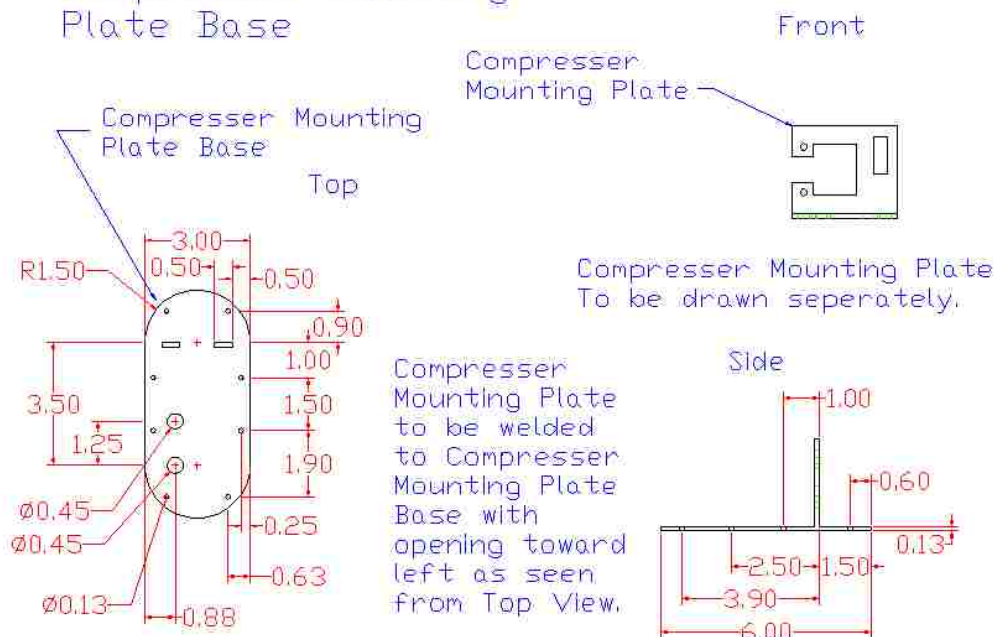


Electronics Holder

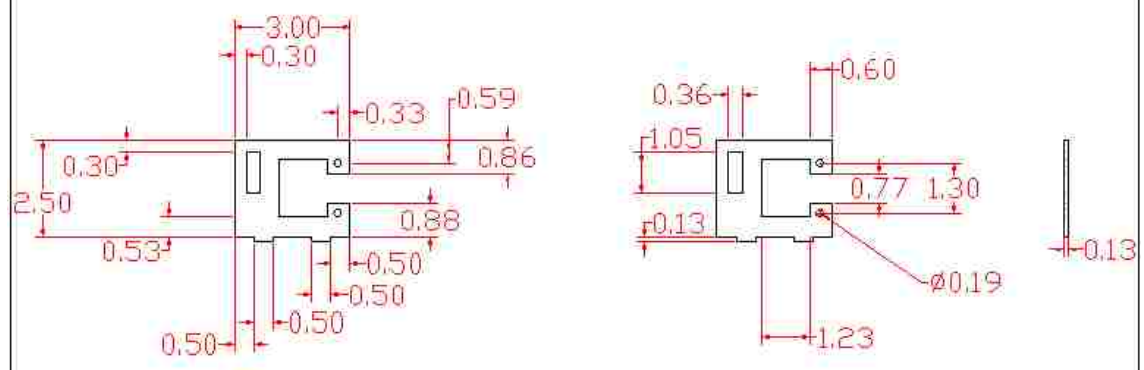
1. Welded to top of Tank as shown in Fuel Tank Top View Assembled.
2. Hook and loop Velcro attached to each side for securing electronic components.



Compressor Mounting Plate Base

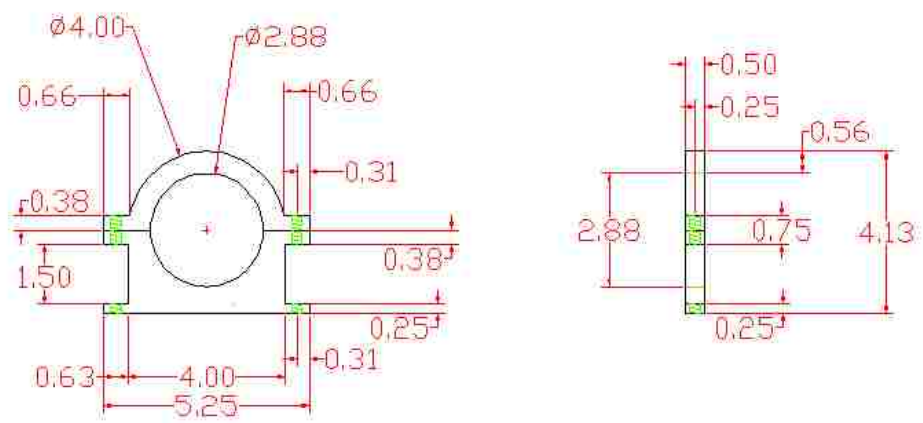


Compressor Mounting Plate



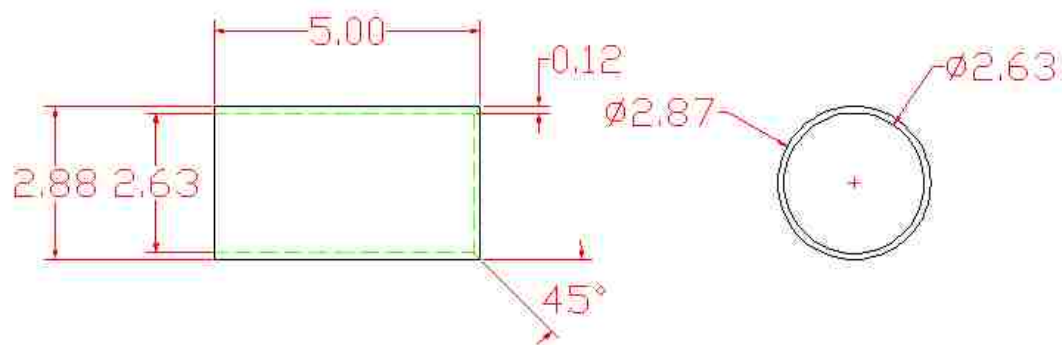
Part to be placed into slots on Compressor Mounting Plate Base then welded from bottom side and ground flush.

Exhaust Bracket



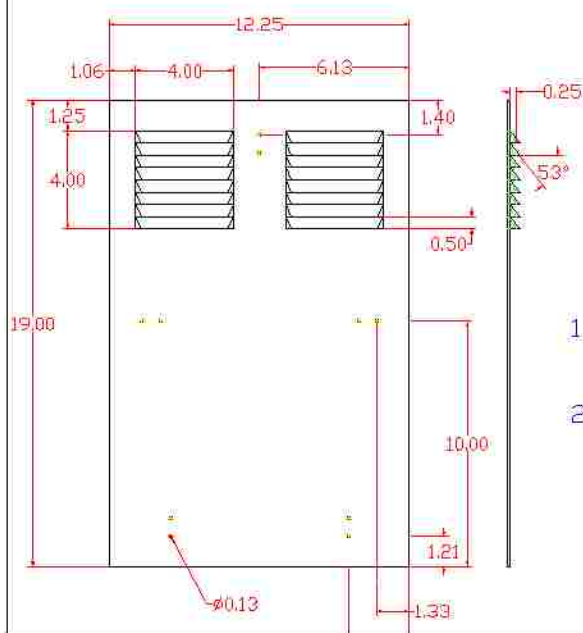
1. Drill and tap bracket for 8-32 in 4 locations with Drill Size #29.
2. 8-32 x 3/4 Inch Socket Head Cap Screws used to attach top and bottom sections.
3. Bracket is bolted to Upper Turbine Encasement in specified location using 8-32 x 1/4 Inch. (see drawing)

Exhaust Pipe



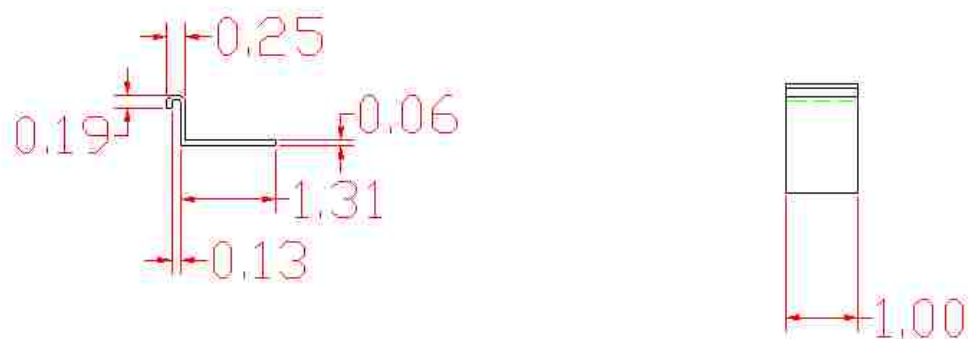
1. Exhaust Pipe mounted in Exhaust Bracket as shown in Upper Turbine Encasement Side View and End View.
2. Material is to be Stainless Steel.

Front



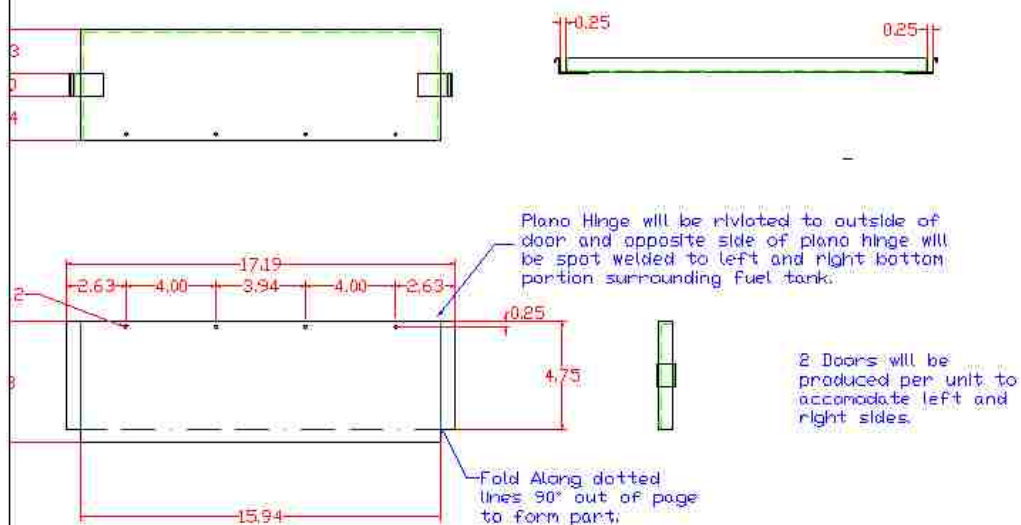
1. Hole Spacing at 0.75 in. center to center, for 10 holes \varnothing 0.13 in for clasps to be riveted on.
2. Drawing is a mirror image of left and right sides, therefore all measurements are transferable.

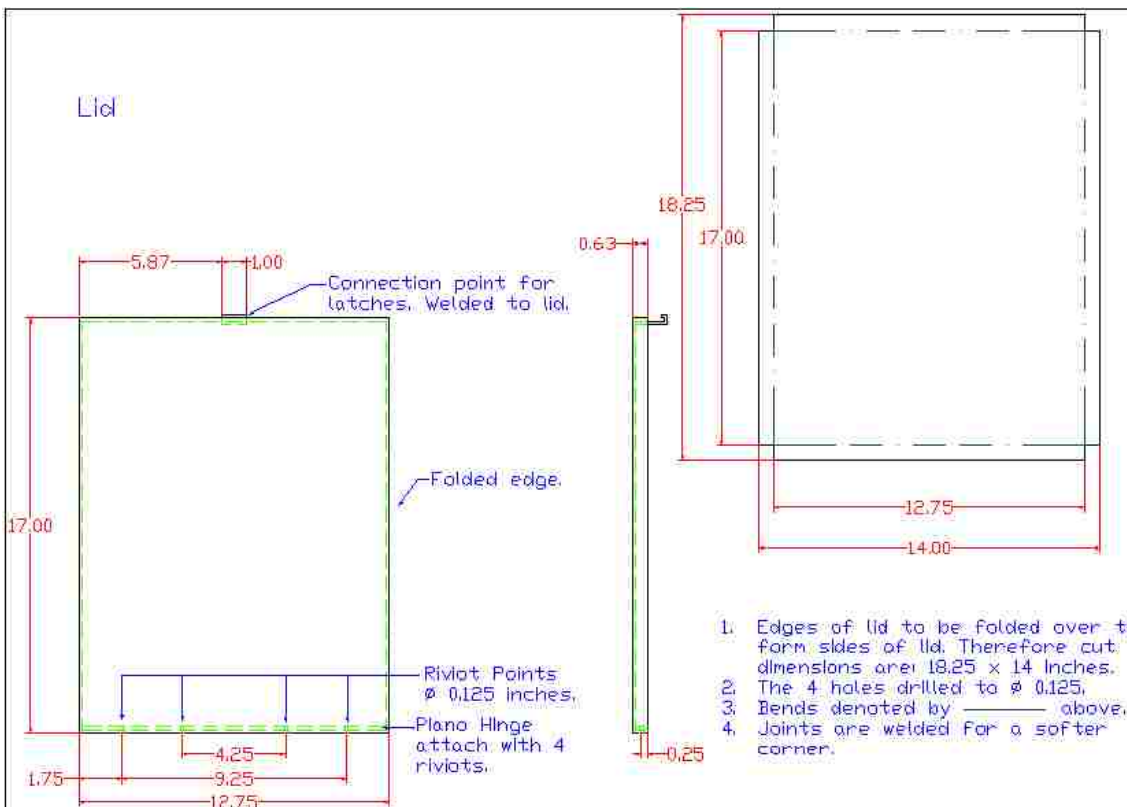
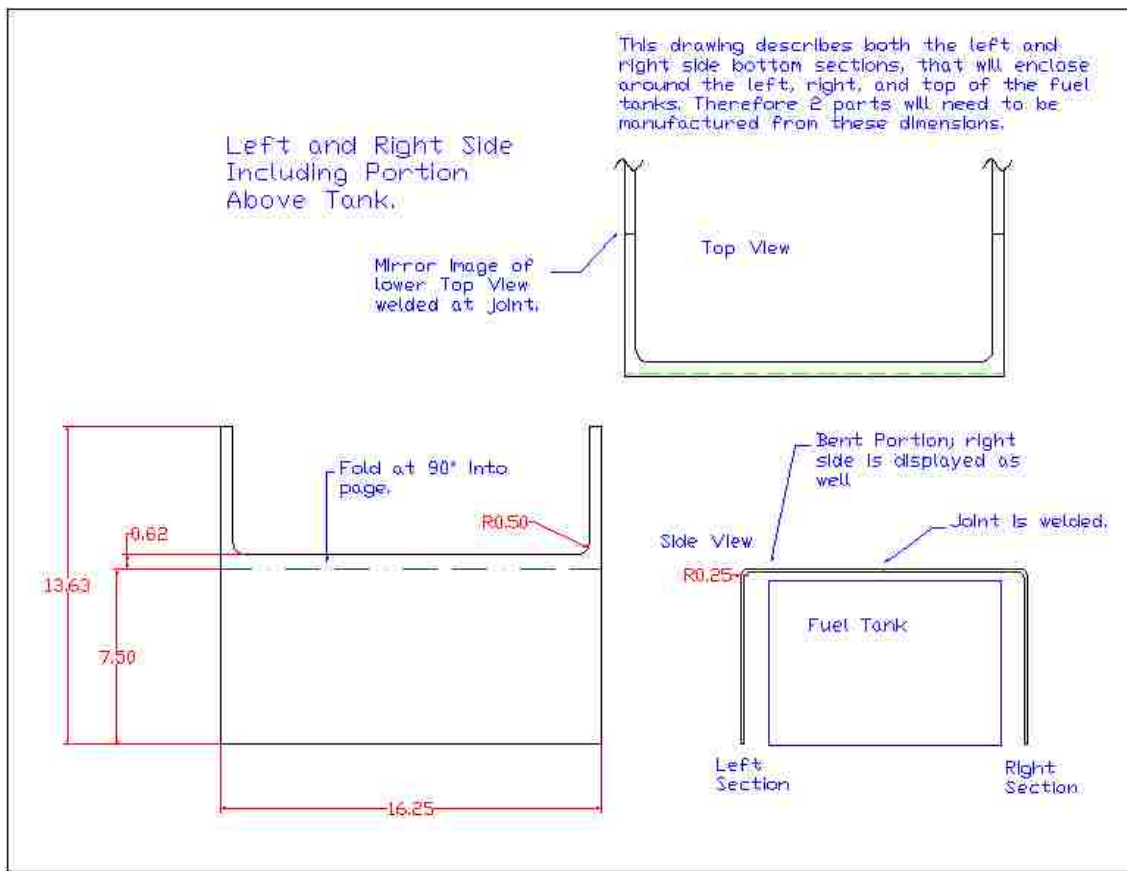
Latch Connector



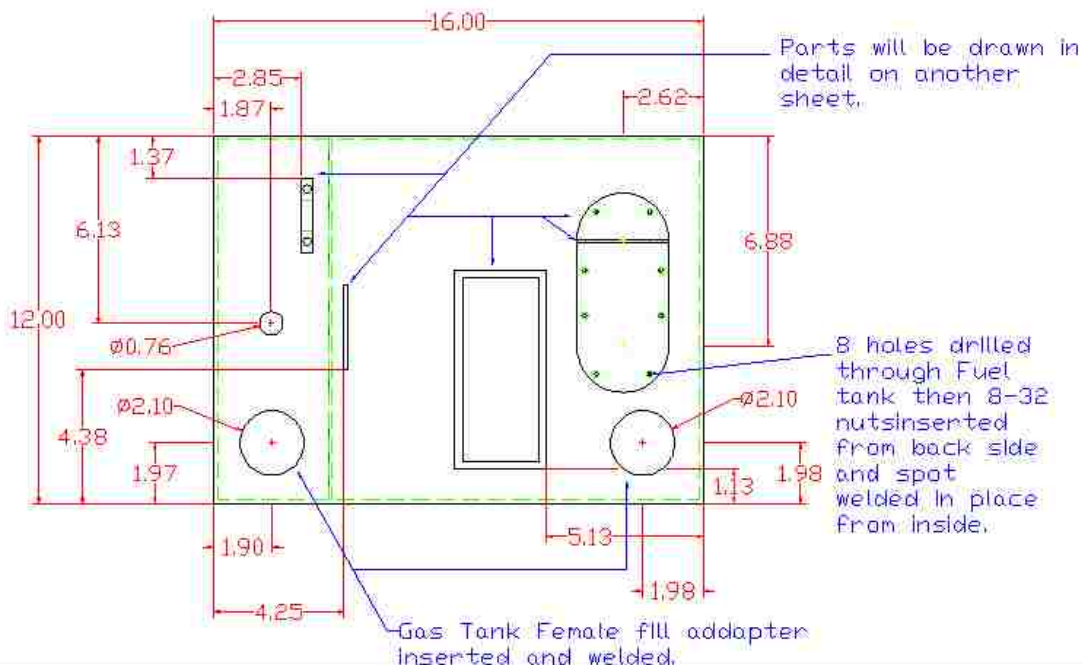
Connector to be welded to indicated locations as per drawings.

Side Doors

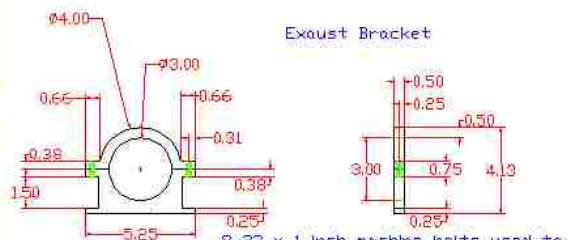




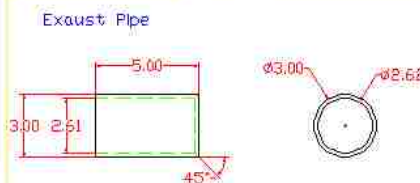
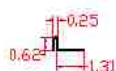
Fuel Tank Top View Assembled



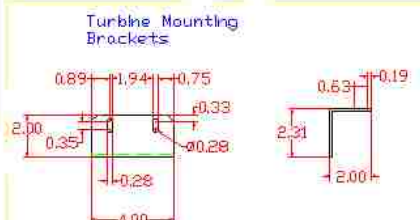
Special Parts



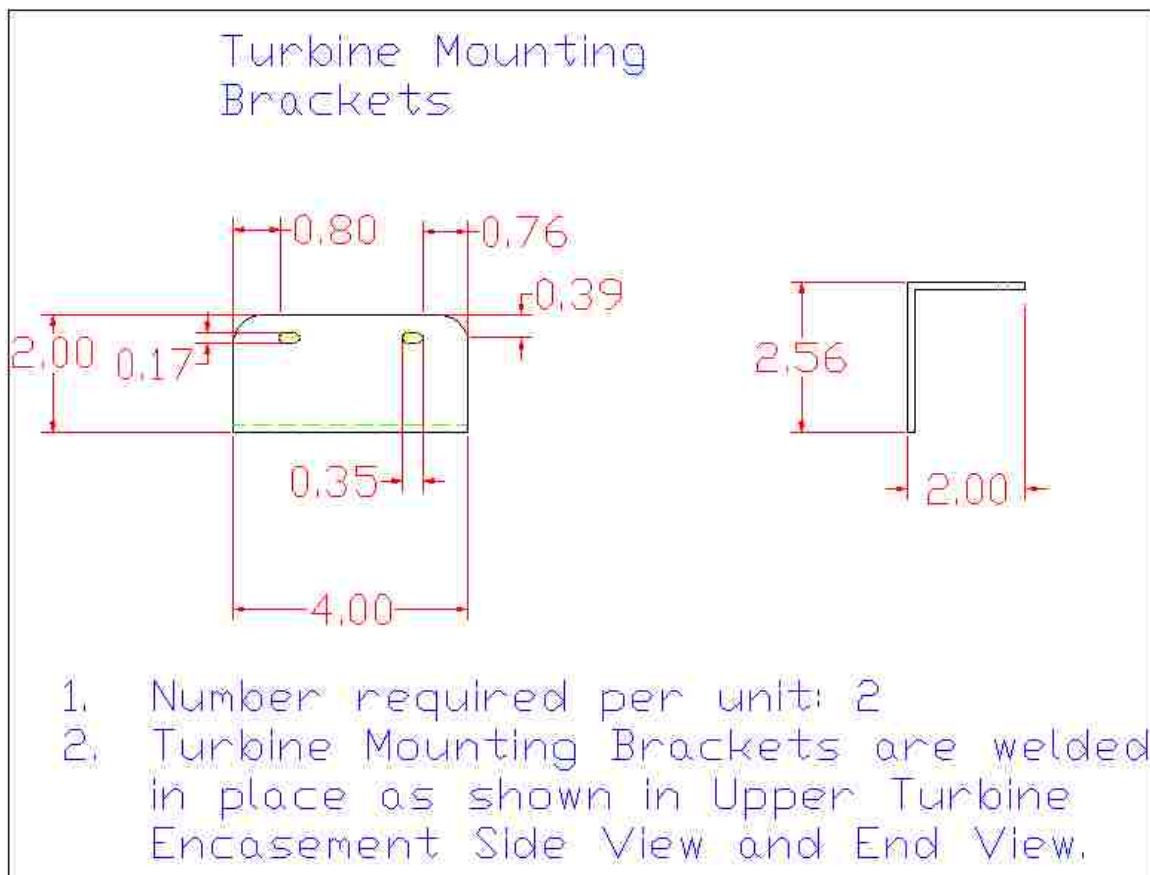
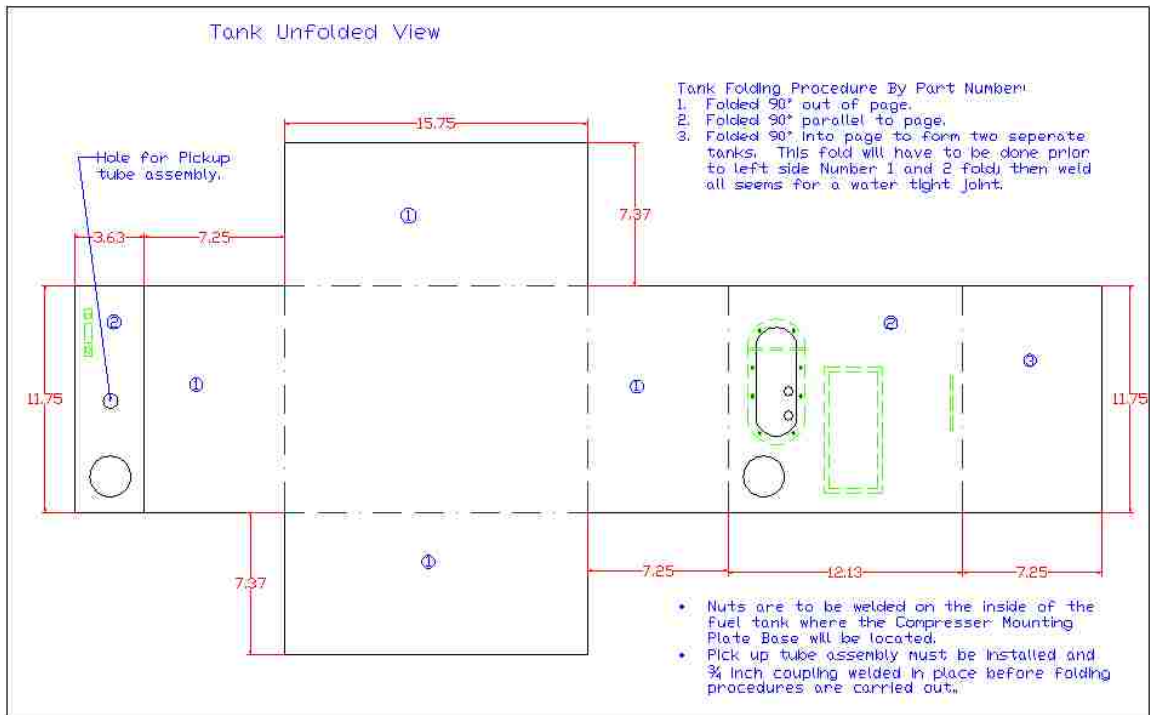
1. Drill and tap bracket for 8-32 in 2 locations.
2. 8-32 x 3/4 inch Socket Head Cap Screws used to attach top and bottom sections.
3. Bracket is welded to Upper Turbine Encasement in specified location. (see drawing)

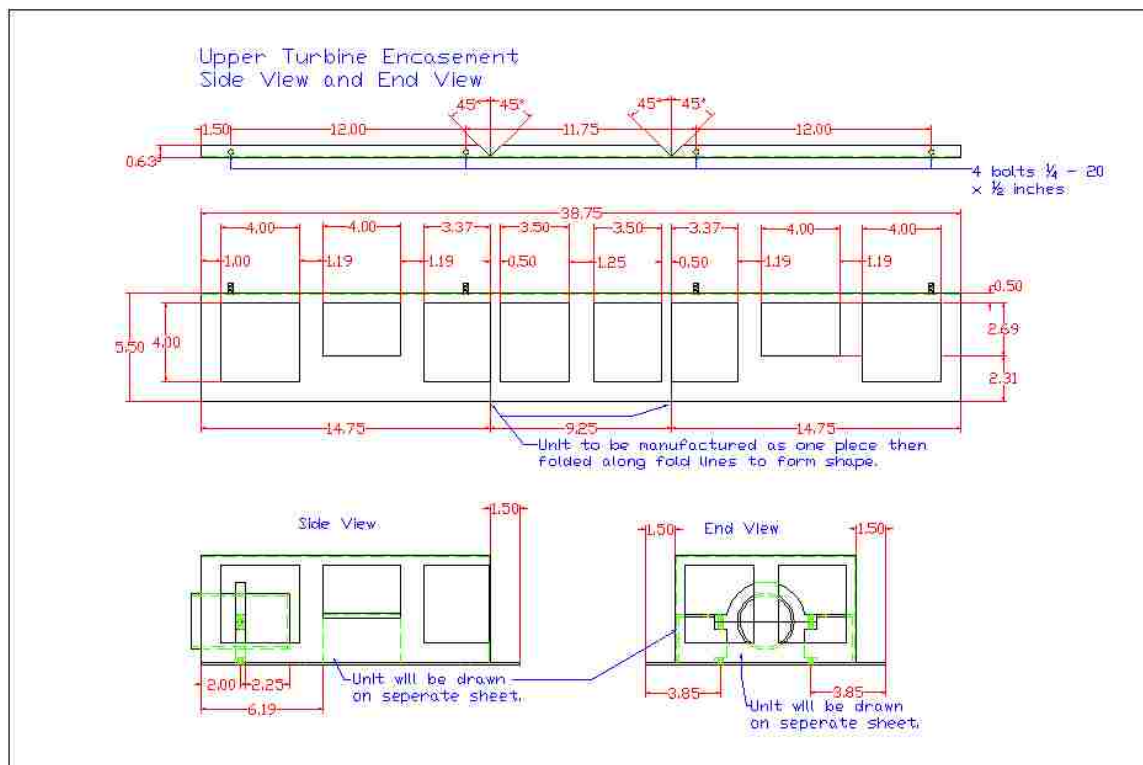
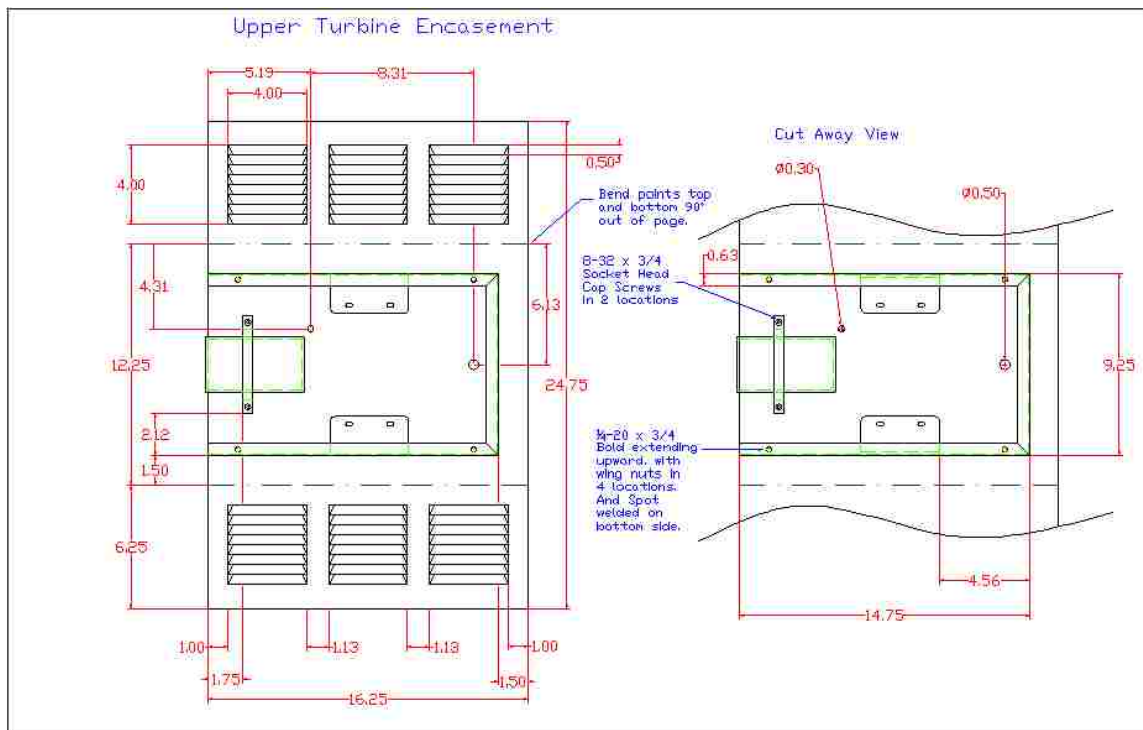


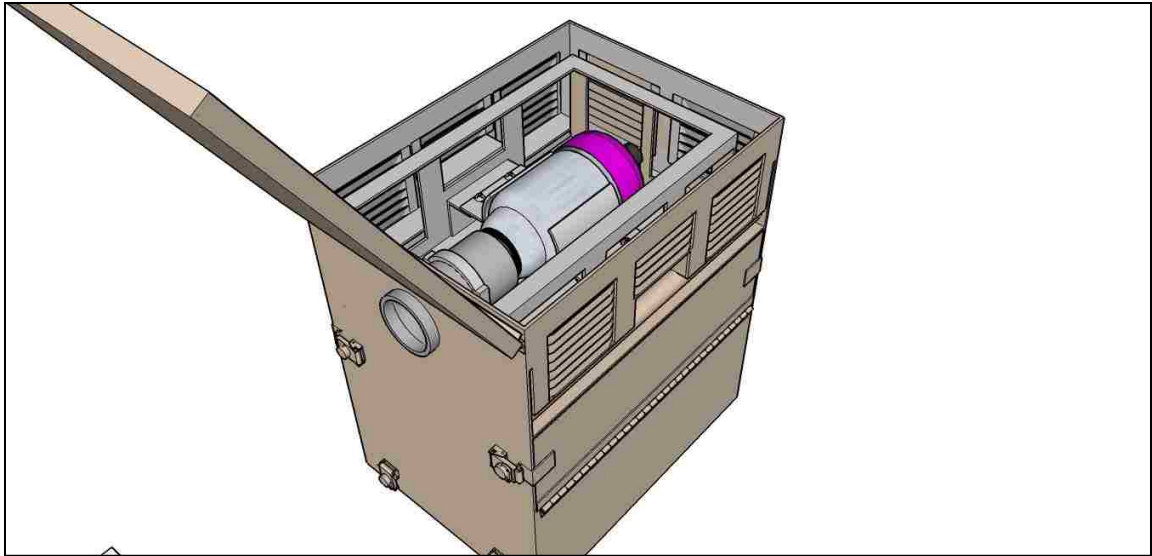
Exhaust Pipe mounted in Exhaust Bracket as shown in Upper Turbine Encasement Side View and End View.



1. Number required per unit 2.
2. Turbine Mounting Brackets are welded in place as shown in Upper Turbine Encasement Side View and End View.







APPENDIX B

COMPACT MAN-PORTABLE OBSCURANT SYSTEM OPERATIONAL MANUAL

The prototype man-portable modular obscurant aerosol generator units developed in this research were based on the JetCat P80 turbojet engine. As such, the standard operating manual for the JetCat P80 is applicable and is available for download at www.jetcatusa.com. However, there were modifications made to make these turbojets function on a Futaba brand radio control receiver and transmitter, so the radio control operations manual created by this research for use with these generators is included in the following pages.

Compact Man Portable Obscurant System

Operational Manual

The Center for Environmental Science and Technology
Missouri University of Science and Technology
Rolla, MO 65409

Edgewood Chemical and Biological Center
United States Army

Version January 2010

Table of Contents

I. Introduction.....	3
II. General Specifications.....	5
III. Design of the Modular Unit and its Features.....	6
IV. Electrical Systems.....	8
V. Fluid Connections.....	12
VI. Tethered Control Operation.....	13
VII. Other Engine Controls Changed with Tethered Controller.....	15
VIII. Radio Controlled Operation.....	17
IX. Troubleshooting.....	20
X. Maintenance.....	24
XI. Additional Notes.....	32

I. Introduction

The threat of asymmetric warfare and terrorism has generated a revived interest in military obscurants. Obscurants provide a thick plume of aerosols that hindering visibility and reducing the ability of the enemy to target individual personnel or equipment. In line with generally applicable doctrine, “You can’t kill what you cannot see.” The caveat exists that if the enemy sees smoke they may suspect the presence of significant targets either in or behind the obscurant plume (smoke) at which they may blindly fire upon, however, since targets cannot be individually singled out the likelihood of any one thing or person being struck is reduced. Smokescreens have been and will likely to be used as a decoy to attract attention away from the real deployments during an assault. It is also possible that if an enemy group were small enough, smoke could be used to cover the enemy so they could not see where to move for a retreat and friendly forces could then entrap the hostiles with flanking movements.

Smokescreens have long been used by forces in combat, but the methods and materials have evolved over time. Initial smokes were created by burning readily available natural materials such as wet leaves, providing combustion products capable of scattering visible light. During the twentieth century a varied of chemicals such as white phosphorus, zinc chloride and other reaction products were used as obscurants. However, use of these such products has been largely been discontinued because of human health and environmental considerations.

Since the Second World War obscurants have been deployed through smoke generators which use a middle distillate of petroleum, fog oil (FO) for obscurant aerosol generation. FO pumped into the hot exhaust of a turbine engine e.g. a helicopter turbine. Oil is volatilized and vapors are emitted with the turbine exhaust. Oil vapors in contact with cool air at ambient temperature and condense into micron size droplets with a relatively long settling time, thus remain suspended in air for several minutes providing effective scattering of light. The micron size particles provide effective obscuration in the visible and the near IR regions of the electromagnetic radiation through Mie scattering.

The major drawback to the current generation obscurant generator (M56) used by the US Army is its size. This wide area obscurant aerosol generator is build around a 240

kg thrust turbine, the generator produces obscurant aerosol from FO at a flow rate of with 1 G min^{-1} . Because of its size and weight the generator is mounted on a dedicated vehicle. The large size and high cost reduce deployment of these units. To overcome these limitations a compact low cost man portable obscurant generator was developed at the Center for Environmental Science and Technology – Missouri University of Science and Technology (A Campus of the University of Missouri), Rolla, MO. The compact unit is less than $1/10^{\text{th}}$ the size of the current obscurant generator, however, can produce obscurant aerosol of the same volume.

A technical description and operating procedure for MOSS are provided in the following sections.

II. General Specifications

Engine: JetCat P80 turbojet

Length: 30 cm

Diameter: 11.1 cm

Weight: 1.32 kg

Starting Substance: Jet A1, 1-K Kerosene

Running Substance: Jet A1, 1-K Kerosene

Bearing Lubricant: 5% Turbine Oil mixed into fuel (1 Quart per 5 Gallons of Fuel)

Operational RPM Range: 35,000-120,000

Exhaust Gas Temperature: 580-690 °C

Fuel Consumption: 270 mL min^{-1} at full RPM

Recommended Maintenance Interval: 25 Hours of Use

Control Methods: Tethered digital controller (provided), or Radio Control Unit (separate)

Thrust Chart

RPM	Thrust (PSI)
35,000	0.8
85,000	8.0
93,000	10.0
101,000	12.5
110,000	15.0
117,000	17.0
123,000	21.0

Integrated Generator Unit

Length: 45.7 cm

Width: 33.0 cm

Height: 49.5 cm

Weight: 45.5 kg (fully loaded)

Input Power: 24 Volts DC (2x12V Series)

Output power: 12V DC (obscurant), 8V DC (engine), 5V DC (radio control); (separate battery for

radio control transmitter is required)

Exhaust tube diameter: 8.5 cm

III. Design of the Integrated Generator

The integrated obscurant generator is comprised of an aluminum box with three compartments. The top compartment houses the mini-turbojet engine, the fuel and obscurant oil manifolds, a glow plug, two obscurant oil spray rings and a stainless steel tube that directs the engine exhaust and obscurant aerosol out of the generator housing. The top compartment is closed with a latched – hinged hatch that can be rotated to provide an easy access to the engine and other components in the compartment. The sides and back covers of the unit contain louvered air intakes to prevent rainwater entry into the unit. The air entering the compartment is filtered with U-shaped air filter enclosed in stainless steel mesh screen to prevent large particulate matter such as sand and debris from entering the turbine, such debris can damage the turbine and pose a safety hazard due flying fan blades released at high velocity. The top is also protected with a stainless steel mesh screen panel held in place with four wing nuts to prevent accidental intake of large materials should the top hatch become opened during operation. The oil sprayer rings are positioned in between the engine exhaust tube and the stainless steel tube obscurant output tube. A photograph of the top compartment is shown in Figure 1.

The middle compartment is accessible through hinged hatches on either side of the unit. The hatches are secured in place with a pair of latches. Components housed in

the compartment can be readily accessed through the openings on either side. Components housed in the compartment include a power converter, battery leads, the tethered push-button digital engine controller and stainless steel tubes that connect the obscurant oil tanks to the sprayer nozzles

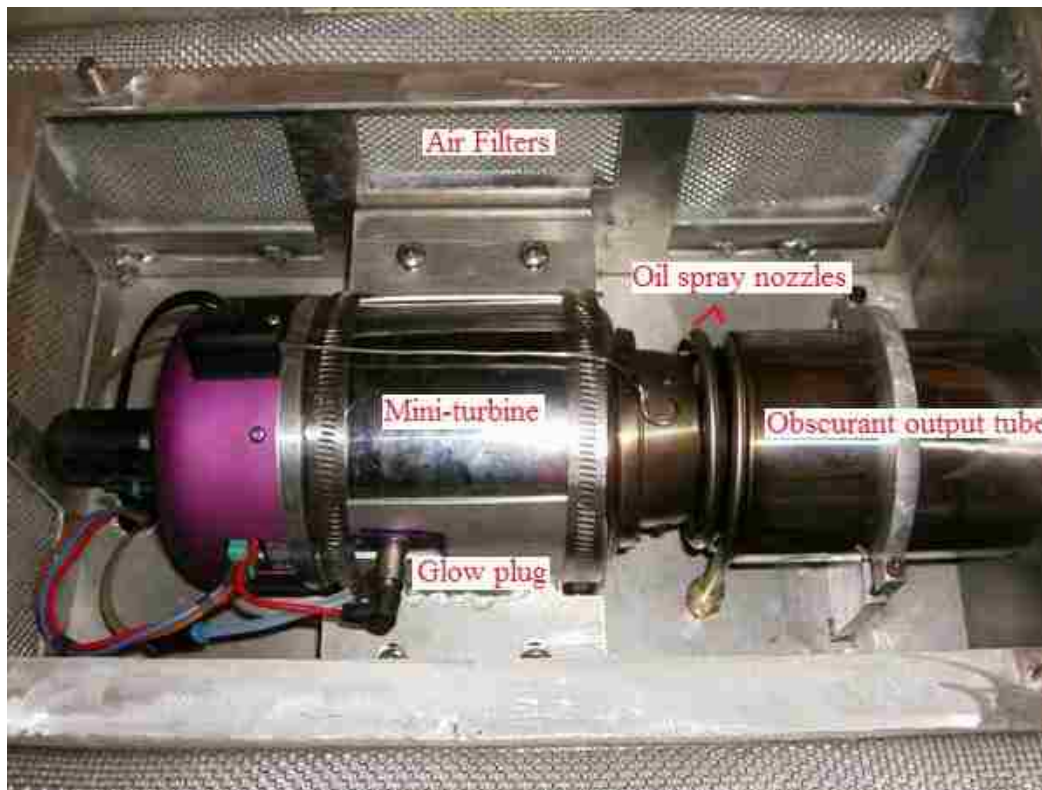


Figure 1: Photograph of the top compartment, top view.

situated in the top compartment, fuel and obscurant oil pumps, solenoid valves, the fuel and oil level indicators, and the fuel and obscurant oil tank refill caps. The fuel or obscurant oil refill caps are readily assessable through the side openings. The power converter has a main power switch to activate the system power output to the individual devices within the unit. Maintenance procedures for the components are provided in the maintenance section of this document.

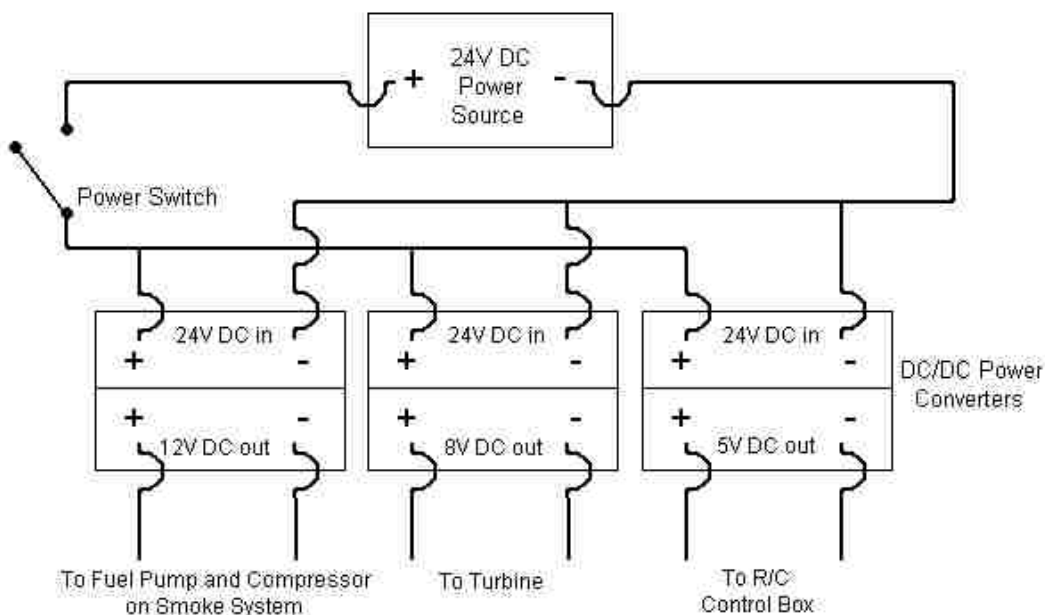
The bottom compartment houses the fuel and obscurant oil tanks. It is accessible by disconnecting the fuel lines and electrical wires from the engine in the top compartment and feeding through the holes to the middle compartment, disconnecting the metal obscurant oil tubes in the middle compartment, removing the four latches around the bottom while the unit is on the floor, and then lifting the outer body of the unit with

the top compartment off of the fuel tank. All electronic controls and fuel systems are attached to the fuel tank assembly. Fuel pumps for the obscurant oil system are located inside the box and are accessible via the small metal nuts holding the assembly in place on the tank. For more information please refer to the Maintenance section.

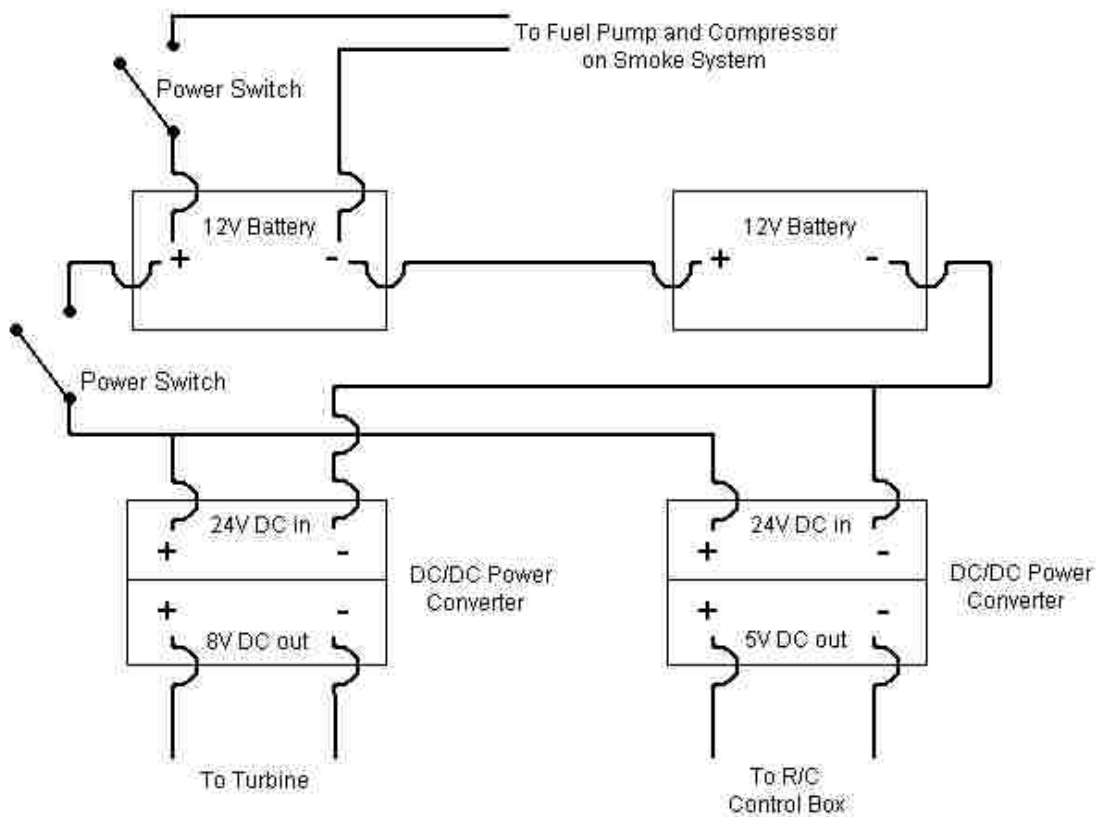
The sides of the box feature fold-out handles accessible from the recessed area found below the center louvered intakes. The design of these handles allows the unit to be slightly more compact when attached to vehicles for transport.

IV. Electrical Systems

Power is provided to the obscurant generator unit through a power converter box. The obscurant fluid systems are powered by 12V DC, the engine and its tethered controller use 8V, and the radio control system uses 5V. This unit is configured to run off of a 24V battery system. The wiring diagram of the box is shown below with two options. The first option is using the military standard of 24V DC power coming into the unit. This 24V source is then routed through three different power converters to give outputs of 12, 8, and 5 Volts. The second option is using two separate 12V batteries, pulling the 12V line directly from one battery, and internally linking both batteries as a series circuit providing 24V so power converters can provide 8V and 5V outputs.



Electrical Diagram of Power Converter for Standard 24V DC Input

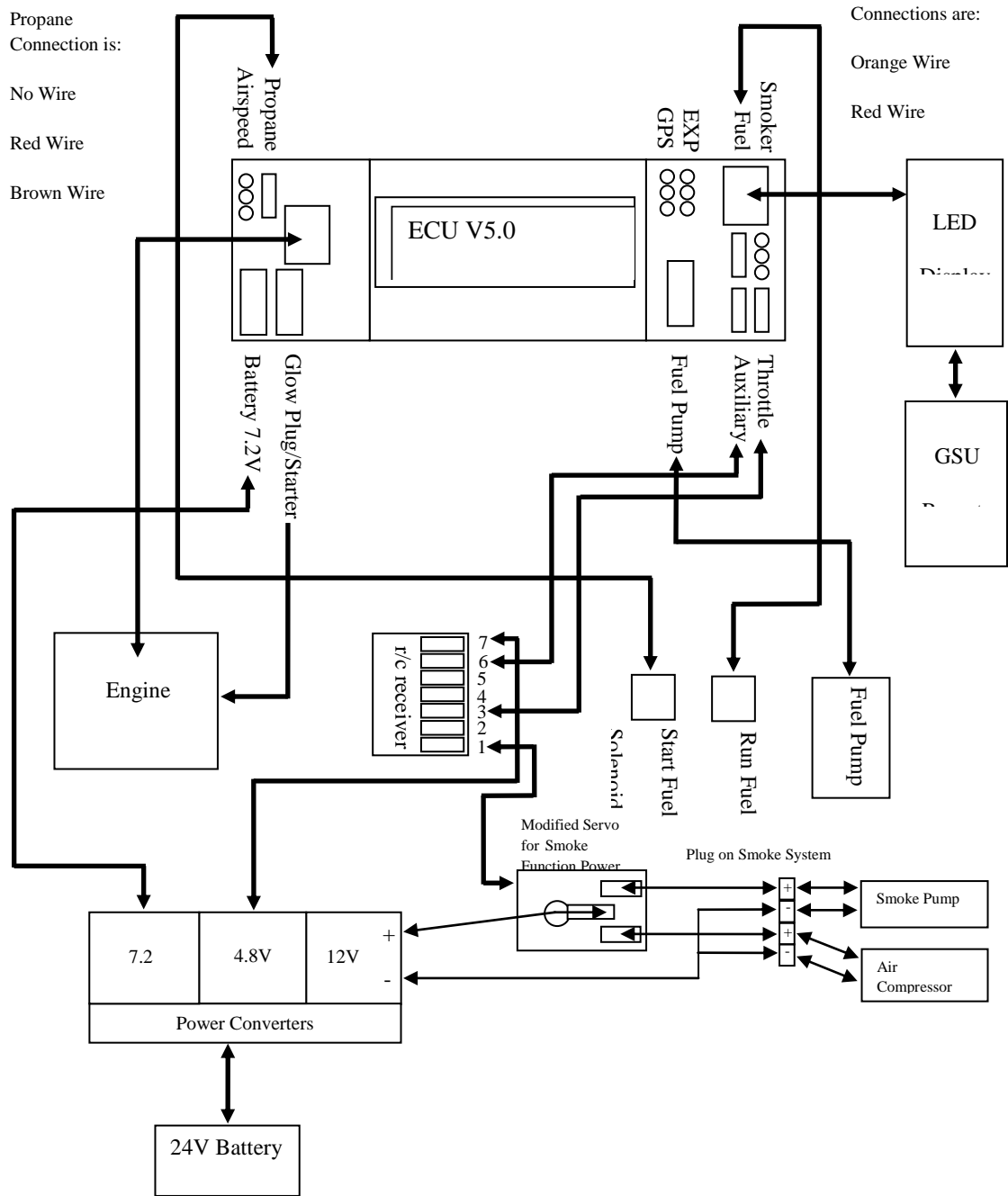


Electrical Diagram of Power Converter for Two 12V DC Inputs

The power converters provide all necessary voltage outputs from a uniform power supply, eliminating the need for various battery voltages and current ratings. This also allows easier system maintenance because it uses fewer batteries and thus fewer battery chargers. By being based on a 24V system, this unit may be modified in the future to directly connect into the power supply used on military vehicles.

The engine is controlled through an ECU (Electronic Control Unit). The generator operator gives commands to the ECU through use of the tethered control or the radio control system, and the ECU then responds by changing operating parameters such as glow stick heating during startup, fuel flow direction for startup or running operation, fuel flow rates for RPM control, and other internal settings to make the engine perform as commanded. Proper ECU operation relies on many electrical connections to the fuel pump, sensors and solenoid valves. The electrical diagram of the ECU is shown ahead for current radio control setup.

If no radio control system is to be used, the diagram is modified by simply disconnecting any wires from the Auxiliary port on the ECU, and rerouting the Throttle wire so it bridges between the Throttle port and the Airspeed port on the ECU.



V. Fluid Connections

There are two fluid systems onboard the modular obscurant generator unit. The first is the fuel system for the turbine engine, and the second is the obscurant oil system for smokescreen production.

The fuel system generally consists of a pickup line inside the fuel tank, passing through a bulkhead penetrator to get out of the tank, then flowing through the fuel filter. After this is the fuel pump which draws the fuel from the tank and pushes it through the rest of the system. Beyond this are the fuel solenoid valves which direct the fuel towards either the glow stick or the main fuel inlet on the engine. Electronically, the fuel pump connects into the ECU for digital control, and the solenoid valves are also connected to the ECU in respective sockets for “propane” (starter fuel line) and “fuel” (main fuel line). It is very important to trace the wires to know which solenoid valve is to serve for which purpose, then ensure that the fuel lines coming out of them are in agreement with those uses on the engine inlets. Crossing these fuel lines will result in the engine being unable to start and will also lead to engine fuel flooding. To remedy the fuel accumulation inside the engine, tilt the generator unit backwards so the engine air intake is pointed downward and the fuel may flow out of the engine. Capture as much of this fuel as possible, and clean the interior of the engine compartment so there is no risk of accidentally engulfing the generator in flames.

The obscurant oil system begins with fuel pumps mounted on a bracket inside the tank. Access is achieved through removing the nuts affixing the mounting bracket plate onto the top of the obscurant oil tank once the tank is removed from the generator unit. These fuel pumps push the oil up through an assembly on top of the mounting plate that houses small air compressors which can be activated to purge the obscurant oil lines beyond this point. The obscurant oil lines then progress upward and connect to the bulkhead penetrators at the interface between the engine compartment and the electronics compartment. The sprayer nozzle rings are affixed to the other side of these bulkhead penetrators. The nozzle ports are installed pointing toward the exhaust tube rather than toward the engine. Control of the obscurant oil sprayers and purging functions is through the use of the radio control handset, or the use of a manual toggle switch.

VI. Tethered Control Operation

WARNING! *It is strongly recommended to **never** engage the obscurant system unless the display shows that the engine is running above 100k RPM. If the obscurant system is engaged while the engine is at a low idle RPM (35k RPM) it has been observed that there is insufficient air flow to push the vaporized oil away from the heat source before ignition, and will produce a sudden large flame that is hazardous to the obscurant generator unit as well as personnel and equipment in close proximity.*

The following steps are used to start and run the modular smokescreen generator with the tethered controller. First, ensure there is fuel and obscurant oil in the appropriate tanks, the obscurant on/off/purge handheld control is connected to the system and in the center 'Off' position, and that the power source is connected. Make sure nothing flammable is within 15 feet of the exhaust tube. Then turn on the power switch(es) on the power converter unit. The screen on the controller will illuminate and display some initial startup screens. Once the screen displays the system status and shows 'ready,' follow the next steps:

Startup.....Simultaneously press 'Manual' + 'Ignition'

Max RPM.....Simultaneously press 'Ignition' + 'Min/Max'

Obscurant On.....Flip 3-Way obscurant switch to position for 'On'

Obscurant Off.....Flip 3-Way obscurant switch to center position for 'Off'

Obscurant Purge.....Flip 3-Way obscurant switch to position for 'Purge'

Min RPM.....Simultaneously press 'Ignition' + 'Run'

Shutdown.....Simultaneously press 'Manual' + 'Ignition'



VII. Other Engine Controls Changed with Tethered Controller

There are numerous other settings for the turbine system that are accessed through use of the tethered controller, including maximum RPM and radio control synchronization. These features are detailed below.

Prime the Fuel Pump: If fuel is not reaching the engine during startup, the fuel line may be primed with this feature. However, this does not include control over the solenoid valves directing fuel between the start and run fuel lines, so if the system is primed in this manner the fuel will likely dump into the engine through the run line. Temporarily disconnect the fuel line from the inlet side of the engine (purple shroud) by pressing in on the plastic connector on the shroud while simultaneously pulling outward on the fuel line. These fittings behave much like Chinese Finger Trap toys in the sense that if you only pull the fingers apart (on the engine, the fuel line), the finger trap (engine fuel line connector) will grip more tightly, and release can only be accomplished by pressing in the ends of the finger trap (engine fuel line connector) to release the

constriction before removing the fingers (fuel line). Hold the fuel line over a small container while priming the system so the fuel will not dump into the engine compartment. When done, remove the container and push the fuel line back into the connector until a small snap is felt which indicates successful recoupling. If successful the fuel line should not move when pulled on. The controls for priming are as follows:

Fuel Pump and Fuel Line Priming:

1. Press and hold 'Select Menu' while repeatedly pressing '-' or '+' until screen displays "Test-Functions Menu" then release all buttons
2. Select "Pump TestVolt" by pressing '-' or '+'
3. Press and hold 'Change Value/Item' then also press and hold either '-' or '+'
4. Once fuel comes out of the fuel line, release all buttons
5. Press 'Run' to display the system status

Non-Running Fan Spin: To test the starter motor or to manually force the turbine to spin without the engine actually running for only passing ambient air through the engine, press and hold 'Ignition.'

System Learn Radio Control: First, ensure that all radio settings are at their off positions. The throttle stick should be all the way down, 3-way position switch all the way back, and all trim tabs centered. With the obscurant generator system power off, press and hold 'Select Menu' followed by switching on the system power. Continue to hold 'Select Menu' until the display reads "Release key to: - learn RC -". Follow the on-screen procedures. "Set throttle to minimum" is when the throttle (left) stick is all the way down. "Throttle trim to maximum" is when the up/down trim adjustment tab is all the way up. "Set throttle to maximum" is when the throttle (left) stick is all the way up. "Set AuxChan. to minimum" is when the 3-way position switch is all the way back. "Set AuxChan. to center" is when the 3-way position switch is in its center position. "Set AuxChan. to maximum" is when the 3-way position switch is all the way near.

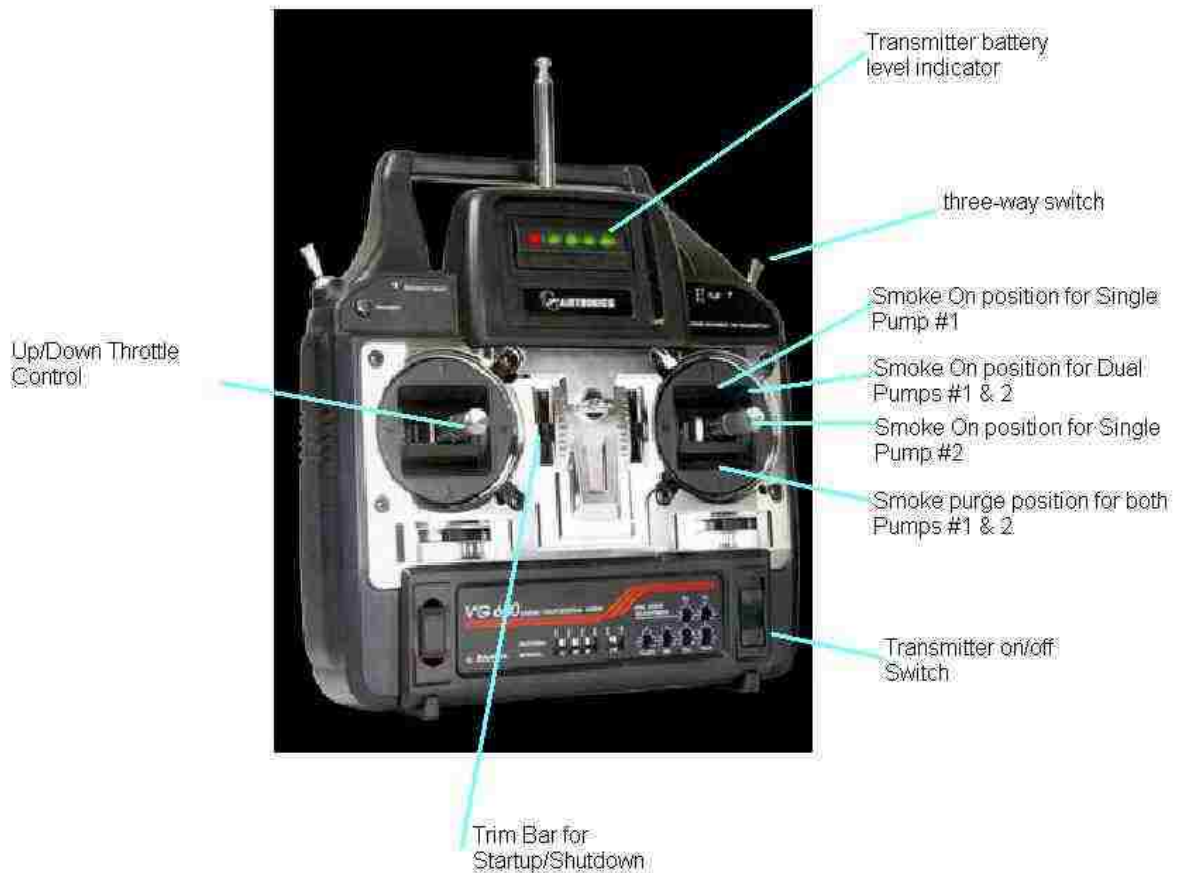
Set Maximum RPM: To set the maximum RPM to a lower value (example 110,000 RPM) to aid in prolonging engine life, press ‘Limits.’ Next, press ‘-’ or ‘+’ repeatedly until the display reads “Maximum RPM :(number).” Then press and hold ‘Change Value/Item’ and repeatedly press ‘-’ or ‘+’ to the desired setting. *It is strongly recommended to keep this value at or higher than 100,000 RPM to prevent accidental obscurant ignition.* Press ‘Run’ to return the display to the normal system status mode.

Additional information can be found in the JetCat manual found in the appendix, but these are expected to be the only normal system modifications that may be needed.

VIII. Radio Controlled Operation

WARNING! *It is strongly recommended to never engage the obscurant system unless the display shows that the engine is running above 100k RPM. If the obscurant system is engaged while the engine is at a low idle RPM (35k RPM) it has been observed that there is insufficient air flow to push the vaporized oil away from the heat source before ignition, and will produce a sudden large flame that is hazardous to the obscurant generator unit as well as personnel and equipment in close proximity.*

Radio controlled operation may look more intimidating than it really is. *When using the radio controlled operation, make sure the radio control transmitter is switched on before turning on the obscurant generator’s system power.* If the obscurant oil sprayer servo switches are powered up before the transmitter is activated they receive no signals and may act erratically, potentially engaging the obscurant oil sprayers without the engine running. This not only creates a large pool of flammable oil inside the engine compartment which *must* be cleaned, but if not cleaned thoroughly has the potential to ignite upon engine startup and engulf the obscurant generator in flames.



Radio Control Startup Procedure:

Engine Startup

1. Make sure the radio control transmitter stick and trim tab are both minimized for throttle, at the rear for the 3-way position switch, and obscurant control trim tabs are centered
2. Turn on the radio control transmitter
3. Turn on the obscurant generator system power switch(es)
4. Slide the throttle trim bar to the maximum (top) position
5. Move the 3-way position switch to the center (on) position
6. Wait momentarily for the system to initialize
7. Slide the throttle stick to its maximum (top) position. The engine will start.
8. Once the engine starts and automatically ramps down to idle, move the throttle stick back down to idle (bottom). The engine RPM will now respond according to the position of the throttle stick.

9. Move the throttle stick back up to its maximum position for full RPM

Obscurant Operation

1. Single Nozzle operation: With the engine at full RPM, move the obscurant stick straight up or straight right to spray obscurant oil. Note: This uses obscurant oil more slowly, lengthening run time.
2. Dual Nozzle operation: With the engine at full RPM, move the obscurant stick to the top right corner to engage both obscurant sprayer systems simultaneously. Note: This uses obscurant oil about twice as fast, shortening run time.
3. Obscurant Off: Release the obscurant stick so it may auto-center
4. Obscurant Sprayer Purge: To force compressed air through the obscurant oil sprayers after use, move the obscurant stick straight down while the engine is at full RPM. This clears the lines from oil to prevent clogging and facilitates cleaner maintenance work should the obscurant oil lines need to be disconnected to remove the fuel tank.

Engine Shutdown

1. Normal Auto-Shutdown Mode: Move the 3-way position switch to its nearest position. The engine will ramp to around 55,000 RPM and then shut off.
2. Emergency Shutdown Mode: Move the 3-way position switch all the way back. The engine will immediately shut down without ramping.
3. After shutdown return all switches to their pre-start positions
4. Turn off the obscurant generator system power
5. Turn off the radio control transmitter

IX. Troubleshooting

The obscurant generator system should be reliable and trustworthy, but every device can have its moments of trouble. Should the system not work properly, refer to this section for assistance.

Issue:***No Power****Batteries**

- Ensure the system is connected to a 24V power source or to two 12V sources
- Check that the power source batteries are fully charged

Wiring Connections

- Check that the wires are securely connected to the power source
- Check that the wires from the power converter are all properly connected
- Check that the wires going into the ECU are all properly connected (see wiring diagram) and that the wire colors are facing the right way. In wire sets with two or three bound wires, brown wires are kept toward the outside edge of the ECU
- Check the wiring connections on the engine

Power comes on but there is no control*Wiring connections**

- Check that the wires going into the ECU are all properly connected (see wiring diagram) and that the wire colors are facing the right way. In wire sets with two or three bound wires, brown wires are kept toward the outside edge of the ECU
- Check that the tethered controller is connected. The controller uses the inboard port rather than the outboard port.

Transmitter power

- Check the radio control transmitter's battery power. If low, recharge or replace.

RC range

- Check if the obscurant generator is located outside the range of the radio control transmitter

*Radio Control Transmitter Power Goes Low Fast

Battery

- If the transmitter battery is charged long enough that it should have a true full charge and it still goes low fast, replace the battery in the transmitter unit.

*Power available, but engine will not start

NOTE: If the engine will not start, tilt the obscurant generator unit backwards so the engine air intake is pointed down. This will allow any fuel accumulation inside the engine to drain, reducing the risk of fire and damage. Fuel accumulation inside the engine also causes a drag on the fan blades, slowing the starter motor RPM and decreasing likelihood of the engine starting. Clean any fuel that drains out so nothing can accidentally ignite in the engine compartment. If the fuel lines are connected to the engine opposite of how the solenoid valves are plugged into the ECU, the engine will not start due to fuel being diverted away from the glow stick. Ensure the proper connections are in place.

Glow Plug

- Check that the Glow Plug gets hot. When the system status indicates “Preheat” the plug should feel hot even while mounted in the engine. If the plug is not hot, refer to the Maintenance section for removal instructions.

Fuel level

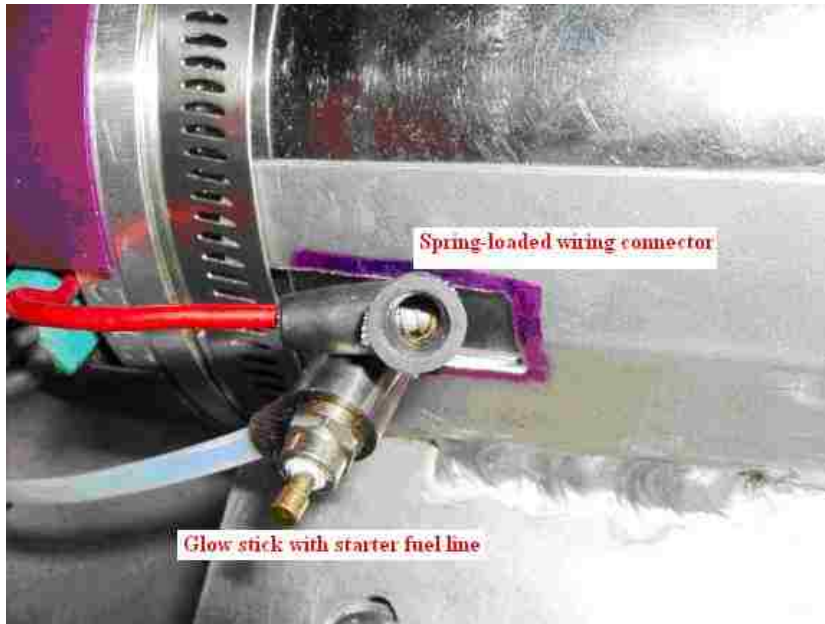
- Check that the fuel tank is full

Fuel Lines

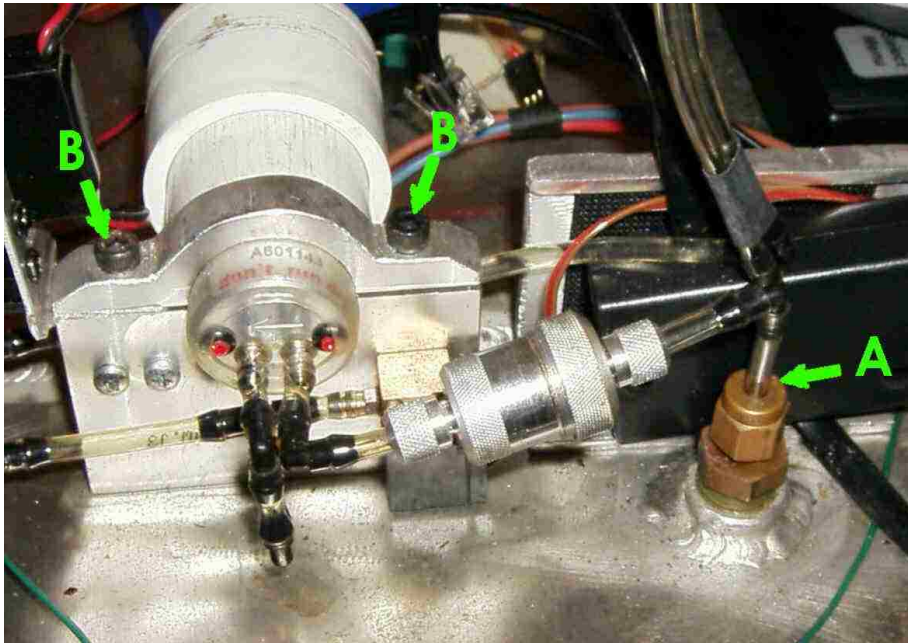
- Check that the fuel lines are connected to the proper ports on the engine

Fuel pump

- Check that fuel moves through the lines by visual inspection in the engine compartment during startup procedures, or when the Priming operation is performed. See the “Other Engine Controls Changed with Tethered Controller” section for this procedure.



Engine Glow Stick with Spring-Loaded Wiring Connector



Engine Fuel Pump Assembly. (A) Tank Pickup Line Connector, with fuel filter in-line to its left, followed by the fuel pump in its mounting bracket. Do not overtighten the bracket screws (B) because this could damage the pump's internal components.

Fuel solenoid valves

- Check that the two fuel solenoid valves controlling starting and running fuel flow are properly connected to the right plugs on the ECU and that they are both functioning. See the wiring diagram for details. The starting fuel line connected the starter line solenoid with the glow plug on the engine. The main running fuel line connects the run solenoid with the air intake side of the turbine.

Battery strength

- Check power source battery strengths. If the batteries are weak the system may appear normal on the status display but can not start. Listen to the sound of the starter motor. If the starter motor begins to sound weaker through the startup process the batteries are likely weak. Recharge or replace the batteries and try again.

Starter motor turns but fan does not spin

- The contact gasket on the end of the starter motor shaft may be damaged or missing. Contact JetCat for the likely recommendation of manufacturer maintenance.

Fan blades will not spin

- With the power off, check to see if the fan blades can be loosened by hand by using a finger to gently try spinning the blades. If the blades begin to freely turn, repeat the starting procedures.

Starter does not make the fan turn fast enough to start

- There is a small rubber O-ring on the end of the starter motor shaft that makes contact with the fan blade spindle, and if the O-ring is damaged or missing the starter shaft will spin without the full amount of grip causing the fan to not spin fast enough.

*Engine startup aborts due to overtemperature

Fuel

- Check that the fuel has had turbine lubricating oil added

Wind speed and direction

- Make sure the unit is not undergoing starting procedures with a strong outside wind blowing backwards through the turbine

Temperature sensor location

- Slightly pull the exhaust temperature sensor wire farther back out of the exhaust. Do not modify this by much because the sensor must remain in contact with the exhaust gases exiting the turbine, but slight changes in position may sometimes overcome this problem.

*Engine starts, but runs rough

Air bubbles in fuel line

- Check connectors to make sure fuel lines are snugly connected and check for leaks along all fuel lines. Also check the fuel line filter to make sure it is snugly screwed together and that the filter is snug on the fuel lines.

*Engine starts, but runs very hot with louder or different noises than usual

Fuel

- Check that the fuel was pretreated with the required amount of turbine lubricating oil in fuel. It has been observed that the engine may have a blue flame, the exhaust port on the rear of the engine glows red-hot before automatically shutting down from “Over-temp”, and the bearings sounds squealing.

Exhaust direction versus wind speed and direction

- If the system overheats during startup and aborts, make sure the exhaust is not facing into the wind. Backdraft can make the fans spin backwards and make startup more difficult.

*Obscurant system unresponsive

Check connections

- Check the wires going from the power converter to the servo switches and on to the fuel pumps in the obscurant oil tank. Also check the leads connecting the servos to the radio control receiver unit.

Check fluid level

- Check that the obscurant oil tank is full

Check servo switches

- Check that the servo switches are functioning properly and that the full range of travel stops on the metal contacts. If the range is too large or too small, change the corresponding endpoint adjustments on the radio control transmitter (near the power switch) with a small screwdriver.

Check power to fuel pumps in obscurant oil tank

- Check that power should be reaching the fuel pumps inside the obscurant oil tank

Check fuel pumps in obscurant oil tank

- Check that the fuel pumps in the obscurant oil tank are both functional using a 12V DC power source

Check for clogged obscurant oil lines

- Ensure that the obscurant oil lines are not clogged with residual oil or burnt oil

*Fluid Leakage

Residual from use

- Check to see if oil accumulation is the result of a leak, from the obscurant oil sprayers being activated before the radio control transmitter was switched on, or if it is residual from normal use

Loose connection

- Check all connections and fittings to make sure they are tight

Broken fitting

- Check all fittings and tubes to make sure there are no cracks or holes. It may help to put the engine through startup procedures so there is fuel movement that may be used to help identify leaks.

X. Maintenance

The obscurant generator system occasionally requires maintenance. Maintenance is divided into two types: User Maintenance and Manufacturer Maintenance.

Manufacturer Maintenance is recommended, as per the JetCat owners manual, every 25 hours of use. The turbine is removed and sent to JetCat for disassembly, inspection, and any necessary maintenance of components such as bearings, fan blades, shafts, and spindle balance. This maintenance requires special machinery and sensors and can not be performed in the field.

User Maintenance may be performed as necessary. Examples of this include glow stick replacement, fuel filter replacement, cleaning the system, and checking the air filters. It is better to be proactive and check components regularly for signs of oncoming trouble than to be reactive and learn of a problem at the most inconvenient of times. It is also recommended as part of user maintenance to regularly take note of normal engine sounds so differences can be detected as a sign of possible maintenance issues.

Manufacturer Maintenance

If any of the following are noticed, remove the turbine engine and return to JetCat for maintenance immediately: fan blade nicks, constant squealing or scratching sounds outside of the normal engine sounds, damage to the body of the engine, a defective starter motor, a starter motor that engages but does not spin the fan, or anything abnormal that is not described in the User Maintenance section.

User Maintenance

Glow Stick Replacement

- The glow stick is located on the side of the turbine engine body. Removal is performed by unscrewing the starter fuel line from the side of the glow stick,

then hold the black wire connector on top of the glow stick and gently pull on the spring-loaded wire so the connector may be pulled up off of the glow plug. Plug removal is performed using an appropriate sized wrench and turning counter-clockwise. Do not lose the washer/gasket which is placed between the engine and the glow stick! Do not touch the ceramic glow stick. Installation is the opposite, turning until the plug has a snug fit and the fuel line is directed off the side of the engine away from any heat.



Fuel tank removal

-To remove the fuel tank, first open the engine compartment and disconnect all fuel lines and sensor wires and feed these through the opening into the electronics bay. In the electronics bay, disconnect the metal obscurant oil tubes from the fittings penetrating into the engine compartment. Release the four latches at the bottom of the fuel tank. Pull the outer body of the obscurant generator unit upwards and off of the tank. Note the location of the main fuel line at the top left, the glow stick halfway down the engine with the starting fuel line, and various sensor and control wires.



Note: The obscurant oil lines must be disconnected before removing the fuel tank from the obscurant generator unit. The photo at left shows the obscurant oil lines coiling before being attached to the bulkhead penetrators (upper left side). Unscrew the fitting where the arrows indicate.

Fuel filter replacement

-To replace the fuel filter, first remove the fuel tank from the generator unit using the procedures above. The fuel filter is an aluminum cylinder about 1-1/2 inches long in line between the fuel tank penetration fitting and the fuel pump. Disconnect the short fuel line from the top of the fuel tank penetration fitting. Holding the fuel pump side of the fuel filter assembly, unscrew the fuel tank side of the same assembly. The fuel filter is located inside. If dirty, flush the inside of the filter assembly before installing a new fuel filter. Installation is the reverse of removal.



Note: The small square shaped fuel solenoid valves are mounted low on either side of the metal mounting bracket between the fluid level indicator gauges. Make sure these are connected to the ECU and the engine in correctly. “Fuel” on the ECU refers to the main fuel line and should be connected to the solenoid valve that feeds to the main fuel inlet on the front shroud of the turbine. “Propane” on the ECU refers to the starter fuel line and should be connected to the solenoid valve that feeds to the starter fuel inlet on the glow stick. Crossing these solenoid valves will cause fuel to dump into the engine through the main fuel line and not ignite, and poses a hazard due to the amount of flammable fuel that accumulates inside the engine. Should this occur, tilt the entire obscurant generator

backwards so the engine air intake is pointing down. Clean any fuel that drains from the engine so it will not present a hazard to the unit or nearby personnel.

Note: The fuel pump is housed on the metal mounting bracket between the fluid level indicator gauges. Removal is performed using the appropriate sized hex key wrench to remove the screws holding the top of the bracket onto the fuel pump. To replace the pump, take note of the fuel flow direction through the fuel pump, then cut the fuel lines off the pump and the adjacent plastic elbows. Replace these pieces of fuel line between the fuel pump and the adjacent plastic elbows, making sure the new fuel pump has the correct fuel flow alignment. Re-attach the metal bracket on the side of the fuel pump, but **do not overtighten because this will damage the fuel pump.**

Cleaning

- It is recommended to keep the system clean since the obscurant oils can be flammable. Periodically wipe dry any fuel or oil that is found in the engine compartment and electronics compartment.

Broken fuel lines or fittings

- Cut the fuel line as near to the fitting as possible for removal of the damaged component. If a longer piece of tubing is necessary remove the entire segment of tubing and replace with the necessary length. Press the fuel tubing onto a new replacement fitting. It may be necessary to stretch the tubing opening with needle nose pliers before installation if it is too tight a fit to make.

Engine Replacement

- If it is deemed that the engine must be replaced, disconnect all fuel lines and sensor and control wires from the engine. Remove the four nut/bolts securing the mounting bracket wings to the generator unit so the entire section can be removed from the compartment. Once removed, loosen the hose clamps but **be careful with the temperature sensor wire**. The hose clamps are fed between the engine housing and the temperature sensor wire. *If the sensor wire is damaged it will cause a sensor malfunction and the engine will not start.* Remove the mounting bracket wings and the hose clamps and reattach to the new engine, making sure the alignment of the glow stick is correct. Reattach

the four nuts/bolts that hold the mounting bracket wings to the engine once the engine is in a straight alignment with the exhaust tube.

Obscurant oil pump replacement

- If the obscurant oil pumps must be accessed, follow the above procedures to remove the fuel tank from the generator unit. The obscurant oil fuel pumps are installed inside the obscurant oil tank and are accessible by removing the large plate bolted onto the top of the tank. Be careful not to lose any nuts and washers, and also be careful not to damage the gasket between the plate and tank. Once removed from the tank, the fuel pumps can be replaced by disconnecting the wiring and unscrewing the bracket holding the pump to the assembly.

XI. Additional Notes

There has been an interest in biofuels as a replacement for petroleum fuels. We have tested the JetCat P80 turbine engine using biodiesel (B99) as the sole fuel source. However, turbine oil must still be added as a lubricant. The P80 electronics package is pre-configured for the properties of Jet-A fuel, not for biodiesel. Biodiesel requires more heat energy for ignition, but the glow stick can not be modified to provide more heat. Instead, we constructed a set of bypass valves so we could manually control the flow of fuel through the fuel lines. By starting at a much lower flow rate it increased the relative amount of heat energy available per unit volume and could ignite. Once ignited the valves were adjusted to slowly increase the flow of fuel into the starter line. Upon the automatic transition to the main fuel line, a similar procedure was followed to start at a lesser flow rate and increase it to full. We have successfully run the engine on methyl soyate biodiesel using this technique, and feel that with factory modifications to the electronics package it would be possible to run the modular obscurant generator unit using a single fluid in dual roles.

It may also be feasible that this obscurant generator unit could be modified to release tactical agents such as OC (pepper spray), and CS (tear gas).

Applications could range from military maneuvers to civilian police and SWAT tactics as well as fire department training. If tactical agents could be used with the generator it could be applied for DEA enforcement and riot control.

Although this system is designed to release large plumes of obscurantscreen, there is a deposition of oil on the ground and surrounding vegetation in near proximity to the generator when it is used. This is expected due to the nature of aerosol particle collisions and particle growth overcoming the weight restrictions for those particles to remain airborne.

A. Radio Control Operation Quick Reference Sheet

A Quick Sheet reference guide was also created for use with the modular obscurant generators. This guide was designed to be printed for use with the system as a refresher for the controls, and is found on the next page.

JetCat P80 R/C QuickSheet

To Turn On and Control Engine:

1. On R/C Transmitter, set the left stick all the way down. Put the left side up/down trim bar (black slider) all the way down. Set the three-position Flaps switch all the way to the back (farthest from user). Put the right side up/down trim bar in its center position.
2. Connect all batteries on the engine (12V obscurant, 7.2V ECU, 4.8V R/C).
3. Turn on the transmitter.
4. Turn on the small on/off R/C Receiver switch inside the obscurant box.
5. Slide the left up/down trim bar to the top.
6. Move the three-position Flaps switch to the central position.
7. Wait a second for the R/c System to initialize, then slide the left stick all the way up. The engine begins startup. It will start, ramp up to a high RPM for a few seconds, then drop down to idle RPM. Slide the left stick to the bottom as it drops down. Wait several seconds for the system to give full throttle control to the Transmitter, then move the left stick up to the desired RPM. All the way up is full RPM.

To Engage/Disengage Obscurant System:

1. Move the right side up/down trim bar to the top **Or** move and hold the right stick to the top position to blow obscurant.
2. Move the right side up/down trim bar to the bottom **Or** move and hold the right stick to the top position to purge the obscurant system.
3. Move the right side up/down trim bar to the center position **Or** release the right stick to turn off the obscurant system.

To Turn Off Engine (Normal):

1. Move the three-position Flaps switch to the uppermost position (“Auto-Off”). The engine will go to approximately 55K RPM, then turn off and begin the cooling process.
2. Reset all switches to the pre-start positions.
3. Turn off Receiver and Transmitter switches (in that order, or Obscurant On/Off servo may engage).

To Turn Off Engine (Emergency):

1. 1. Move the three-position Flaps switch all the way to the back (“Off”). **Or** Turn off the Receiver power switch inside the box.
 2. Reset all switches to the pre-start positions.
- Turn off Receiver and Transmitter switches (in that order, or Obscurant On/Off servo may engage)

BIBLIOGRAPHY

- ¹ “Smoke Screen.” *Online Etymology Dictionary*. Douglas Harper, Historian. 05 Nov. 2011. <Dictionary.com [http://dictionary.reference.com/browse/smoke screen](http://dictionary.reference.com/browse/smoke%20screen)>.
- ² “Smoke.” *Field Manual 8-285 Treatment of Chemical Agent Casualties and Conventional Military Chemical Injuries*. Department of Defense, Washington DC. 22 Dec. 1995. Retrieved 11 Nov. 2011. <GlobalSecurity.org <http://www.globalsecurity.org/wmd/library/policy/army/fm/8-285/>>.
- ³ *Toxicity of Military Smokes and Obscurants: Volume 2*. National Academy Press, Washington DC. 1999. Retrieved 11 Nov. 2011. <The National Academies Press <http://www.nap.edu/catalog/9621.html>>
- ⁴ *ERDEC-CR-071 Environmental and Health Effects Review for Obscurant Fog Oil*. C. Driver, M. Ligothe, J. Downs, B. Tiller, T. Poston, E. Moore, Jr., and D. Cataldo. Edgewood Research, Development & Engineering Center, Aberdeen Proving Ground, MD. Sep. 1993.
- ⁵ *ECBC-CR-073 Development and Evaluation of Biogenic Obscurants, Robotic Obscurant Projectors, and Obscurant Simulation Models*. V. Flanigan and S. Kapila. Edgewood Chemical Biological Center, Aberdeen Proving Ground, MD. Sep. 2004.
- ⁶ *DEP TM 3-1040-289-10 Operator’s Manual: Generator, Smoke, Mechanical: Motorized for Dual Purpose Unit, M56E1*. Headquarters, Department of the Army, Washington DC. 27 Sep. 2004.
- ⁷ *Toxicity of Military Smokes and Obscurants: Volume 1*. National Academy Press, Washington DC. 1997. Retrieved 11 Nov. 2011. <The National Academies Press <http://www.nap.edu/catalog/5582.html>>
- ⁸ *Assessment of Biodegradability and Mutagenicity of Methyl Soyate and Mineral Oils*. S. Mathkar. Missouri S&T Thesis. 2003.
- ⁹ *Obscurant Oil Characterization Produced Through Vaporization By Exhaust Gas of Mini-Jet Turbine Engine*. Maj. D. Bahaghighat. Missouri S&T Thesis. 2008.
- ¹⁰ “Nanofabrication and Packaging Strategies for Bispectral Obscurants.” *Proceedings for the 2011 Obscurants Symposium: 21st Century Countermeasures for the 21st Century Warfighter*. J. Holecek, S. Oldenburg, J. Icuss, D. Sebba, and C. Bruce. U.S. Army Edgewood Chemical Biological Center. May 2011.

¹¹ “Ultra-High Extinction Coefficients in Visible and Near-IR Wavelengths Using Plasmonic Nanoparticles.” *Proceedings for the 2011 Obscurants Symposium: 21st Century Countermeasures for the 21st Century Warfighter*. S. Oldenburg, D. Sebba, J. Holecek, and J. Icuss. U.S. Army Edgewood Chemical Biological Center. May 2011.

VITA

Robert W. Schaub is a native of Rolla, Missouri. In May 1999 he graduated from Rolla High School with Salutatorian honors. That fall he started his undergraduate research at University of Missouri-Rolla (now Missouri University of Science and Technology) working towards a degree in chemistry. In 2000 he started working as a student laboratory assistant with Dr. Paul Worsey in the Explosives Research Laboratory, and in 2003 earned the Missouri Limestone Producers' Association Blaster's Certification. In December 2003 he attained his Bachelors of Science degree with Cum Laude honors.

Beginning in January 2004 he joined the research group of Dr. Shubhen Kapila at Missouri S&T to begin working towards a Doctor of Philosophy degree in analytical chemistry. For several years he presented his research at the Pittsburgh Conference (PITTCO). Along the way he served as a laboratory teaching assistant for three chemistry courses. In the fall of 2011 he began teaching chemistry courses at a community college while completing his dissertation.

As an undergraduate Mr. Schaub was a member of the Missouri S&T student-affiliated chapter of the American Chemical Society, and has been a member of the American Chemical Society itself since 2005. He was also a member of the International Union for Pure and Applied Chemistry (IUPAC). In his spare time he volunteered with the Phelps County Historical Society to promote an appreciation for the study of history.

